# MCP3909 / dsPIC33FJ128GP206
# 3-Phase Energy Meter
# Reference Design

 

# Table of Contents



 

**NOTES:**

# Preface

## NOTICE TO CUSTOMERS

**All documentation becomes dated, and this manual is no exception. Microchip tools and documentation are constantly evolving to meet customer needs, so some actual dialogs and/or tool descriptions may differ from those in this document. Please refer to our web site (www.microchip.com) to obtain the latest documentation available.**

**Documents are identified with a "DS" number. This number is located on the bottom of each page, in front of the page number. The numbering convention for the DS number is "DSXXXXXA", where "XXXXX" is the document number and "A" is the revision level of the document.**

**For the most up-to-date information on development tools, see the MPLAB® IDE on-line help. Select the Help menu, and then Topics to open a list of available on-line help files.**

## INTRODUCTION

This chapter contains general information that will be useful to know before using the MCP3909 / dsPIC33F 3-Phase Energy Meter Reference Design. Items discussed in this chapter include:

- Document Layout
- Conventions Used in this Guide
- Recommended Reading
- The Microchip Web Site
- Customer Support
- Document Revision History

## DOCUMENT LAYOUT

This document describes how to use the MCP3909 / dsPIC33F 3-Phase Energy Meter Reference Design as a development tool to emulate and debug firmware on a target board. The manual layout is as follows:

This document describes how to use the MCP3909 / dsPIC33F 3-Phase Energy Meter Reference Design as a development tool. The manual layout is as follows:

- **Chapter 1. "Meter Overview"** - Summarizes the meter specifications and a quick getting started section
- **Chapter 2. "Hardware Description"** - A detailed explanation of the different circuit blocks, their function, and implementation
- **Chapter 3. "Firmware"** - All the calculations performed by the dsPIC33F are described here
- **Chapter 4. "Meter Calibration"** - Explains how the meter is calibrated to accuracy
- **Chapter 5. "PC Software" -** Includes screen shots of the viewer/calibration software included with the system
- **Chapter 6. "Meter Communications Protocol"** - The UART commands used to communicate to the meter
- **Appendix A. "Schematics and Layouts"** - Both PCB, SCH files are located here for the 2 board system
- **Appendix B. "Bill Of Materials (BOM)" -** Part number and ordering information for all components of the energy meter
- **Appendix C. "Power Calculation Theory" -** A detailed explanation of the theory behind the calculations described in **Chapter 3. "Firmware"**
- **Appendix D. "50/60 Hz Meter Operation"** - Instructions on converting the meter for use in a 60 Hz line frequency environment

## CONVENTIONS USED IN THIS GUIDE

This manual uses the following documentation conventions:

**DOCUMENTATION CONVENTIONS**

| Description | Represents | Examples |
|---|---|---|
| **Arial font:** | | |
| Italic characters | Referenced books | *MPLAB® IDE User's Guide* |
| | Emphasized text | ...is the *only* compiler... |
| Initial caps | A window | the Output window |
| | A dialog | the Settings dialog |
| | A menu selection | select Enable Programmer |
| Quotes | A field name in a window or dialog | "Save project before build" |
| Underlined, italic text with right angle bracket | A menu path | *File>Save* |
| Bold characters | A dialog button | Click **OK** |
| | A tab | Click the **Power** tab |
| N'Rnnnn | A number in verilog format, where N is the total number of digits, R is the radix and n is a digit. | 4'b0010, 2'hF1 |
| Text in angle brackets < > | A key on the keyboard | Press <Enter>, <F1> |
| **Courier New font:** | | |
| Plain Courier New | Sample source code | `#define START` |
| | Filenames | `autoexec.bat` |
| | File paths | `c:\mcc18\h` |
| | Keywords | `_asm, _endasm, static` |
| | Command-line options | `-Opa+, -Opa-` |
| | Bit values | `0, 1` |
| | Constants | `0xFF, 'A'` |
| Italic Courier New | A variable argument | *`file`*`.o`, where *`file`* can be any valid filename |
| Square brackets [ ] | Optional arguments | `mcc18 [options]` *`file`* `[options]` |
| Curly brackets and pipe character: { \| } | Choice of mutually exclusive arguments; an OR selection | `errorlevel {0\|1}` |
| Ellipses... | Replaces repeated text | `var_name [, var_name...]` |
| | Represents code supplied by user | `void main (void)`<br>`{ ...`<br>`}` |

## RECOMMENDED READING

This user's guide describes how to use MCP3909 / dsPIC33F 3-Phase Energy Meter Reference Design. Other useful documents are listed below. The following Microchip documents are available and recommended as supplemental reference resources.

**MCP3909 Data Sheet, *"Energy Metering IC with SPI Interface and Active Power Pulse Output"* (DS22025)**

This data sheet provides detailed information regarding the MCP3909 device.

**AN994 Application Note *"IEC61036 Meter Design using the MCP3905/6 Energy Metering Devices"* (DS00994)**

This application note documents the design decisions associated with using the MCP390X devices for energy meter design and IEC compliance.

## THE MICROCHIP WEB SITE

Microchip provides online support via our web site at www.microchip.com. This web site is used as a means to make files and information easily available to customers. Accessible by using your favorite Internet browser, the web site contains the following information:

- **Product Support** – Data sheets and errata, application notes and sample programs, design resources, user's guides and hardware support documents, latest software releases and archived software
- **General Technical Support** – Frequently Asked Questions (FAQs), technical support requests, online discussion groups, Microchip consultant program member listing
- **Business of Microchip** – Product selector and ordering guides, latest Microchip press releases, listing of seminars and events, listings of Microchip sales offices, distributors and factory representatives

## CUSTOMER SUPPORT

Users of Microchip products can receive assistance through several channels:

- Distributor or Representative
- Local Sales Office
- Field Application Engineer (FAE)
- Technical Support

Customers should contact their distributor, representative or field application engineer (FAE) for support. Local sales offices are also available to help customers. A listing of sales offices and locations is included in the back of this document.

Technical support is available through the web site at: http://support.microchip.com

## DOCUMENT REVISION HISTORY

### Revision A (November 2009)

- Initial Release of this Document.

# Chapter 1. Meter Overview

## 1.1 INTRODUCTION

The MCP3909 / dsPIC33F 3-Phase Energy Meter Reference Design is a fully functional energy meter with many advanced features such as harmonic analysis, per phase distortion information, voltage sag detection, four quadrant energy measurement, and active and reactive power calculation. It uses Microchip's powerful 16-bit dsPIC33F Microcontroller Unit (MCU).

The MCP3909 / dsPIC33F 3-Phase Energy Meter Reference Design is unique in the fact that all calculations take advantage of the dsPIC33F DSP engine, and all output quantities are calculated in the frequency domain through the use of direct fourier transforms (DFT). This approach yields a large volume of outputs for a variety of meter designs, from simple active power only energy meters, to advanced energy meters requiring harmonic analysis.

Another significant advantage of this design, is that the dsPIC firmware implements a quasi-synchronous sampling algorithm, eliminating the need for external zero-crossing detection and PLL (Phase Locked Loop) circuit for the synchronization of ADC samples to line frequency. The line frequency is measured in software and corrected for measurement errors caused by frequency fluctuations in the power grid. This additional processing on the dsPIC reduces the overall meter cost by eliminating the requirement for a PLL circuit.

## 1.2 METER DESIGN PARAMETERS

- Accuracy Class: 0.2S
- Rated Current Ib: 3 X 5(20)A
- 3-phase 4-wire System
- Line Frequency Range: 47-53 Hz or 57-63 Hz (firmware option, see **Appendix D. "50/60 Hz Meter Operation"**)
- ADC Sampling Rate: 12.8 ksps to 3.2 ksps
- Voltage Input:
  - 3 x 220/380V
  - 3 x 57.7/100V (3-Phase, 4-Wire)
- Starting Current: 0.001 $I_B$
- Active Power Measurement Range: 0-13200W, Precision Class: 0.2.
- Reactive Power Measurement Range: 0-13200VAR, Precision Class: 0.2.
- Power Factor (PF) Precision Class: 0.2.
- Frequency Measurement: Precision Class: 0.2, Max. Error 0.1 Hz
- Harmonic Component Measurement of Voltage Input: $2^{ND}$-$31^{ST}$ Harmonic
- Harmonic Component Measurement of Current Input: $2^{ND}$-$31^{ST}$ Harmonic
- Creeping: Anti-creeping Design (<0.0008 $I_B$)
- Two Pulse Outputs: Total Phase Active Power, Total Phase Reactive Power
- Pulse Constant: 3200 Imp/kWh

## 1.3 POWER CALCULATIONS

A summary of all the calculations performed by this energy meter are summarized below.

**Chapter 3. "Firmware"** provides an explanation on the firmware implementation, **Appendix C. "Power Calculation Theory"** is included to show the theory behind this firmware.

- Power Grid Frequency
- RMS Voltage Of Each Phase
- RMS Current Of Each Phase
- RMS Neutral Current
- Active Power Of Each Phase
- Reactive Power Of Each Phase
- Apparent Power Of Each Phase
- Power Factor Of Each Phase
- Fundamental Active Power Of Each Phase
- Fundamental Reactive Power Of Each Phase
- Harmonic Active Power Of Each Phase
- Harmonic Reactive Power Of Each Phase
- Total Active Power:
  - The Algebraic Sum Of Active Power Of Three Phases
- Total Reactive Power:
  - The Algebraic Sum Of Reactive Power Of Three Phases
- Total Apparent Power:
  - The Algebraic Sum Of Apparent Power Of Three Phases
- Total Power Factor
- Phase Missing / Line voltage sag detection and alarm
- Total Active Energy:
  - The Algebraic Sum Of Positive/negative Active Energy
- Positive/negative Active Energy
- Positive/negative Reactive Energy
- Four-quadrant Reactive Energy
- Voltage/current Harmonic Content Of Each Phase

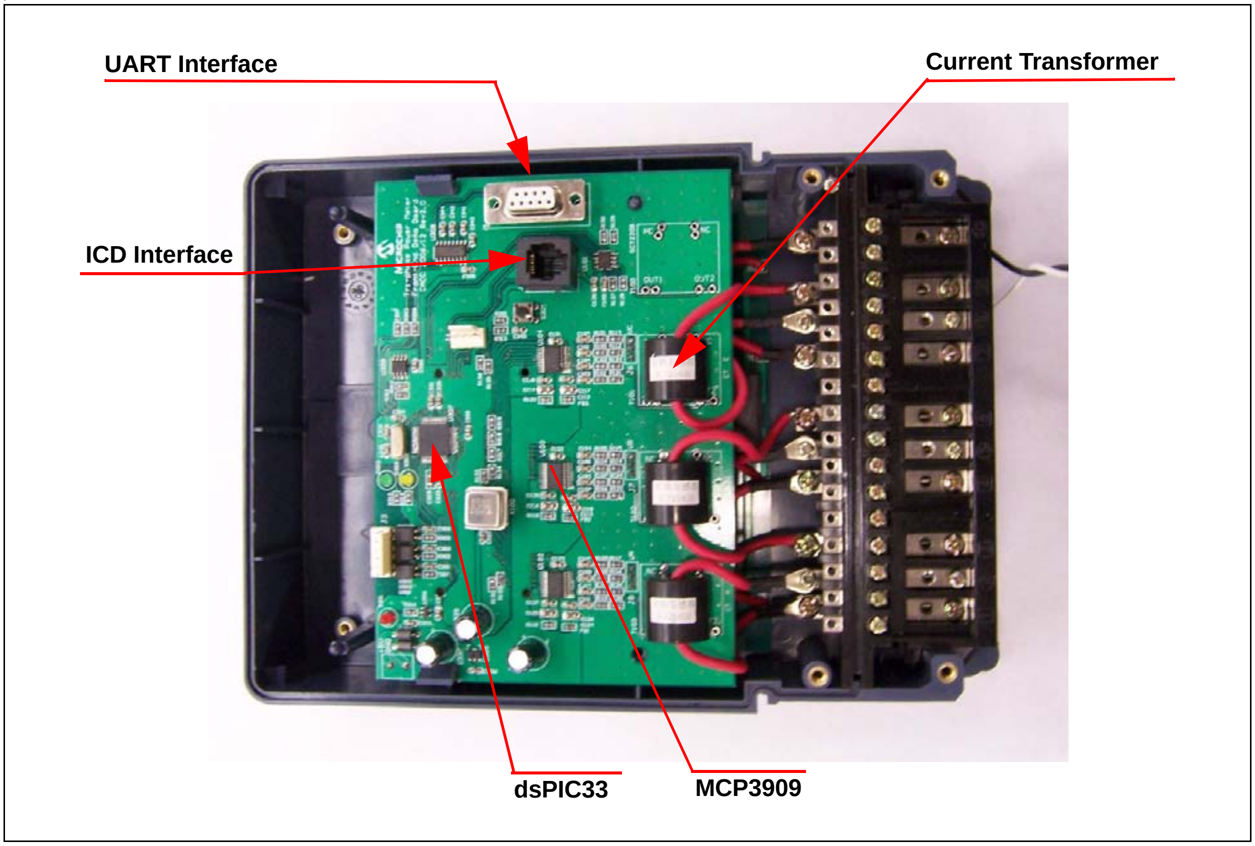


***FIGURE 1-1:*** *MCP3909 / dsPIC33F 3-Phase Energy Meter Reference Design.*

## 1.4 GETTING STARTED

To describe how to use the MCP3909 / dsPIC33F 3-Phase Energy Meter Reference Design, the following example is given using a 4-wire, 3-phase, 220VAC line voltage and connection. The rated current of the energy meter is 5(20)A.

The energy meters are not shipped fully calibrated, and a full calibration should be performed to show the true meter accuracy. See **Chapter 4. "Meter Calibration"** for more information.

All connections described in this section are dependent on the choice of current sensing element and a secondary external transformer may be required in higher current meter designs.

### Step 1: Connect the meter to 220V line and load

The diagram below shows where the voltage and current connections should be made. It is not required to connect all 3 phases for the meter to be operational.

220VAC should be placed between either $V_A$, $V_B$, $V_C$ and $N_{IN}$, $N_{OUT}$.

The AC load for a given phase should then be connected to the $I_{IN}$ and $I_{OUT}$ of a given phase.

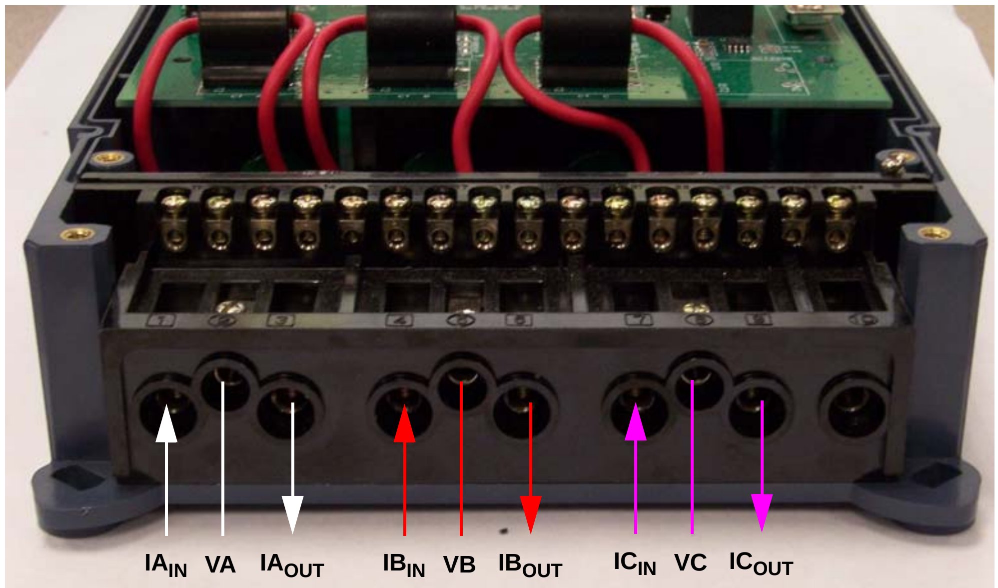


***FIGURE 1-2:*** *Meter Case Bottom.*

### Step 2: Turn On Line/Load Power to the Meter

Turn on the power to the energy meter. D1 should be lit showing the meter has power. At this point, if a load is connected and the meter is measuring power, the power LED, D1, should be blinking.

### Step 3: Connect the RS-232 Cable

1. Connect the RS-232 cable from the energy meter to a Personal Computer (PC), using either COM1, COM2, or COM6.

### Step 4: Run the PC Calibration Software

After installing and running the PC energy meter software on a PC running a Windows™ Operating System, and selecting the proper comm port for RS-232 communication, the following screen should show real-time meter results. The following chapters include more detail on the firmware, calculation, and PC software.

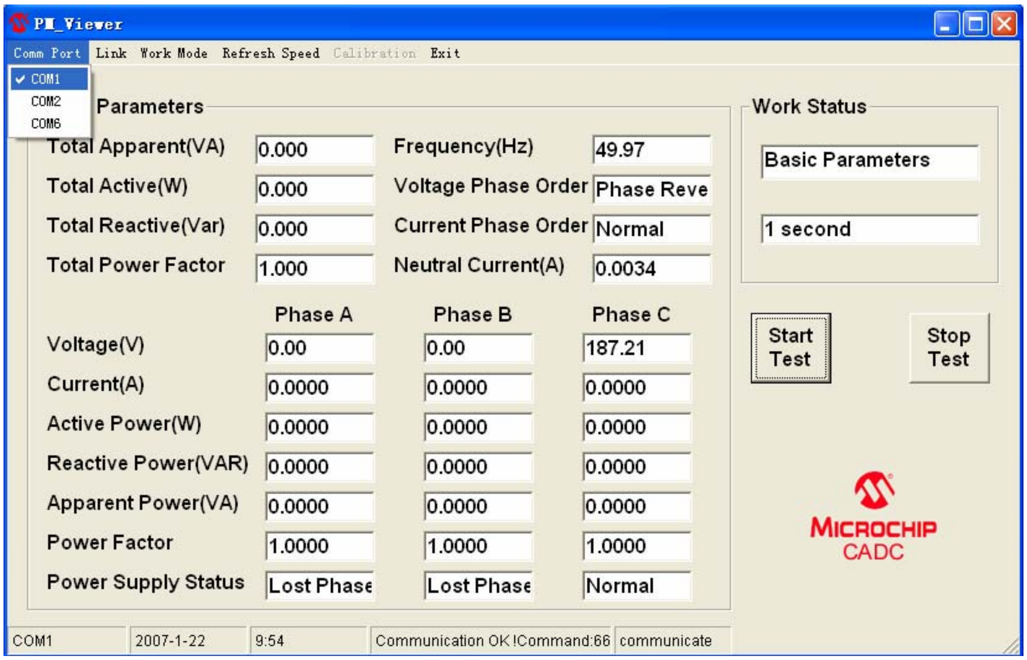


*FIGURE 1-3: "PM_Viewer" or Power Meter Viewer PC Software.*

**NOTES:**

# Chapter 2. Hardware Description

## 2.1 OVERVIEW

Figure 2-1 is the basic hardware block diagram of the MCP3909 / dsPIC33F 3-Phase Energy Meter Reference Design. The hardware includes the dsPIC33F and ICD 2 interface, analog signal conditioning for 3-phase voltage/current inputs and current using the MCP3909 Energy Meter IC, neutral current measurement using external op-amp on-board dsPIC33F ADC, UART interface to PC, ICD2 interface for MCU programming, and power supply circuits. Note there are two PCBs comprising this energy meter, the power supply PCB, and the MCU/AFE PCB. Refer to **Appendix A. "Schematics and Layouts"** for more information.

Three-phase voltage and current signals are connected to the meter through transformers, and connected to the MCP3909 A/D converter through a simple signal conditioning circuit. The MCP3909 device samples the signal and performs the analog-to-digital conversion (ADC). The MCP3909 device sends the digital conversion results to the dsPIC device via the SPI interface.

The MCP3909 / dsPIC33F 3-Phase Energy Meter Reference Design uses a quasi-synchronous sampling algorithm via the dsPIC33F, therefore eliminating the need for voltage zero-crossing detect and clock generating circuit, which are otherwise needed in a synchronous sampling algorithm. The clock of the MCP3909 device is an active external 3.2768 MHz crystal.

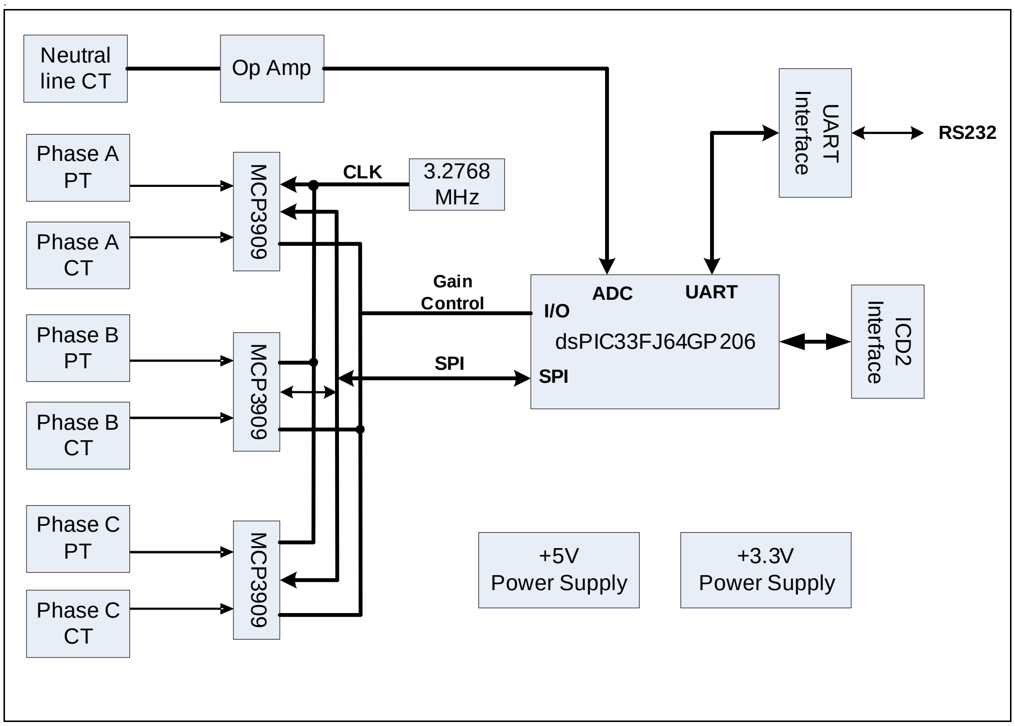


***FIGURE 2-1:*** *Hardware Block Diagram.*

## 2.2 ANALOG FRONT END CIRCUITRY

For safety, current transformers are used between the voltage and current input signals and the measurement module to isolate it from the 3-phase power supply.

The transformer used for the voltage path is a 1:1 transformer, SPT204B from Beijing Singure Measurement & Control Technology Co., with non-linearity less than 0.1%, and rated input/output current of 2 mA/2 mA.

The transformer used on the current side is a SPT254FK, from Yhehua Shanghai, with rated input /output current of 20A/2 mA, non-linearity less than 0.1%, and linear range of 0-20 A. See **Appendix B. "Bill Of Materials (BOM)"** for more information on the input circuitry.

Using phase A as an example for the voltage signal path, a 150 kΩ ($R_1$) resistor is used before the CT to transform the signal to an appropriate current. After the CT, burden resistors $R_{125}$ and $R_{126}$ are needed to transform the current signal to a differential voltage signal for the MCP3909 device to sample. Signals are coupled into the MCP3909 device's signal input port via $R_{110}$ and $R_{111}$. $C_{111}$ and $C_{112}$ are used to filter high-frequency signals.

Using phase A as an example for the current signal path, transformation of the current signal is similar to that of the voltage signal. The burden resistors $R_{125}/R_{126}$ and $R_{116}/R_{117}$ are chosen to be 20Ω for the current channel and 100Ω for the voltage channel after considering the following 3 factors:

- The MCP3909 device's differential voltage input range: 1V for voltage channel and 0.705V for current channel
- Maximum current/voltage for the meter: rated current of 5A, maximum current of 20A, and maximum voltage of 300V)
- Transformer ratio for the current and voltage transformer.

A non-isolated voltage input circuit is included. In practice, a voltage divider network of resistors is often used for sampling AC voltage input. This measuring method is therefore included in the hardware design. In Figure 2-2, voltage divider resistors $R_3$, $R_4$, and sampling resistor $R_1$ construct a network for sampling AC voltage.

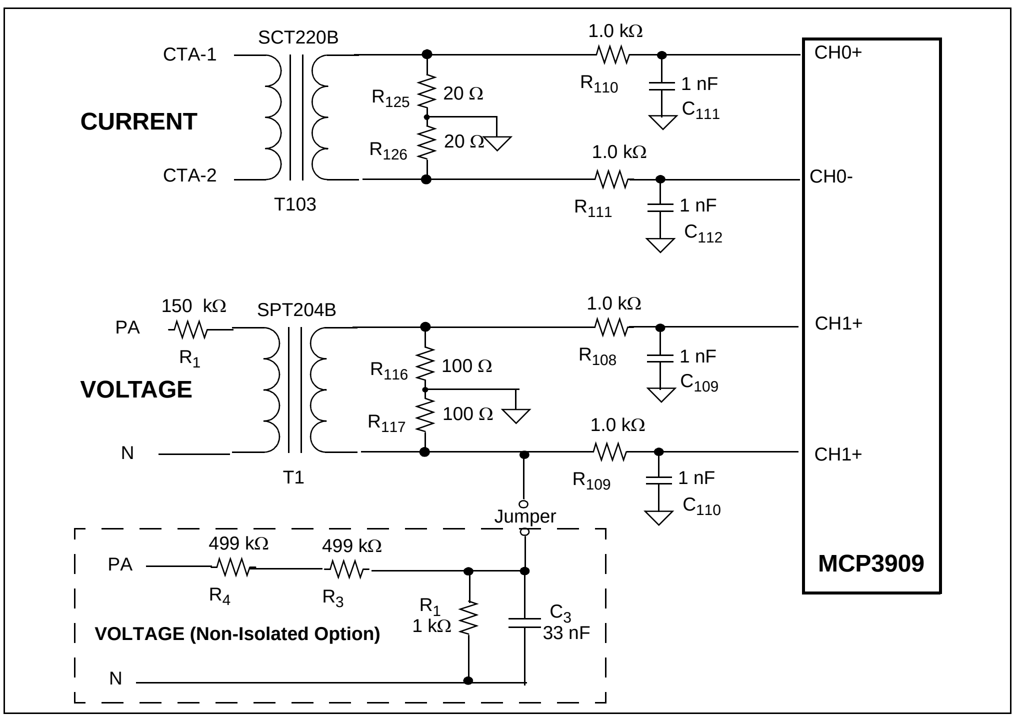


***FIGURE 2-2:*** *Input Signal Conditioning Circuit (Phase A).*

### 2.2.1 Burden Resistor Temperature Coefficient

The high precision class 0.2S requirement for the energy meter makes it crucial to select proper burden resistors for the output of the current transformers.

Metal film resistors with low inherent noise and temperature coefficient are ideal. Given that the secondary current of the CT is I, then the input voltage of the MCP3909 device is U = IR, where R is the resistance of $R_{125}$ and $R_{126}$ (Using Phase A as an example). If the temperature varies by $\Delta T$, and the temperature coefficient of sampling resistor R is $\beta$ ppm/°C, then the output voltage is:

**EQUATION 2-1:**

$$U' = I(R + \Delta T \times \beta \times R)$$

The voltage variation is:

**EQUATION 2-2:**

$$\Delta U = U' - U = I \times \Delta T \times \beta \times R = U \times \Delta T \times \beta$$

This relationship shows that the output voltage variation caused by temperature variation is in proportion to the temperature coefficient of the burden resistor.

In addition, a smaller temperature coefficient benefits meter start stabilization after startup. It takes a longer time for resistors with larger temperature coefficient to stabilize. Therefore, accurate measurements would require a longer wait after power-up. This affects the efficiency, or speed of meter calibration.

## 2.3 ANALOG-TO-DIGITAL CONVERSION

This meter design uses Microchip's MCP3909 energy meter ICs. Small-signal current inputs can be amplified by the programmable gain amplifier inside the MCP3909 device. The programmable range for the MCP3909's PGA is 16:1 V/V. The MCP3909 PGA gain can be configured by G0 and G1 (Pin 15 and 16 of the dsPIC33F).

The MCP3909 device's clock is provided by a 3.3768 MHz active crystal (for 50 Hz system, see **Appendix D. "50/60 Hz Meter Operation"** for 60 Hz line frequency information). The MCP3909 device's output data rate is 12.8 ksps. The clock lines and MCLR lines of all 3 MCP3909 devices are connected together, which ensures that the 3 phases are strictly synchronous.

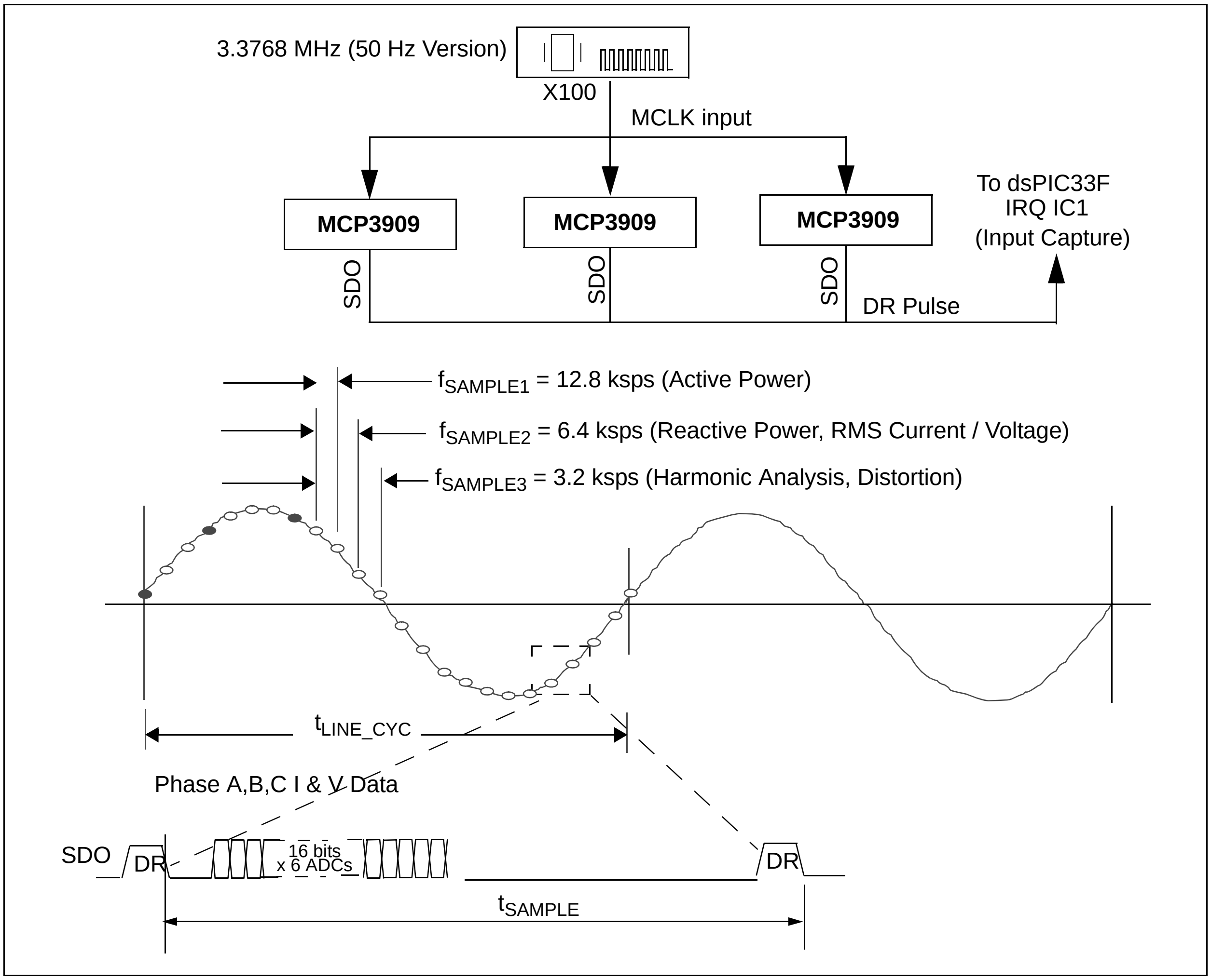


***FIGURE 2-3:*** *Clock Generation, Sampling Times and Calculation Frequencies.*

### 2.3.1 Samples And Processing

Input capture $IC_1$ on the dsPIC33F is used to detect if A/D conversion is complete. However, not all MCP3909 device samples are stored in the MCU, depending on the parameter being calculated. The ADC conversion rate of the MCP3909 device is determined by the frequency of the master clock (3.378 MHz for the case of a 50 Hz line), and the output data rate is MCLK/256 or 12.8 ksps. After each conversion is complete, a Data Ready signal is generated by the SDO of the MCP3909 device. The signal is fed into $IC_1$, allowing the Interrupt Service Routine (ISR) of $IC_1$ to read the data. When the MCP3909 device outputs data, it first sends an ADC result of the voltage channel, then an ADC result of the current channel, with MSB first.

As noted, not all MCP3909 device samples are used for calculating all the parameters. In practice, 6.4 ksps sampling rate is required, which means only 1 output data is used for every 2 data sampled. For 50 Hz input signal, 6.4 ksps sampling rate will take 128 samples for each cycle. For example, the active power metering is computed based on this condition.

But for other parameters for which precision is not critical, such as reactive energy, voltage, current and frequency, the sampling rate may be reduced to save data storage space and processing time. In this design, the 3.2 ksps sampling rate is used, which means only 1 result is stored for every 4 ADC conversions.

After each conversion, a positive pulse with the width of 4 clock cycles is output by the SDO pin of the MCP3909 device. $IC_1$ is used to detect the falling edge of the pulse and generate an interrupt for every 2 falling edges, i.e., 1 data is read for every 2 conversions, thus realizing 6.4 ksps sampling rate.

## 2.4 DSPIC33F HARDWARE CONNECTION AND PERIPHERAL USAGE

Table 2-1 is the pin allocation for the dsPIC33FJ64GP206 MCU.

**TABLE 2-1: FUNCTIONAL ALLOCATION FOR dsPIC33F PINS**

| dsPIC Pin | Pin Function Name | Corresponding Name in Schematic Diagram | Functional Description |
|---|---|---|---|
| 62, 1 | RG14, RG15 | G0A, G1A | MCP3909's gain control for Phase A |
| 2, 3 | RC1, RC2 | G0B, G1B | MCP3909's gain control for Phase B |
| 13, 12 | RB3, RB4 | G0C, G1C | MCP3909's gain control for Phase C |
| 14 | RB2 | CSA | MCP3909's chip-select signal corresponding to Phase A |
| 15 | RB1 | CSB | MCP3909's chip-select signal corresponding to Phase B |
| 16 | RB0 | CSC | MCP3909's chip-select signal corresponding to Phase C |
| 4, 5, 6 | SCK, SDI, SDO | SPI I/F | Interface signal of SPI2. SPI interface operates under master mode, used for the MCP3909 device communications |
| 42 | INT1 | SDO | SDO line of SPI interface, for detecting MCP3909's A/D conversion complete flag |
| 49-51 | RD1-RD3 | PULSE1, PULSE2, PULSE3 | PULSE1 is total phase active power pulse output, PULSE2 is total phase reactive power pulse output. PULSE3's function is to be determined. |
| 61 | RG0 | AD_MCLR | Master clear signal of 3 MCP3909 devices (tied together) |
| 53 | RC13, RC14 | LED1, LED2 | LED drive pins, can be used as energy pulse output indicator, for meter calibration. Its function is similar to those of PULSE1 and PULSE2 |
| 36, 37 | SDA1 / SCL1 | SDA/SCL | $I^2C$™ interface, used to read/write EEPROM externally |
| 33, 34 | U1TX / U1RX | RF3/RF2 | UART interface |
| 33, 34, 35 | SDO1/SDI1/SCK1 | RF3/RF2/RF6 | SPI1 interface, can be designed by customers, used for communication with host MCU to obtain measurement results and calibrate a meter. Its function is the same as UART interface, but have a faster communication rate and higher efficiency. SPI operates in slave mode. If UART interface is used to communicate with host MCU, then this interface cannot be used. |
| 27 | AN12 | Current_N | Detect neutral current |
| 28 | AN13 | Ref_V | Detect boost voltage of neutral current |
| 17, 18 | ICSPCLK, ICSP-DAT | ICSP I/F | Online debugging/programming interface |
| 7 | MCLR | MCLR | Master clear input |

### 2.4.1 UART and SPI1 Interface

The UART and SPI1 interfaces are multiplexed. Through the UART or SPI1 interface, the host MCU can communicate with the metering front-end to perform calibration or obtain metering results. The SPI interface may also be used if high-speed data transfer is desired. In this case, the SPI interface of the dsPIC device works in the slave mode. The UART and SPI1 share a common pin, so only one of the two interfaces can be used at a time. Since the reference design uses a PC to simulate the host MCU, the UART interface is chosen as the communication interface. SPI and RS232 interfaces are not isolated from the PC. A general-purpose transceiver device, MAX232, is used for the UART interface.

### 2.4.2 Energy Pulse Output Interface

Three sets of outputs for energy measurement pulses are available in this design, corresponding to the I/O pins of RD1-RD3. Two of them, output total active energy and total reactive energy, respectively, and the other is not yet specified. Outputs are isolated by a photo-electronic coupling device, $U_3$. The photo-electronic coupler is active when corresponding I/O pin is high.

In addition, the design also provides two sets of LED outputs for energy meter calibration. The output pins for these LEDs are RC13 and RC14. The LED is on when the output is low. Figure 2-4 is the circuit of energy pulse output interface.

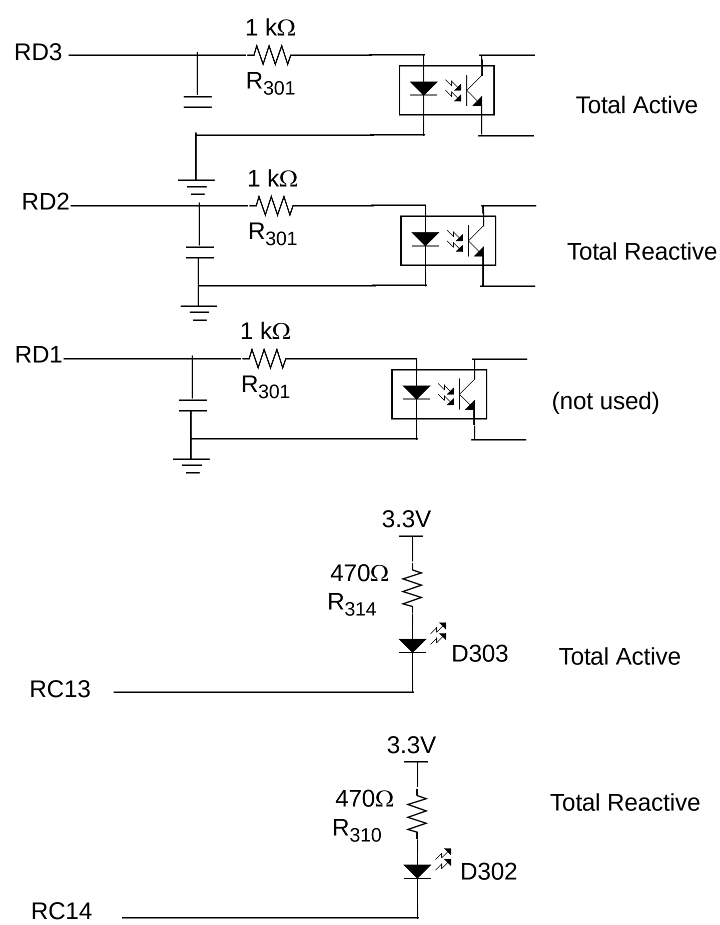


*FIGURE 2-4: Energy Output Pulse Configuration.*

### 2.4.3 Neutral Current Detection

Detection of neutral wire tampering is performed by the on-chip A/D of the dsPIC device. The purpose of the detection is to prevent electricity theft, balance 3-phase signals and detect electricity leakage. Since the precision is not critical, a dsPIC on-chip A/D is sufficient.

Figure 2-5 shows the circuit for neutral current detection. The neutral input uses $R_{128}$ for sampling. To bias the AC signals to the A/D measurement range, a 3.3V power supply is divided by $R_{130}$ and $R_{129}$ and connected to the emitter-follower of the MCP6002 device to output a boost voltage REV_V of 1.65V. The biased voltage is then connected to the CT in series. The CT's sampling voltage is connected to Op-amp B of the MCP6002 device via $R_{127}$ as emitter-follower output, generating the sampling voltage, Current_N, for the current. Both Current_N and 1.65V $V_{REF}$ signals are sampled and measured by the dsPIC on-chip A/D.

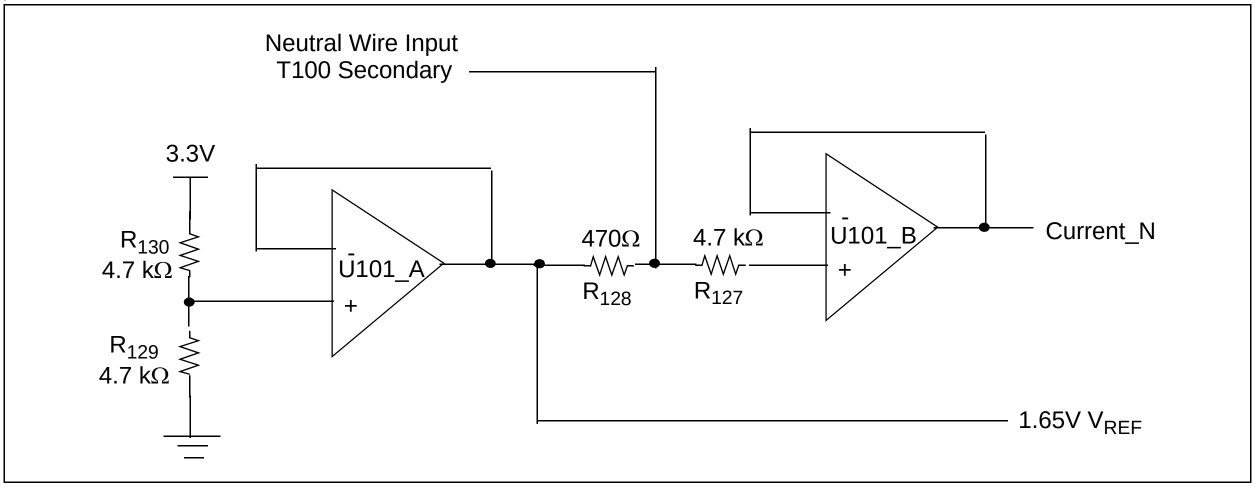


***FIGURE 2-5:*** *Circuit of Neutral Line Detection.*

 

## 2.5 POWER SUPPLY

The power supply used in this design provides 3.3V and 5V. Since the energy meter for a 3-phase 4-wire system is required to operate properly when any one phase is active, a switching power supply module is used for convenience. T4 is the switching power supply module.

Prior to the input of this module, additional protection circuitry is included with the meter design. Figure 2-6 shows the input to the switching power supply module and the additional filtering and protection circuitry. In Figure 2-6, $R_5$ is the integrated ferrite bead, $C_1$, $C_4$, $C_6$, RV1, RV2 and RV3 are $C_{BB}$ capacitors and varistors. They are used to improve anti-surge performance of the system.

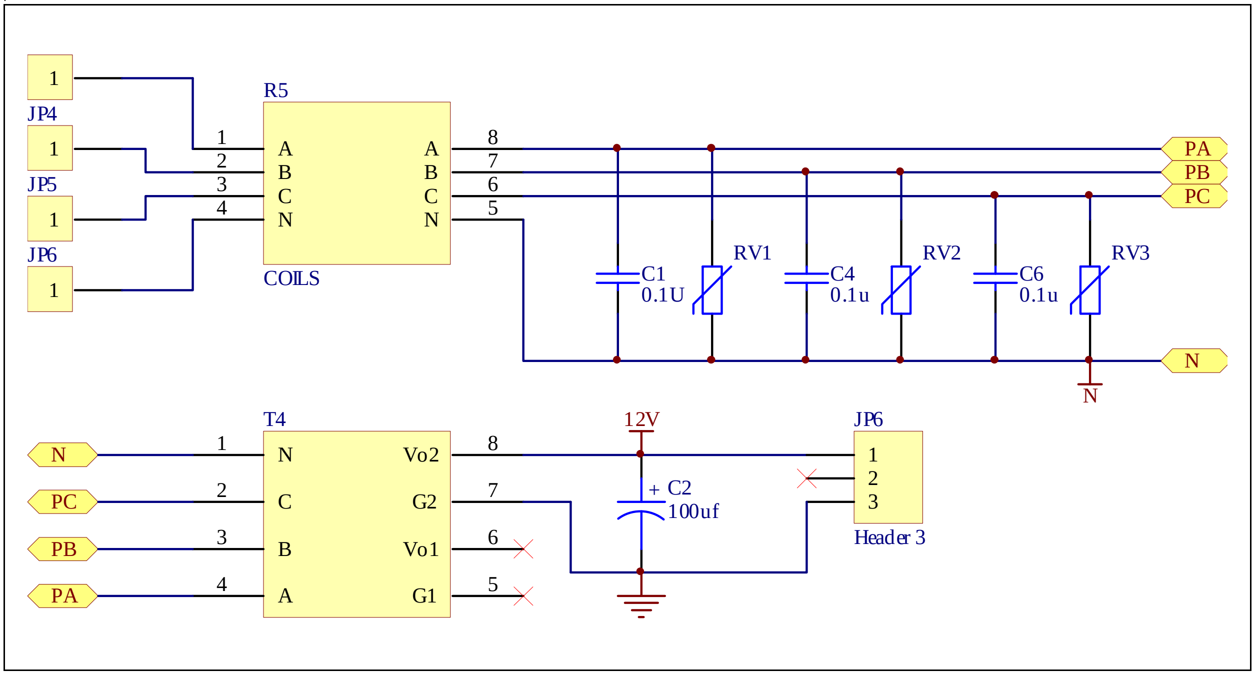


**FIGURE 2-6:** *Switching Power Supply Module (T4) and Additional Input Protection Circuitry.*

An LDO is connected in series at the output of the switching power supply to obtain a more stable power supply. Figure 2-7 shows this circuit. Microchip's MCP1701 device and MCP1700 device, low drop-out high efficiency LDOs, are selected for use.

D301 is the power LED for the meter and is active when the meter is connected to the proper line input voltage.

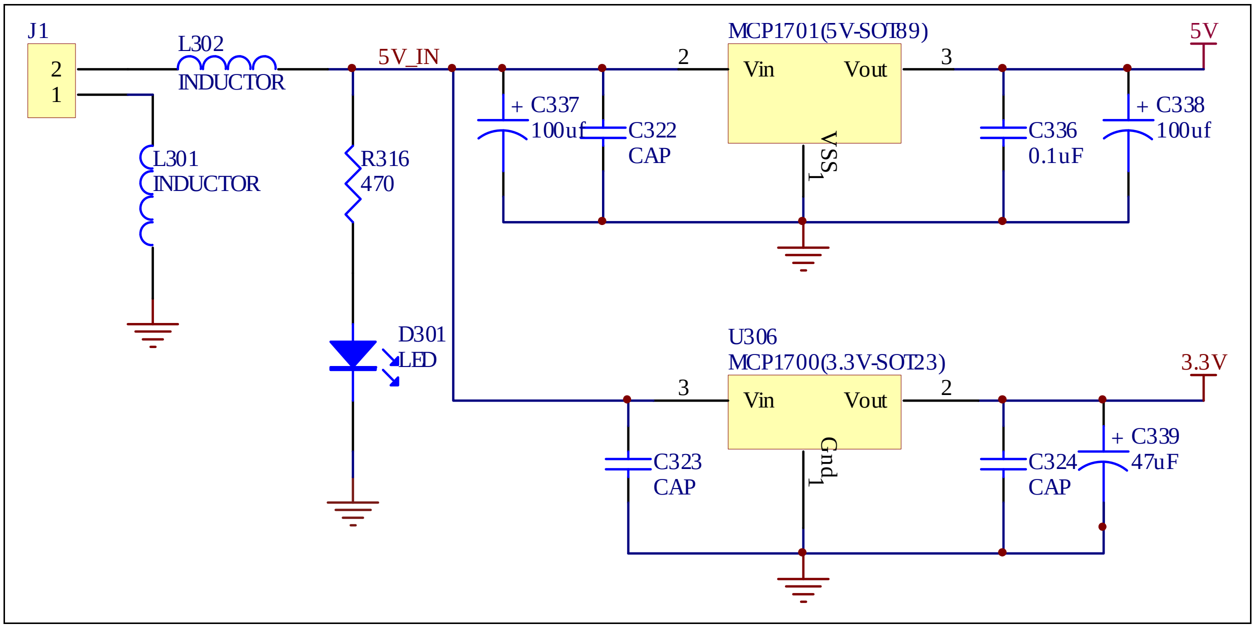


**FIGURE 2-7:** *5V and 3.3V LDO Modules.*

# Chapter 3. Firmware

## 3.1 OVERVIEW

This section discusses the dsPIC firmware structure, peripheral resources, important program flows, and explanations of project files included in the firmware zip files included with the system. See **Appendix D. "50/60 Hz Meter Operation"** for converting to 60 Hz code.

- Calculate all electrical parameters in frequency domain
- MCP3909 device communication
- Detect voltage/current phase order, and determine missing phases
- Generation imp/kWh power pulse
- UART communication

## 3.2 MAIN LOOP

The main loop of the entire dsPIC33F program is shown in Figure 3-1.

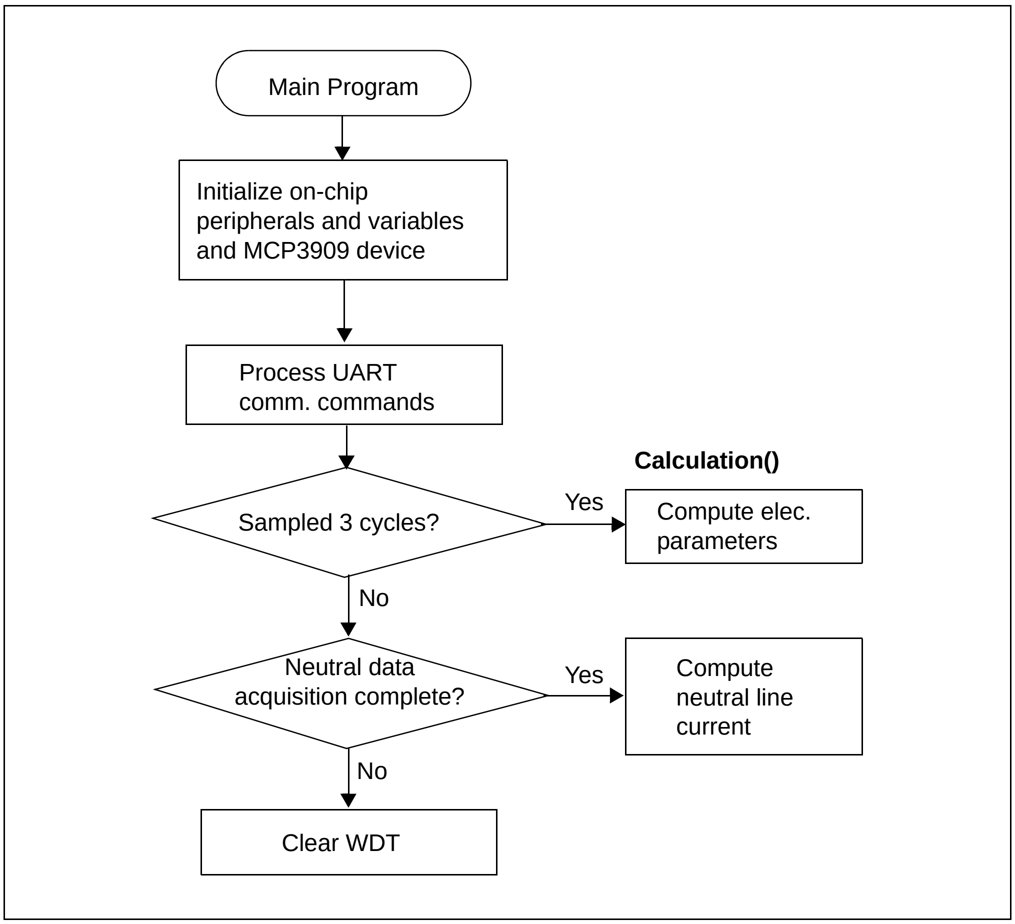


***FIGURE 3-1:*** *Main Loop Chart.*

After system power-up, the MCU enters the initialization process, which includes proper configuration of the I/O ports and on-chip peripherals (such as timer, UART, SPI and IC). At the same time, the system control parameters can be loaded from the external EEPROM and variables are all initialized.

Since most tasks of this system are accomplished through interrupts, only three tasks are carried out in the system main loop, which are interpreting/processing UART communication protocol, calculating parameters, and detecting neutral current. The UART communication is performed in function **UART_process()**, the executing frequency of which depends on the polling frequency of the upper computer.

Parameters are calculated by the function **Calculation()**, which is executed once every 3 cycles of the power grid. Neutral current is detected by function **ComputeNeutral-Current()**, and computing is performed once every 16 cycles of the power grid.

## 3.3 CALCULATION() - CALCULATING ELECTRICAL PARAMETERS

All power parameters are calculated with the function ***Calculation()****,* which is executed once every 3 cycles of the power grid. As shown in Figure 3-2, all calculations are performed post DFT (direct fourier transform), in the frequency domain.

- RMS Voltage/current Of Each phase
- Phase Angle
- Measuring Line Frequency
- Active, Reactive, Apparent Power Of Each Phase
- Positive and Negative Active Power
- Positive/negative Reactive Power
- 4-quadrant Reactive Energy
- Total Active Power, Total Reactive Power, and Total Apparent Power
- Total Power Factor
- Voltage and Current Distortion Of Each Phase
- Voltage and Current Harmonic Contents Of Each Phase

**Note:** Algorithms for all calculations are shown in **Appendix C. "Power Calculation Theory"**.

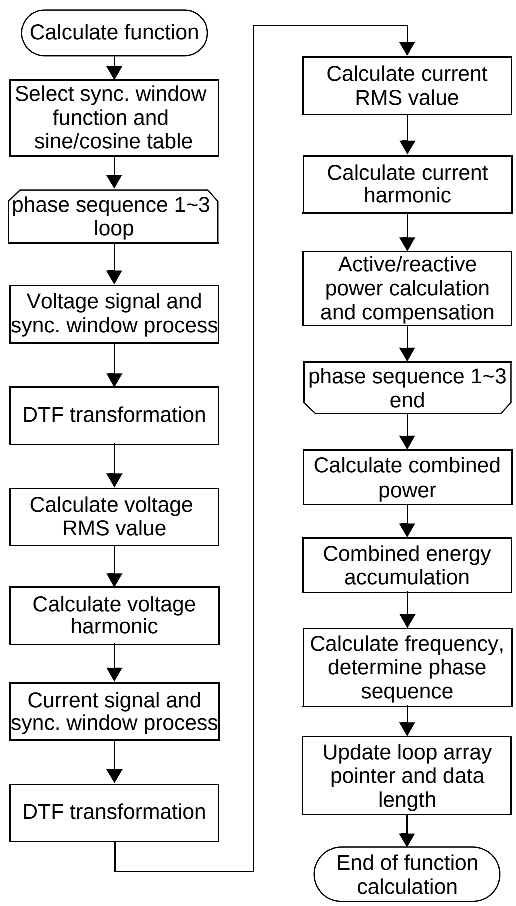


***FIGURE 3-2:*** *Calculation() Flow Chart.*

Each block can be categorized into one of three types of calculations:

1. Calculation for an individual phase
2. Calculation for all 3 phases
3. Calculation of power accumulation (Energy)

### 3.3.1 Process Quasi-Synchronization Window

The first blocks of the calculation flow are to determine how many samples to use for the quasi-synchronization sampling algorithm. See **Appendix C. “Power Calculation Theory”** for more information on this approach.

The firmware selects the proper quasi-synchronization window function (array of data) and corresponding sine/cosine table according to the number of sampling points in present current cycle.

The number of sampling points is obtained from the last calculation of frequency function. As the line frequency fluctuates in slow motion and typically varies by a small amount over three (3) line cycles, the period of line frequency measurements of the previous cycle can be used to determine data length of sampling.

The quasi-synchronization window function is an array established in advance, and its length is the same as that of the sampling data, which is obtained by the weight coefficient multiplied by 32768. In this design, the method of quadrature by complexification echelon is used, corresponding weight coefficient is calculated with three (3) iterations. Three iterations implies that the length of the input original data is equal to the number of sampling points in three cycles. The number of sampling points in each cycle is usually different from the input signal cycle, but it will be close to an integral multiple of the input signal cycle. For example, at a sampling rate of 3.2 ksps, 50 Hz input signal corresponds to 64 sampling points for each cycle, and 50.1 Hz input signal would also be close to 64 sampling points for each cycle. Again, 51 Hz input signal would be close to 63 sampling points for each cycle. Therefore, at different input frequencies, the corresponding numbers of sampling points in each cycle are different. Consequently, the corresponding quasi-sync window function and sine/cosine table need to be established according to different numbers of sampling points. The sine/cosine table is established by evenly dividing a cycle into a number of segments equal to the number of sampling points, calculating corresponding sine/cosine values and then multiplying the values by 32768. The purpose of the multiplication is to change the original operation of floating point numbers into that of fixed-point numbers. Adjustments will be performed in the final stage of calculation.

The processing of the original signal being processed by the quasi-synchronization window function is actually a process of array multiplication, i.e. the original input signal is multiplied with a corresponding array of window functions. It's accomplished by the function ***qusi_syn_wnd(),*** which is written in assembly to take full advantages of DSP features.

### 3.3.2 DFT Transformation

A Direct Fourier Transform (DFT) is performed on the collected sets of data. Processing of the original signal by quasi-synchronization window can effectively reduce spectrum leakage caused by non-entire-cycle sampling during DFT transformation.

The data length is not a power of 2, therefore, the FFT algorithm cannot be used in DFT transformation. DFT transform is accomplished by function ***DFT()***, which is written in assembly to take full advantages of the DSP feature of accumulated multiplication.

Since an FFT algorithm cannot be used, and it takes longer to perform a DFT calculation, this is the most time-consuming process in the entire system.

 

### 3.3.3 Calculating RMS Voltage/Current

After the data set of either a voltage or current signal (of each phase), has been DFT transformed, the voltage or current magnitudes of the different harmonics can then be calculated. The total effective voltage or current (RMS) can be obtained by further calculaton, by simply combining the results of the individual harmonics (including the fundamental or the $1^{ST}$ harmonic).

Computing the magnitude of the voltage or current is accomplished by function ***ComputeMagnitude*()**. The result, called amplitude, is a long integer, and is the squared magnitude of voltage or current. To speed up the computation, fixed-point operation is used. The ***ComputeMagnitude***() routine is written in assembly language.

After the magnitude is computed, there is an adjustment process which is based on a floating-point operation. The limited number of computations will not affect the operation speed, and will instead greatly improve precision.

Parameter ***ratio1*** in the firmware is a coefficient related to the number of sampling points (see Equation 2-2). Division is accomplished by a simple shift operation in firmware. If the sampling cycle is not a power of 2, it cannot be accomplished by shifting. However, division by shifting can be accomplished by multiplying a compensating coefficient ***Coeff.data.linear.V_channel[]***. This is the calibration coefficient for ratio errors.

Since the current signal has a wide dynamic range, for small signals, the ADC output data range is small and is limited by DSP's bit resolution (16-bit MCU). If division by shift is used in the same way that is used for large signals in computation, precision may be affected. Therefore, for computing magnitudes of small signals, ***ComputeSmallMagnitude()*** function is used instead. This function is similar to ***ComputeMagnitude(),*** the only difference being that the shift length is shortened in division operation, and will be compensated during data adjustment. The computation precision will not be affected as the data adjustment process uses float-point operation.

### 3.3.4 Calculating Harmonics

Computing harmonics is accomplished in assembly language, by the function ***ComputeHarmonic().*** The computation is based on Equation C-62, in **Appendix C. “Power Calculation Theory”**. The result is the ratio of the magnitude of K-th harmonic to fundamental magnitude, and is given in a percentage.

| | |
|---|---|
| **Note:** | Since the output of ***ComputeHarmonic()*** is the squared harmonic magnitude, extraction of square root is needed in computation. The calculated harmonic content is stored as a fixed-point number, and the actual value stored is the harmonic content multiplied by 10. |

### 3.3.5 Calculating Power

Computing power is accomplished in assembly language by the function ***ComputePower()*** based on Equation C-39 and Equation C-40 in **Appendix C. “Power Calculation Theory”**.

After the ***ComputePower***() function is complete, an adjusting process for computed power is required. First, the computed result is adjusted according to the gain of current amplifier. Then the calibrating coefficient ***ratio2*** is determined according to present number of sampling points.

Additional compensation to the power calculation is required, for phase compensation. This compensation is based on the present load current. The difference between signal frequency and the central frequency is also taken into consideration. Consequently computed power is compensated.

 

### 3.3.6 Active Energy Accumulation

Energy accumulation is done by calculating the total energy, which is the algebraic sum of energy of each phase. Active energy is obtained by accumulating the multiplication of voltage and current of each sample, which ensures the high accuracy of measurement.

### 3.3.7 Reactive Energy Accumulation

The required measurement accuracy of reactive energy low, so in this design, it is obtained by accumulating the product of the present measured reactive power and the time interval between two measurements.

### 3.3.8 Output Pulse Generation

Refer to **Section 2.4.2 "Energy Pulse Output Interface"** for pulse output. To ensure the uniformity of output pulses, the calculation is divided in the measurement cycle into in a number of equal sections, and accumulate them. For simplification and lowering computation complexity, a counter is used to substitute the process of accumulation. The counter is only enabled when accumulated energy approaches to the threshold of the pulse output.

### 3.3.9 Line Frequency Calculation

Frequency calculation is based on Equation C-52 and Equation C-53, in **Appendix C. "Power Calculation Theory"**. The dsPIC33F collects 3-line cycles worth of data. The first two cycles of data of all sampled data is analyzed, and then the frequency of two successive cycles is used.

The data of two successive cycles are transformed via DFT for the fundamental, which is accomplished by assemble function ***DFT_Fundamental***(). This is followed by the computation of the initial phase angle of the first two line cycles. Then the phase lag and frequency offset of the two line cycles of signal can be calculated.

When measuring frequency, only the first two cycles of data are used. It must be assumed the input frequency is 50 Hz and the chosen appropriate sine/cosine table to carry out DFT transform for fundamentals of the 1st and 2nd cycles of data. See **Appendix D. "50/60 Hz Meter Operation"** for 60 Hz firmware.

Frequency offset is calculated by determining the initial phase angle for each line cycle. The greater the frequency offset, the greater the measurement error.

Since one of the 3 phases may be missing, if the voltage magnitude for phase A is less than the threshold, it is necessary to switch to phase B. Consequently, if sufficient voltage magnitude of phase B is not detected, it is necessary to switch to phase C.

The basic algorithm for measuring line frequency is based on the method described in Appendix A, **Section C.4 "Measuring The Voltage/current Rms Value And Power Using Quasi-synchronous Sampling Algorithm"**.

Frequency will be measured once for every 3 times the data is sampled.

## 3.4 ADC SAMPLING SCHEME FOR CALCULATIONS

The ADC conversion rate of the MCP3909 device is determined by the frequency of master clock, MCLK, and the rate will be MCLK/256. After each conversion is complete, a DataReady signal (4-CLK length) is generated by the SDO of the MCP3909 device. The signal is fed into IC1 (Input Capture 1 on the dsPIC33F), allowing the Interrupt Service Routine (ISR) of IC1 to invoke data-read function of the MCP3909 device. When the MCP3909 device outputs data, it first sends the ADC result of the voltage channel, then that of the current channel, with the MSB first.

The frequency of the master clock, MCLK, of the MCP3909 device is 3.2768 MHz, and ADC outputs @12.8 ksps. In practice 6.4 ksps sampling rate is used in the program, which means only 1 output data is used for every 2 data sampled. For a 50 Hz input signal, a 6.4 ksps sampling rate will take 128 samples for each cycle. The active power calculation is computed based on this condition.

The other parameters for which precision is not critical, such as reactive energy, voltage, current and frequency, the sampling rate may be reduced to save data storage space and processing time. In this design, the 3.2 ksps sampling rate is used, which means only 1 result is stored for every 4 ADC conversions.

In the program, sampling and calculation are carried out concurrently, and data is stored in the cyclic array in the dsPIC33F RAM. A calculation may be performed after either 1 cycle, 2 cycles or 3 cycles of data are sampled, which can be configured in the program. The user should note that frequent calculations will increase the measurement precision at the price of system overhead and response speed, therefore making proper tradeoffs based on practical requirement. In this design, 3 cycles of signals are sampled before an AC electrical parameter calculation is performed. Refer to Figure 3-3.

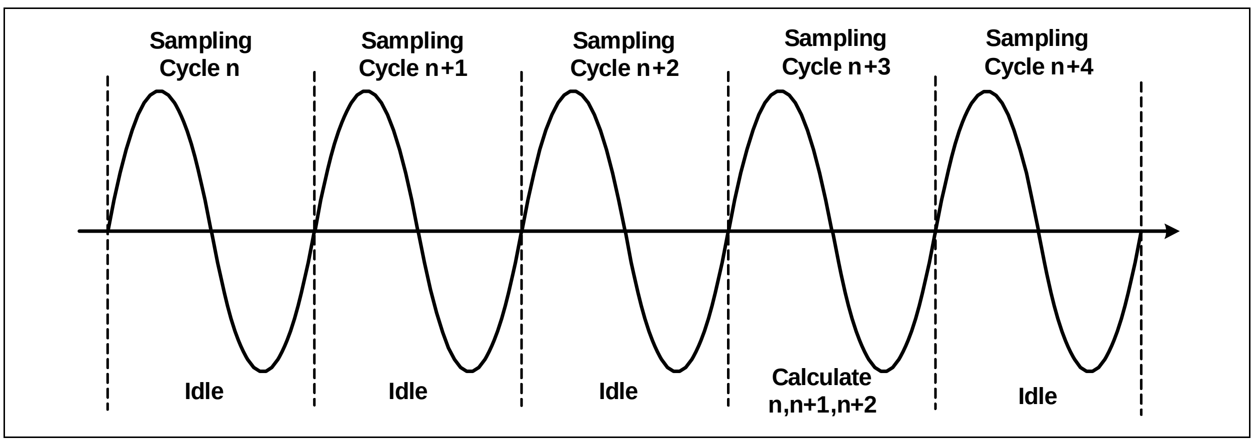


***FIGURE 3-3:*** *AC Signal Sampling alnd Computing.*

### 3.4.1 Processing IC1 Interrupt

Input capture IC1 is used to detect if the A/D conversion is complete. After each conversion, a positive pulse the width of 4 clock cycles is outputted by the SDO pin of the MCP3909 device. IC1 is used to detect the falling edge of the pulse and generate an interrupt for every 2 falling edges, i.e., 1 data is read for every 2 conversions, thus realizing 6.4 ksps sampling rate.

In addition to reading the data of the MCP3909 device, the IC1 interrupt service routine (ISR) also controls the energy pulse output generation. Energy pulse processing consists of active/reactive energy pulse processing. For the pulses to be outputted more uniformly, the clock resolution used to generate the pulses must be as high as possible. The interval of the IC1 interrupt is 156.25 µs, therefore, the resolution generated by the pulse can be up to 156.25 µs.

The energy pulse processing program only begins when the level is close to outputting pulse level. To simplify the process and shorten the ISR execution time, a counter is used in place of the energy accumulation function for each pulse and to determine if a pulse will be outputted. When the count is greater than the threshold of pulse output, an energy pulse will be outputted, and the appropriate amount of energy will be subtracted from the energy accumulating register. Output toggling will then be processed. Once the width of the output pulse exceeds 80 ms, the pulse output will be turned off.

The program flow chart is shown in Figure 3-4.

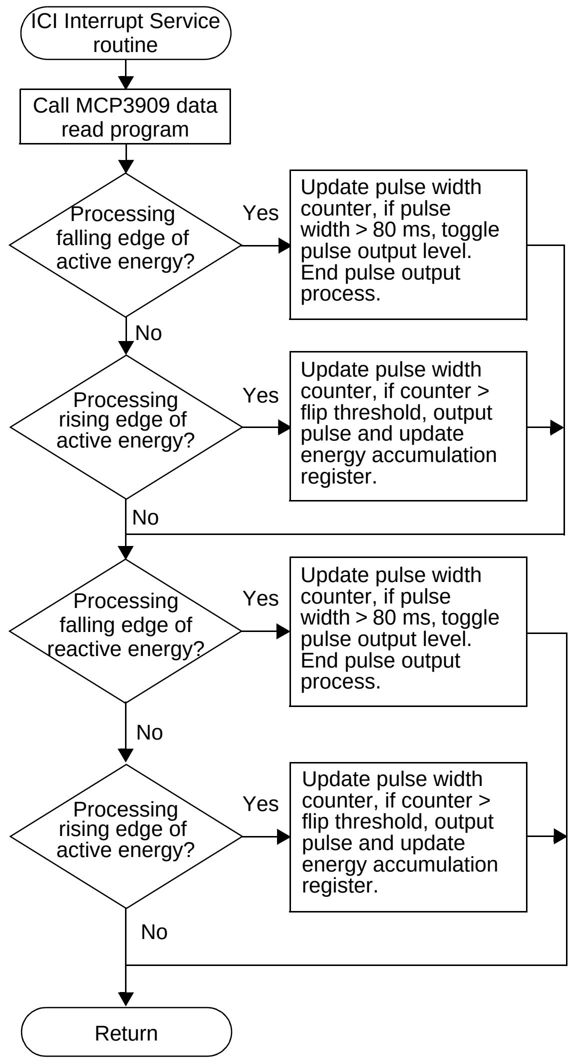


***FIGURE 3-4:*** *IC1 Interrupt Service Routine.*

## 3.5 READING A/D DATA OF THE MCP3909 DEVICE

All three MCP3909 devices use the same clock source and reset signal, so all 6 A/D channels of the 3 MCP3909 devices are synchronous. Only a single Data Ready (SDO) signal of any of the MCP3909 device is required to read A/D data of the 3 phases in turn. This module is invoked by IC1 interrupt triggered by the "data ready" signal on the SDO of the MCP3909 device. IC1 is set to generate an interrupt for every two falling edges. Therefore, only one of the two sampling data of the MCP3909 device is read.The flow of reading the MCP3909 device's data is as follows:

- Retrieve all values of 3-phases, both current channel and voltage channel data. Bits 0-15 of each phase data are voltage channel data, bits 16-31 are current channel data
- Accumulate the active power of each phase. On every other interrupt, the current and voltage values are stored into RAM in the cyclic sampling array
- Update the pointer of sampling array and length of sampling data. If the length of sampling data is 3-line cycles long, set the sampling complete flag, and then the calculation function ***Calculate***() will be called by the main flow to start computing all corresponding parameters.

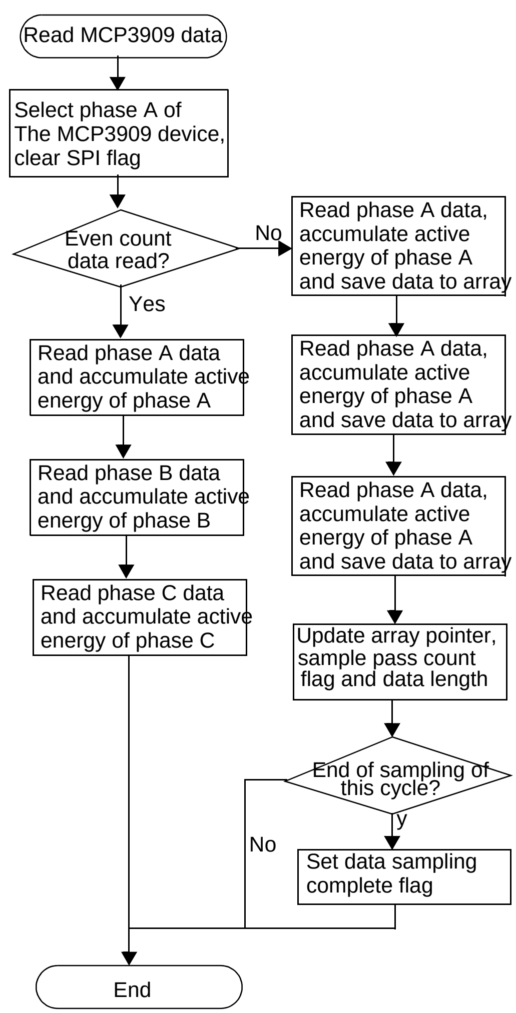


***FIGURE 3-5:*** *Flow Chart of Read A/D Data.*

### 3.5.1 Initialize and Configure MCP3909 Operation Mode

The task of this module is to enable the MCP3909 device to enter the "Channel Output" mode. This design uses the "Channel Output" mode of the MCP3909 device. In this mode, the current and voltage data channels measured by the ADC is sent through the MCP3909 device's SPI port. To enable the MCP3909 device to enter the Channel Output mode, certain instructions must be sent to the device via the SPI interface within a specified time (32CLK) after resetting the MCP3909 device.

- Enable all MCP3909 devices: enable ADCS1, ADCS2 and ADCS3, and configure MCU's SPI to 8-bit mode
- Reset the MCP3909 device through the RESET pin. The pin must be pulled low for no less than 1 clock cycle of the MCP3909 device
- After the RESET pin is pulled high, wait for 4 clock cycles for the MCP3909 device pin functions to reset
- Send Instruction 0x94 to the MCP3909 device through the SPI Interface
- Configure the SPI interface to 16-bit mode and strobe the MCP3909 device for Phase A

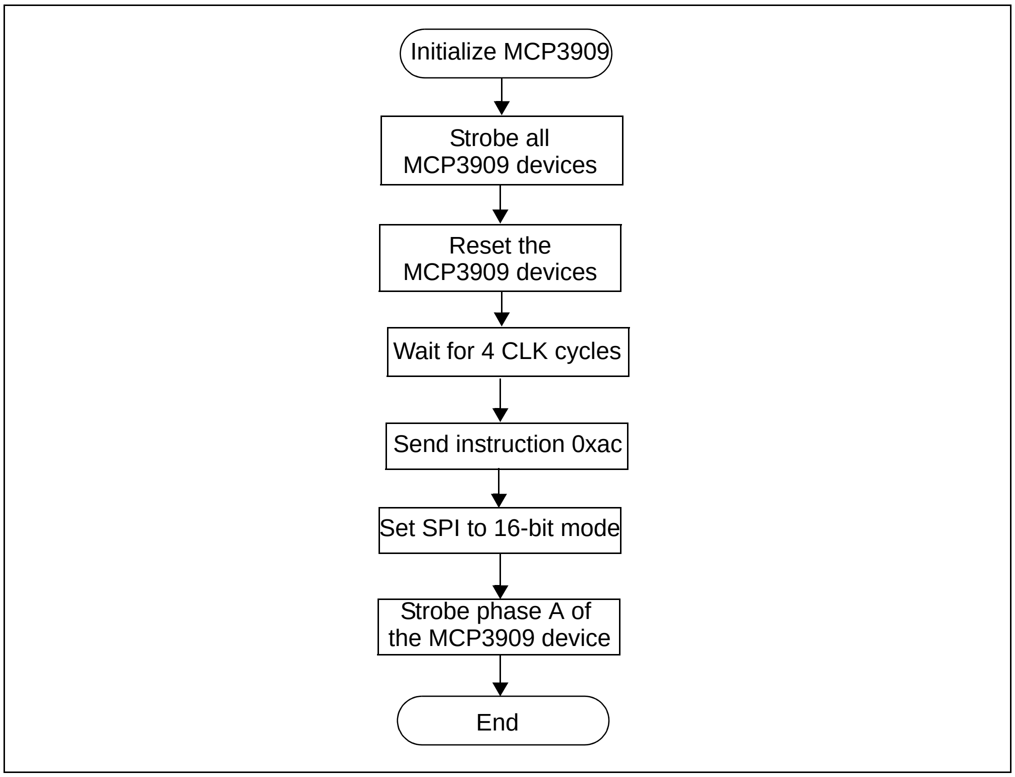


***FIGURE 3-6:*** *Initializing the MCP3909 Device Flow Chart.*

 

## 3.6 COMMUNICATION OF UART INTERFACE

The UART interface is used to communicate with the upper computer (MCU or PC). Via the UART interface, the upper computer reads the measured parameters of the power grid, and may also send system parameters and calibration parameters to the target board as well.

The communication interface is a bidirectional interface based on UART, using master/slave half-duplex mode. The baud rate is 19,200 bps, with 1 start bit, 8 data bits and 1 stop bit. Communication is done by frames with non-fixed-length frame structure, definition of which is shown in Table 3-1. The Communication protocol is specified in a master-slave structure. The system in this design is the slave, and the upper computer is the master. The master sends commands to the slave, and slave responds to the master.

Each command is defined in **Chapter 6. "Meter Communications Protocol"**.

**TABLE 3-1: FRAME STRUCTURE OF COMMUNICATION PROTOCOL**

| Sync Field | Command Type | Data Length | Data Field | Checkout Byte | End Byte |
|---|---|---|---|---|---|
| 2 bytes | 1 byte | 1 byte | N bytes | 1 byte | 1 byte |

## 3.7 RESOURCE CONFIGURATION

Details of the MCU resources used in this design and their configurations are listed in Table 3-2.

**TABLE 3-2: CONFIGURATION OF MCU RESOURCES**

| Resource Name | | Interrupt Priority | Functional Description |
|---|---|---|---|
| System Clock | | | Fcy = 29.4912M, provided by an external 7.3728 Mz timer through an internal PLL frequency doubler. |
| Timer | Timer2 | 1 | System clock, used for timing. Its cycle is 10 ms. The interrupt flag may be set in the IRS. Used to extend the indication of timer. Also used to deal with UART reception overtime. |
| | Timer3 | none | Used to detect ADC's sampling synchronization of neutral current. After the frequency of the power grid is measured, the period of TMR3 is adjusted accordingly. 16 points are sampled by ADC for each cycle of power grid. |
| Interrupt | TMR2 | 1 | ditto |
| | IC1 | 5 | Driven by a 3.2768 MHz clock. The MCP3909 device can generate 12.8 ksps of data output.<br>Sampling input capture. An interrupt is generated for every two MCP3909 device samplings. 6.4 ksps sampling rate is realized.<br>In fact, active power is cumulated at 6.4 ksps sampling rate (128 sampling points each cycle at 50 Hz), but other parameters are cumulated at 3.2 ksps sampling rate |
| | UART RX | 2 | Receive data of UART communication |
| | UART TX | 2 | Transmit data of UART communication |
| | ADC | 2 | Detect current of neutral line |
| SPI2 | | none | Used in communicating with the MCP390X device - set the MCP390X device's modes and read A/D results |
| SPI1 | | none | Unused, but the interface is reserved and may be used to communicate with upper computer in substitution of the UART interface |

## 3.8 DESCRIPTION OF PROJECT FILES

**TABLE 3-3: FILE DESCRIPTION**

| File Name | Description |
|---|---|
| main.h<br>main.c | Main program |
| global.h<br>global.c | Mainly define important system macros, key data structures, and declare global variables. |
| MCP390x.h | Declare macros, constants, local global variables, some of the global variables and functions used in the MCP390X device. |
| MCP390x.c | Functions involved with the MCP390X device, including set SPI, initialize the MCP390X device and read data. |
| calcu.h | Declare macros, constants, local global variables, some of the global variables and functions used in calcu.c. |
| calcu.c | Main module to calculate parameters, including calculate frequencies, current/voltage RMS, power, power factors and energy, and analyze harmonics. |
| uart_comm.c | Declare macros, constants, local global variables, some of the global variables and functions used in uart.c. |
| uart.c | Receive, transmit, process protocol and so forth for UART communication. |
| Calibrate.c | Program for Ratio error calibration, power calibration and phase lag calibration, it stores and initializes calibration data. |
| Calibrate.h | Declare constants, local variables and global variables used in calibration. |
| Adc.c<br>Adc.h | On-chip ADC operation, detecting the current of neutral wire. |
| I2Csubs.h<br>I2Csubs.c | Control EEPROM of off-chip $I^2C$ interface. |
| interrupt.h | Declare macros, constants, local global variables, some of the global variables and functions used in interrupt.c. |
| interrupt.c | Set interrupts and ISRs. |
| Asmcode.c | Some assemble functions used in calculation. |

# Chapter 4. Meter Calibration

## 4.1 INTRODUCTION

Meter calibration consists of using standard electrical power equipment that supplies the power to the meter and calculates the error and correction factor at each calibration point. This equipment must be accurate in order to calibrate the energy meter. The supplied PC software is then used to send calibration commands and correction factors down to the dsPIC33F, completing meter calibration.

### Why Is Calibration Necessary?

An energy meter usually consists of errors due to transformers, $V_{REF}$ tolerance, ADC gain errors, and other passive component errors. Energy meters are factory calibrated before shipping to eliminate the impact from such elements and reduce the error. The non-linearity and inconsistency of signals in the path of sampling circuit and A/D conversion circuit cannot be ignored in high-accuracy measurement. The impact needs to be corrected to improve measurement accuracy.

The calibration described in this chapter are calibrated with the help of the PC software PM_Viewer, described in detail in the next chapter. To summarize the process, the measurement error is fed into the software, and the data is then sent to the meter to via the UART. The details of this procedure are detailed in the next chapter, "PC Software".

## 4.2 CURRENT/VOLTAGE CALIBRATION

Current and voltage calibration is a ratio error calibration from the upper computer by sending commands and data for correction to the MCU. The dsPIC33F will call a firmware module after receiving the command from the host PC. The flow is as follows:

1. Determine the phase to be calibrated and the magnitude of current and voltage being applied to the meter, and read measurement (RMS) values of that channel.
2. Calculate the calibration coefficient of the ratio error by the ratio of standard value received to the measured value.
3. Multiply the original coefficient by calibration coefficient and obtain the calibration coefficient after correction.
4. Store the final calibration coefficient after correction into EEPROM.

| | |
|---|---|
| **Note:** | Voltage and current calibration is a two step process using 100% and 10% $I_B$. |

Since the dynamic range of the voltage channel is usually very small, single-point calibration is enough to meet the accuracy requirements for full range. However, the dynamic range of the current channel is larger, and the transformer has different ratio errors at different current loads.

The MCP3909 device’s current channel, CH0, contains a PGA with gain options of 1, 2, 8, 16. For high-accuracy energy meters, current ratio error needs to be segmented and calibrated for different current loads. The ratio error calibration of current channel uses a two-point calibration method. One point is calibrated when the load is at the rated current ($I_B$) and the PGA gain is 1. The second point is calibrated under small-signal input condition (0.1 $I_B$) and the PGA gain is 16.

 

### 4.2.1 Current/Voltage Calibration Process

The process of calibration is as follows:

1. Supply the meter with balanced load, PF = 1.0, $V_{CAL}$ = 220V, $I_B$ = 5A.
2. Load the dsPIC33F with the proper correction factors. Automatically done using the PC software. See **Chapter 5. "PC Software"**.

Repeat these following steps for the second point at 10% IB:

1. Set the three-phase balance input conditions PF = 1.0, $V_{CAL}$ = 220V, $I_{CAL}$ = 0.1 $I_B$ or 500 mA.
2. Load the dsPIC33F with the proper correction factors. Automatically done using the PC software. See **Chapter 5. "PC Software"**.

If accuracy is not critical, the single-point calibration method can be used. The number of calibration points can be defined in the header file of the program.

## 4.3 APPARENT POWER CALIBRATION

Apparent Power calibration function is implemented by the upper computer by sending the commands. Before the power calibration process can be entered, power calibration mode command needs to be sent first. The error data of the calibration workbench and channel information to be calibrated are sent to the metering front-end. When the front-end receives the command, it calls this module. The flow is as follows:

1. Determine the phase to be calibrated according to the parameters received.
2. Calculate new power calibration coefficient according to the error value received and the measured value, together with the original power calibration coefficient.
3. Store the coefficient after correction into the EEPROM.

### 4.3.1 Apparent Power Calibration Process

The process of calibration is as follows:

1. Set the input condition as: Phase A PF = 1.0, $V_{CAL}$ = 220V, input current is the current when region N is being calibrated, the voltage and current inputs of phase B and C are zero.
2. Choose the energy pulse output to be the apparent power output mode Refer to **Chapter 6. "Meter Communications Protocol"**. At this time, the energy pulse is the accumulated multiplication of power and time.
3. Load the dsPIC33F with the proper correction factors. This is automatically done using PC software. See **Chapter 5. "PC Software"**.
4. Repeat steps 1 - 3 for phase lag calibrations for all current regions of phase A.

> **Note:** At this time, the phase lag has not been calibrated, so when the input PF = 1.0, the measured value of the reactive power isn't equal to zero.

5. Repeat the above steps for Phases B and C.

 

## 4.4 PHASE LAG CALIBRATION

The phase lag calibration function is implemented by the upper computer by sending the proper commands via the UART. When calibrating phase lag, error from the calibration equipment and channel information to be adjusted are sent to the dsPIC33F energy meter. When the front-end receives the command, it calls this module. The flow is as follows:

1. Determine the phase to be calibrated according to parameters received.
2. Calculate new phase lag calibration coef. according to the error value received and the measured value.
3. Store the coefficient after correction into the EEPROM.

This meter design supports single, two, and five point calibration for phase lag error correction.

The purpose of phase lag calibration is to eliminate the impact of phase lag introduced by the current transformer (CT), and voltage transformer (PT) over the power measurement range.

The voltage transformer usually has a constant load, thereby introducing a phase lag that varies insignificantly. The dynamic range of current is larger, and under different current loads, phase lags caused by CT vary greatly. In order to meet the requirements of measurement accuracy in the entire range, it is usually necessary to segment the phase lag and calibrate.

In this design, current is partitioned into 5 regions.

**TABLE 4-1: CURRENT REGIONS FOR PHASE CALIBRATION**

| Region | Current Range |
|---|---|
| 1 | 0 - 0.075 $I_B$ |
| 2 | 0.075 $I_B$ - 0.2 $I_B$ |
| 3 | 0.2 $I_B$ - 0.75 $I_B$ |
| 4 | 0.75 $I_B$ -1.5 $I_B$ |
| 5 | 1.5 $I_B$ - 4.0 $I_B$ |

The partition limit for the current region can be modified in the header file of the program. If accuracy is not critical, single-point calibration and two-point calibration can be used to improve the efficiency of meter calibration.

### Single, Two, or Five Point Calibration

Single-, two- or five-point calibration method can be configured by modifying the header file. When using the single-point calibration, the phase lag compensation values of all regions are the same; When using two-point calibration, the compensation values of region 1 and 2 (0-0.075 $I_B$, 0.075 $I_B$ - 0.2 $I_B$) are the same, and the phase lag compensation values for region 3, 4 and 5 (0.2 $I_B$ - 0.75 $I_B$, 0.75 $I_B$ - 1.5 $I_B$, 1.5 $I_B$ - 4.0 $I_B$) are the same.

### 4.4.1 Phase Lag Calibration Process

The process of phase calibration is as follow:

1. Setup input condition: Phase A, voltage input 220V, current input is the current for region 1, voltage and current inputs of phase B and phase C are zero.
2. Load the dsPIC33F with the proper correction factors. This is automatically done using the PC software. See **Chapter 5. "PC Software"**.
3. Repeat steps 1 and 2 for phase lag calibrations for all current regions of phase A.

> **Note:** If the power metering error still can not meet the requirement, the meter can be calibrated a few more times. When doing so, simply input a new error value into the front-end of the meter.

4. Repeat for Phases B & C.

# Chapter 5. PC Software

## 5.1 OVERVIEW AND INSTALLATION

The PC software “PM_Viewer” or “Power Meter Viewer” has two main functions: view the calculated parameters and calibrate the meter. The PC software has seven output display screens, or “work modes”, selected from the toolbar pull-down menu.

- Basic Parameters
- Phase A Harmonic
- Phase B Harmonic
- Phase C Harmonic
- Distortion Rate
- Harmonic Power
- Energy Accumulation

In addition, the PC software has four calibration screens, selected from the toolbar pull-down menu.

- Reset All Calibration
- Linearity Calibration
- Apparent Power Calibration
- Phase Lag Calibration

### 5.1.1 System Required

- HDD space > 25 MB
- Microsoft Windows OS98 or later
- Hardware COM interface

### 5.1.2 Installation

1. Unzip PM_Viewer setup.zip.
2. Double click on setup.exe.
3. Finish the installation according the prompt.
4. To PM_Viewer.exe - Start -> Program -> Energy Meter ->PM_Viewer.exe.

## 5.2 ESTABLISH COMMUNICATION

1. Open PM_Viewer.
2. Click on Comm Port selection, and select the com port (com1, com2, or com3) that you will use on the menu, noting the baud rate is 19200 bps in 1-8-1 format, and can not be changed.
3. Click on the Link to establish communication with the demo. “Communication OK!” will be displayed on the bottom, if communication is established.

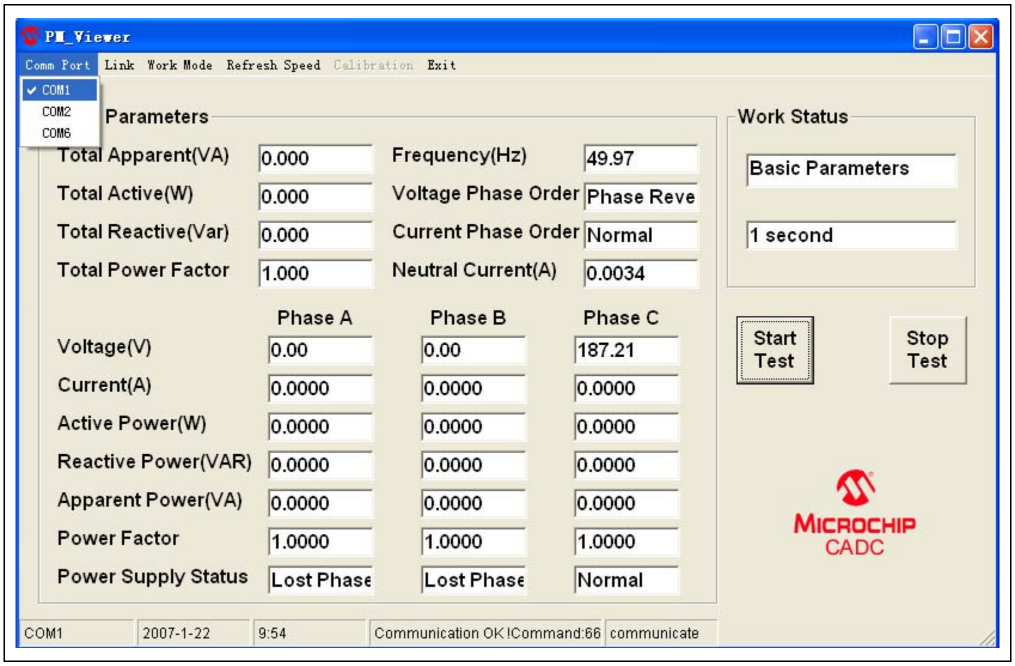


*FIGURE 5-1: Establising Communications.*

## 5.3 BASIC PARAMETERS OUTPUT SCREEN

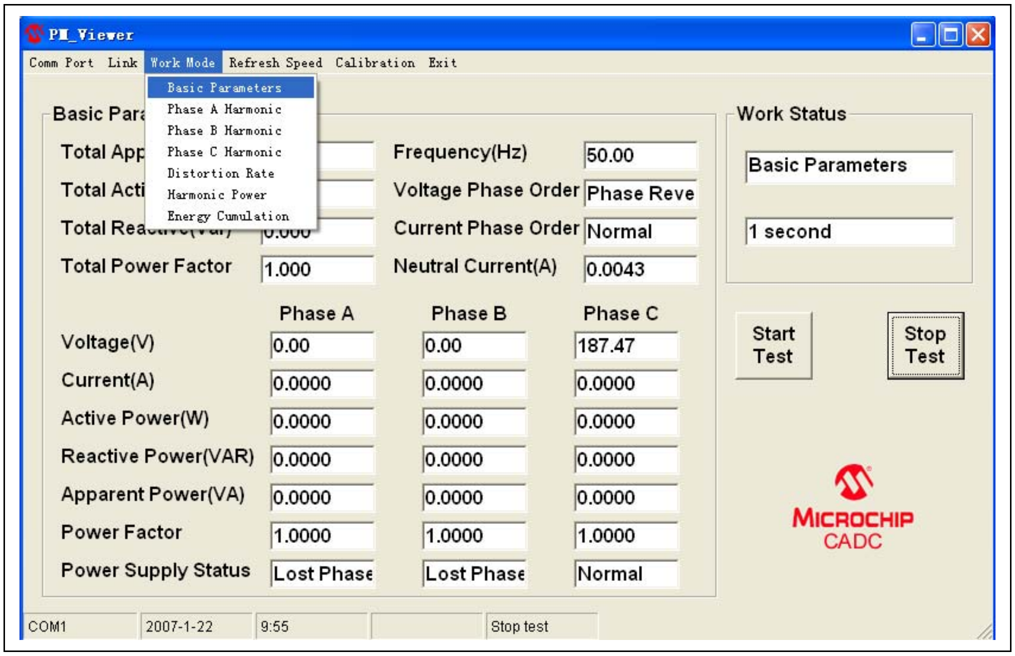


***FIGURE 5-2:*** *Basic Parameters Work Mode Screen.*

## 5.4 PHASE A/B/C HARMONIC OUTPUT SCREEN

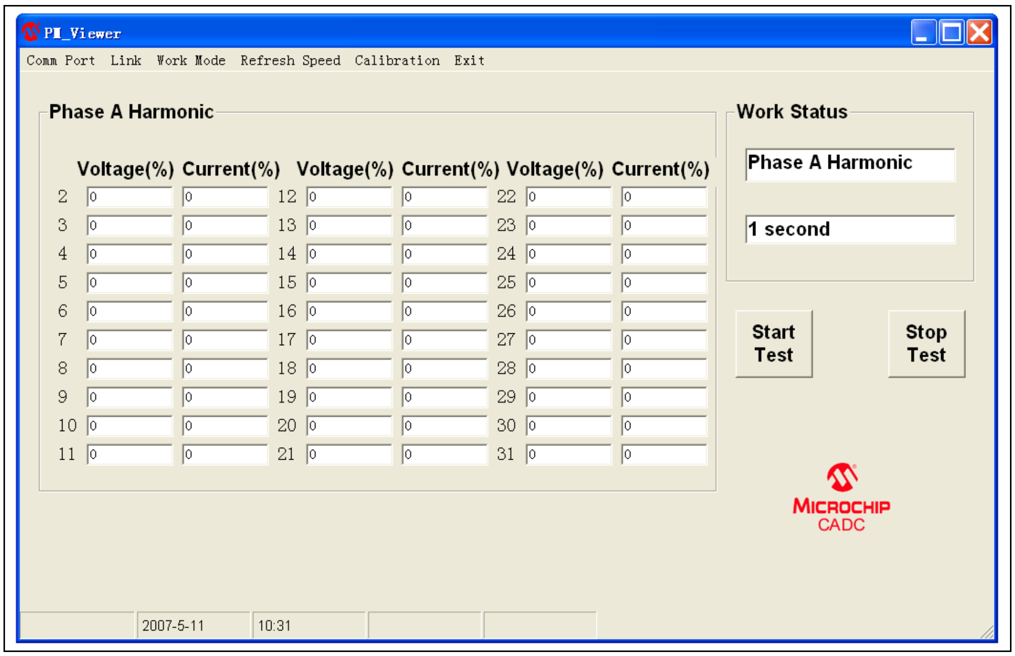


***FIGURE 5-3:*** *Phase N Harmonic Work Mode Screen.*

## 5.5 DISTORTION RATE

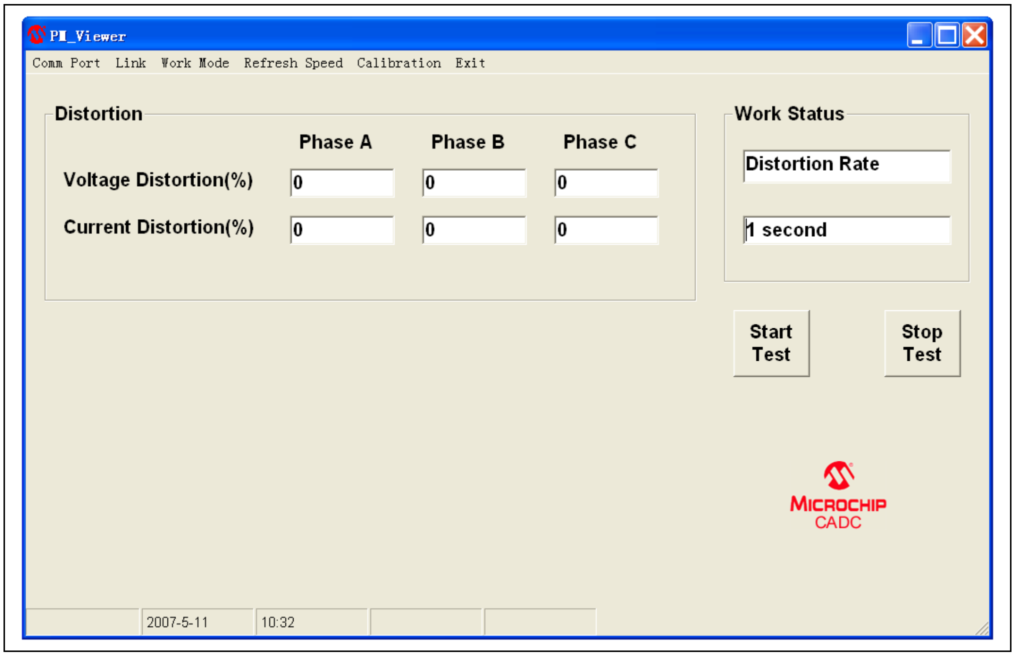


*FIGURE 5-4: Distortion Mode Screen.*

## 5.6 HARMONIC POWER

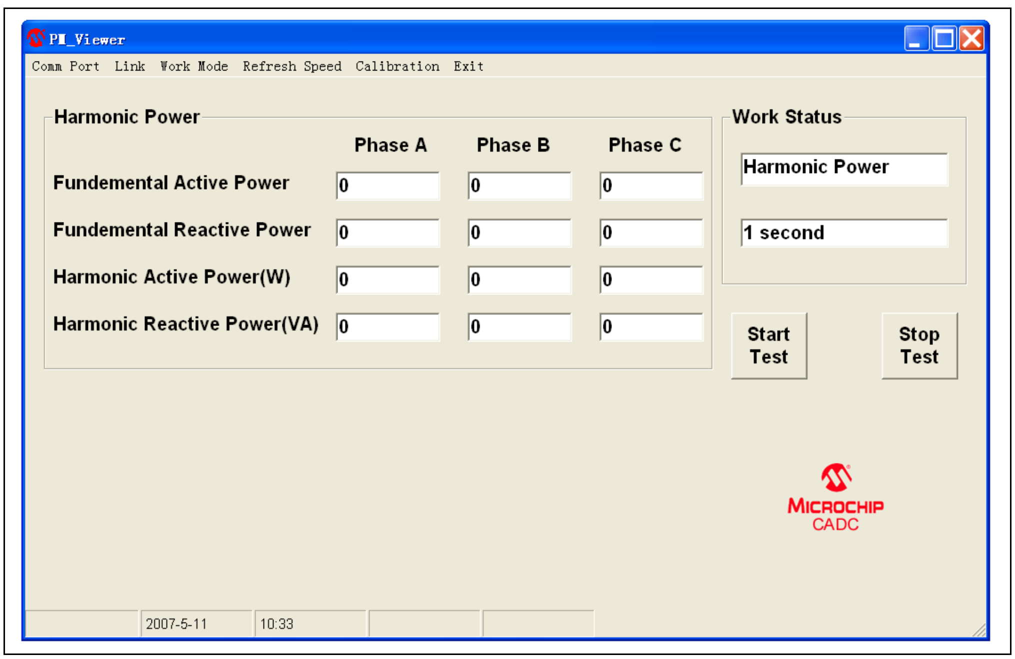


*FIGURE 5-5: Harmonic Power Work Mode Screen.*

## 5.7 ENERGY ACCUMULATION

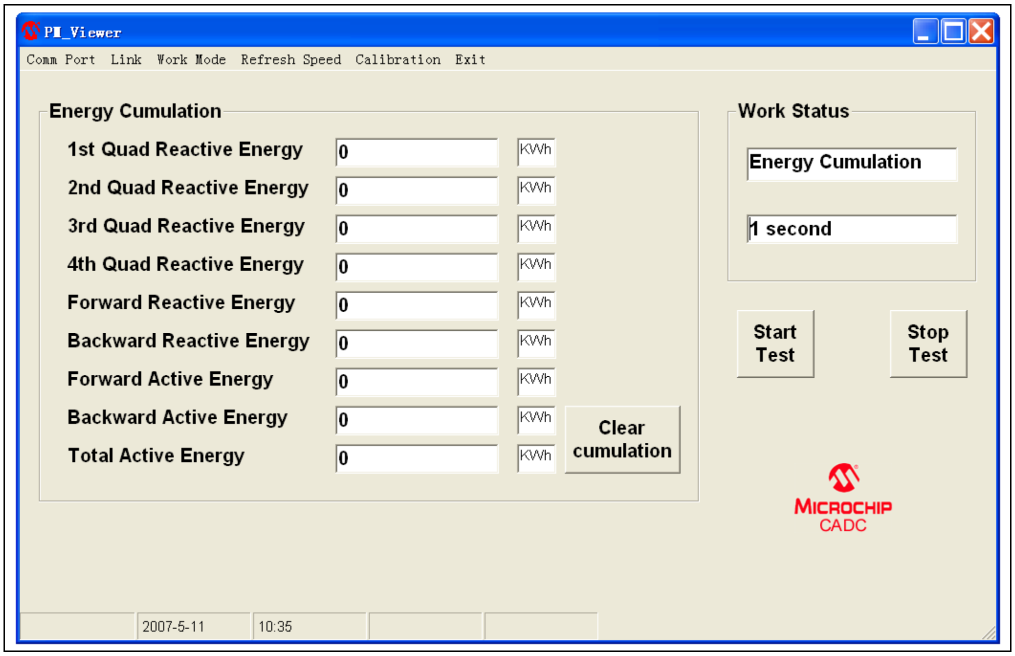


*FIGURE 5-6: Energy Accumulation Work Mode Screen.*

## 5.8 CALIBRATION STEP 1 - RESET ALL CALIBRATION

1. Select **Reset All Calibration** from the toolbar menu.
2. Meter Calibration Values are Reset.

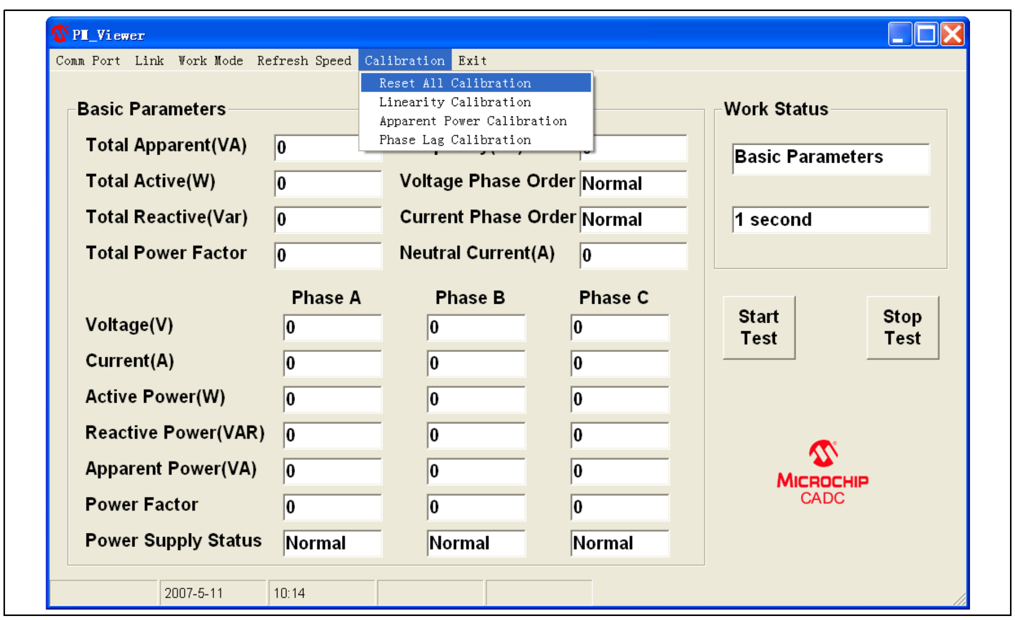


*FIGURE 5-7: Reset All Calibration Command.*

## 5.9 LINEARITY CALIBRATION

1. Select **Channel**, either **Voltage** or **Current**.
2. Select **Phase A**, **B** or **C**.
3. Select **Region**, either **100%** or **10%**.
4. Using a standard meter, supply the input conditions given here.
5. Enter the error recorded from the standard meter here.
6. Click the **Set** button.

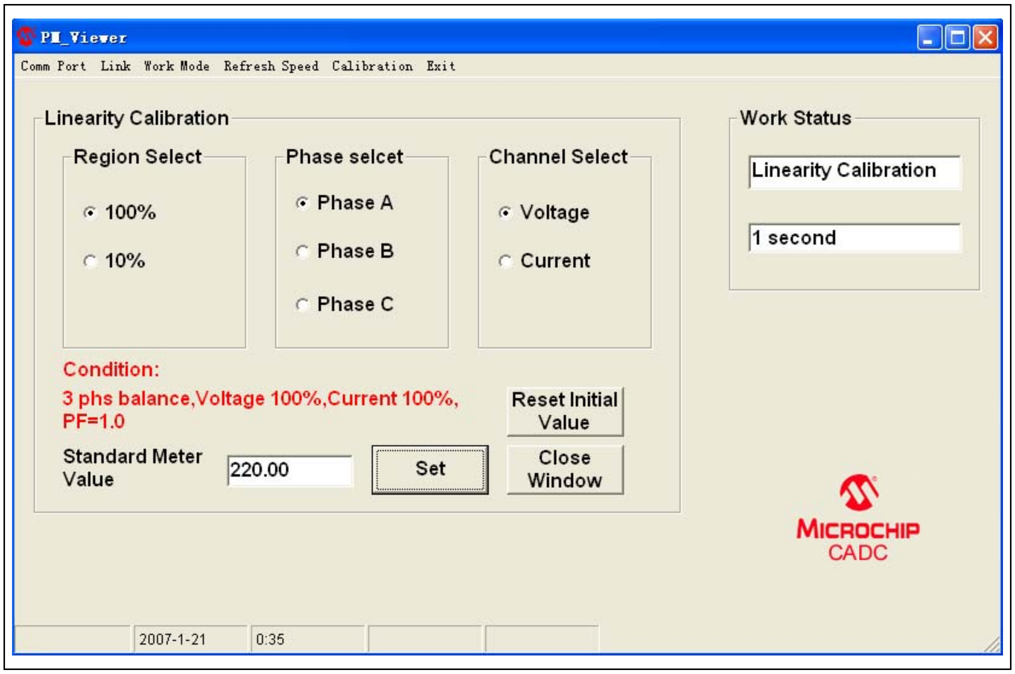


 

## 5.10 APPARENT POWER CALIBRATION

1. Select **Phase A**, **B** or **C**.
2. Select **Region n**.
3. Using a standard meter, supply the input conditions given here.
4. Click the **Set Apparent** button.
5. Enter the error recorded from the standard meter here.
6. Click the **Set** button.
7. Repeat steps 2-5 for the different regions.
8. Repeat for other 2 phases.

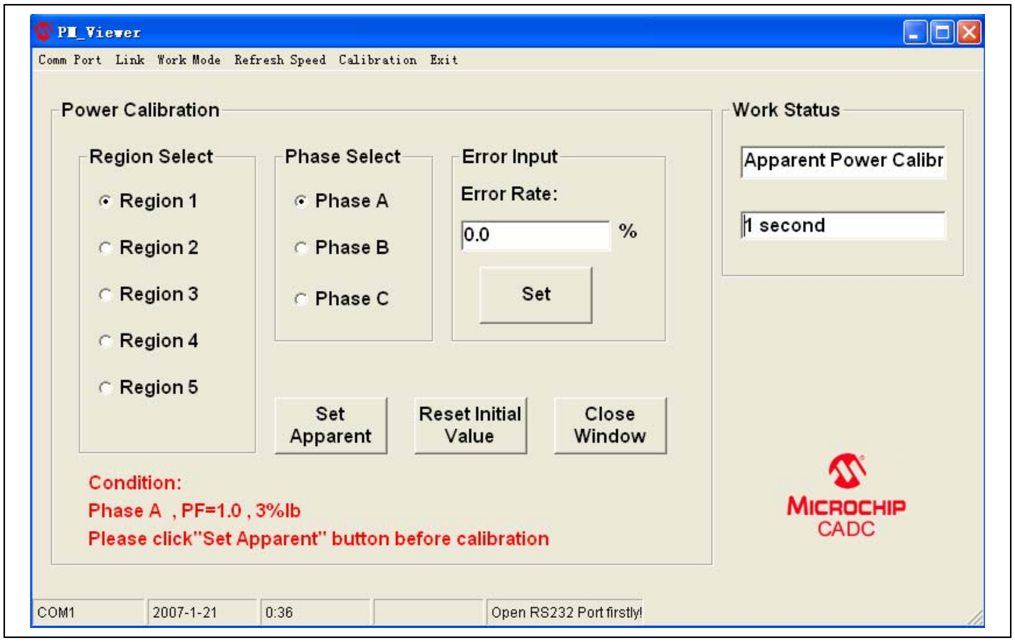

## 5.11 PHASE LAG CALIBRATION

1. Select **Phase A**, **B** or **C**.
2. Select **Region n**.
3. Using a standard meter, supply the input conditions given here.
4. Enter the error recorded from the standard meter here.
5. Click the **Set** button.
6. Repeat steps 2-5 for the different regions.
7. Repeat for other 2 phases.

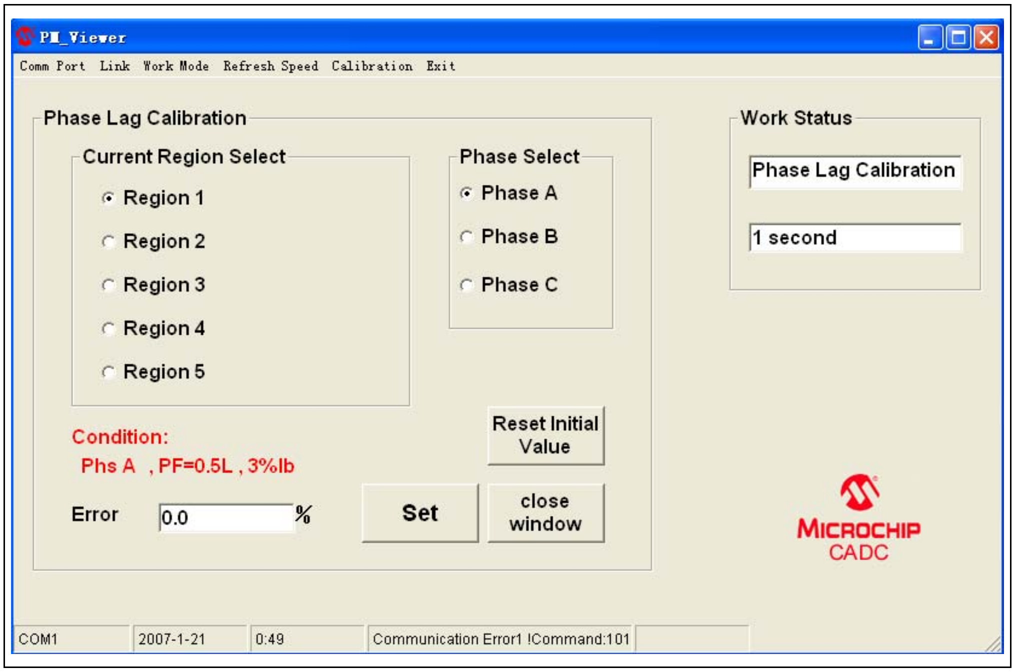

# Chapter 6. Meter Communications Protocol

## 6.1 INTRODUCTION

The UART interface is used to communicate with the upper computer (MCU or PC). Via the UART interface, the upper computer reads the measured parameters of the power grid, and may also send system parameters and calibration parameters to target board as well.

The communication interface is a bidirectional interface based on UART, using master/slave half-duplex mode. The baud rate is 19,200 bps, with 1 start bit, 8 data bits and 1 stop bit. Communication is done by frames with non-fixed-length frame structure, definition of which is shonw in Table 6-1. Communication protocol is specified in master-slave structure. The system in this design is the slave, and the upper computer is the master. The master sends commands to the slave, and the slave responds to the master.

UART communication uses half-duplex mode. The data format is 8-1-1 and the rate is 19,200 bps. The PC is the host computer, and the target board is the slave.

There are 14 command strings that the meter uses. These command strings are defined in Table 6-1

**TABLE 6-1: COMMAND STRINGS**

| Command Description | Command |
|---|---|
| Test Connection | 0x41 |
| Total Data Request | 0x42 |
| Harmonic Content, Phase A | 0x43 |
| Harmonic Content, Phase B | 0x44 |
| Harmonic Content, Phase C | 0x45 |
| Total Harmonic Distortion | 0x46 |
| Energy | 0x47 |
| Stop Energy Measurement and Clear Energy Values | 0x48 |
| Harmonic Power | 0x49 |
| Write Calibration Values to Meter | 0x62 |
| Write Phase Lag Calibration Values to Meter | 0x63 |
| Write Power Calibration Values to Meter | 0x64 |
| Write Energy Pulse Configuration - Active/Apparent | 0x65 |
| Reset All Calibration Values | 0x66 |
| Write Energy Pulse Constant | 0x67 |

 

Variant-length frame structure is used and data communiate in bytes. The command protocol structure is defined as following.

**TABLE 6-2: TYPICAL PROTOTOL**

| START | Command | Data Length | Data Field | Check Sum | STOP |
|---|---|---|---|---|---|
| 2 Bytes | 1 Bytes | 1 Byte | N Bytes | 1 Byte | 1 Byte |

- The START word has 2 bytes, which are 0x00, 0xFF ( PC to target board) or 0xFF, 0x00 (target board to PC)
- Command word is 1 byte which indicates the type of the command
- Data length word is 1 byte that indicates the length of data field
- The data field word has multiple byte(s) that varies with command types
- Checksum word is a single byte, whose content equals to the XOR value of all bytes sent before it
- Stop word is 1 byte with the content of 0xE0

## 6.2 TEST CONNECTION COMMAND

This command is sent from the PC to the meter to setup and test the connection.

**TABLE 6-3: PC TO METER (7 BYTES)**

| START | Command | Data Length | Data Field | Check Sum | STOP |
|---|---|---|---|---|---|
| 0xFF, 0x00 | 0x41 | 0x00 | 0x00 | XX | 0xE0 |

**TABLE 6-4: METER RESPONSE (8 BYTES)**

| START | Command | Data Length | Data Field | Check Sum | STOP |
|---|---|---|---|---|---|
| 0xFF, 0x00 | 0x42 | 0x02 | 0xA5, 0X5A | XX | 0xE0 |

## 6.3 TOTAL DATA REQUEST

This is the main command retrieves all the calcuated data from the dsPIC33F. This command gathers data from all 3 phases including total energy, power, and power factor data.

**TABLE 6-5: PC TO METER (7 BYTES)**

| START | Command | Data Length | Data Field | Check Sum | STOP |
|---|---|---|---|---|---|
| 0xFF, 0x00 | 0x42 | 0x00 | 0x00 | XX | 0xE0 |

**TABLE 6-6: METER RESPONSE (104 BYTES)**

| START | Command | Data Length | Data Field | Check Sum | STOP |
|---|---|---|---|---|---|
| 0xFF, 0x00 | 0x43 | 0x62 | 98 bytes | XX | 0xE0 |

**TABLE 6-7: METER RESPONSE, TOTAL REQUEST FRAME, DETAILED DESCRIPTION**

| Data Field Byte | Name | Value |
|---|---|---|
| 1,2 | Status | See Definition Below |
| 3-6 | Frequency | Float, 4 Bytes Total |
| 7-10 | Phase A Voltage | Float, 4 Bytes Total |
| | Phase B Voltage | Float, 4 Bytes Total |
| | Phase C Voltage | Float, 4 Bytes Total |
| | Phase A Current | Float, 4 Bytes Total |
| | Phase B Current | Float, 4 Bytes Total |
| | Phase C Current | Float, 4 Bytes Total |
| | Neutral Current | Float, 4 Bytes Total |
| | Active Power, Phase A | Float, 4 Bytes Total |
| | Reactive Power, Phase A | Float, 4 Bytes Total |
| | Apparent Power, Phase A | Float, 4 Bytes Total |
| | Power Factor, Phase A | Float, 4 Bytes Total |
| | Active Power, Phase B | Float, 4 Bytes Total |
| | Reactive Power, Phase B | Float, 4 Bytes Total |
| | Apparent Power, Phase B | Float, 4 Bytes Total |
| | Power Factor, Phase B | Float, 4 Bytes Total |
| | Active Power, Phase C | Float, 4 Bytes Total |
| | Reactive Power, Phase C | Float, 4 Bytes Total |
| | Apparent Power, Phase C | Float, 4 Bytes Total |
| | Power Factor, Phase C | Float, 4 Bytes Total |
| | Total Active Power | Float, 4 Bytes Total |
| | Total Reactive Power | Float, 4 Bytes Total |
| | Total Apparent Power | Float, 4 Bytes Total |
| 94-98 | Total Power Factor | Float, 4 Bytes Total |

## 6.4 STATUS REGISTER

This register contains the gain register.

**REGISTER 6-1: STATUS REGISTER**

| R-0 | R-0 | R-0 | R-0 | R-0 | R-0 | R-0 | R-0 |
|---|---|---|---|---|---|---|---|
| CPO | VPO | PHC_S1 | PHC_S0 | PHB_S1 | PHB_S0 | PHA_S1 | PHA_S0 |
| bit 7 | | | | | | | bit 0 |

| **Legend:** | | | |
|---|---|---|---|
| R = Readable bit | W = Writable bit | U = Unimplemented bit, read as ‘0’ | |
| -n = Value at POR | ‘1’ = Bit is set | ‘0’ = Bit is cleared | x = Bit is unknown |

bit 7 **CPO:** Current Phase Order
- `1` = Problem Detected
- `0` = Normal

bit 6 **VPO:** Voltage Phase Order
- `1` = Problem Detected
- `0` = Normal

bit 5:4 **PHC_S:** Phase C Status
- `11` = High Votage
- `10` = No Input
- `01` = Low Voltage
- `00` = Normal

bit 3:2 **PHB_S:** Phase C Status
- `11` = High Votage
- `10` = No Input
- `01` = Low Voltage
- `00` = Normal

bit 1:0 **PHA_S:** Phase C Status
- `11` = High Votage
- `10` = No Input
- `01` = Low Voltage
- `00` = Normal

## 6.5 HARMONIC CONTENT COMMAND

**TABLE 6-8: PC TO METER (7 BYTES)**

| START | Command | Data Length | Data Field | Check Sum | STOP |
|---|---|---|---|---|---|
| 0xFF, 0x00 | 0x43 | 0x00 | 0x00 | XX | 0xE0 |

**TABLE 6-9: METER RESPONSE (134 BYTES)**

| START | Command | Data Length | Data Field | Check Sum | STOP |
|---|---|---|---|---|---|
| 0xFF, 0x00 | 0x44 | 0x80 | 128 bytes | XX | 0xE0 |

**TABLE 6-10: HARMONIC ANALYSIS DETAILED DESCRIPTION**

| Data Field Byte | Description | Value |
|---|---|---|
| 1,2 | Fundamential or 1st Harmonic, Voltage Content | Unsigned Int, 2 bytes |
| 3,4 | 2nd Harmonic, Voltage Content | Unsigned Int, 2 bytes |
| 5-56 | 3-31st Harmonic, Voltage Content | Unsigned Int, 2 bytes |
| 57,58 | Total Voltage Harmonic Content (not including Fundamental) | Unsigned Int, 2 bytes, / 1000 * (100%) |
| 59,60 | Fundamential or 1st Harmonic, Current Content | Unsigned Int, 2 bytes |
| 61,62 | 2nd Harmonic, Current Content | Unsigned Int, 2 bytes |
| 63-126 | 3-31st Harmonic, Current Content | Unsigned Int, 2 bytes |
| 127,128 | Total Current Harmonic Content (not including Fundamental) | Unsigned Int, 2 bytes, / 1000 * (100%) |

## 6.6 TOTAL HARMONIC DISTORTION (THD) COMMAND

**TABLE 6-11: PC TO METER (7 BYTES)**

| START | Command | Data Length | Data Field | Check Sum | STOP |
|---|---|---|---|---|---|
| 0xFF, 0x00 | 0x46 | 0x00 | 0x00 | XX | 0xE0 |

**TABLE 6-12: METER RESPONSE (29 BYTES)**

| START | Command | Data Length | Data Field | Check Sum | STOP |
|---|---|---|---|---|---|
| 0xFF, 0x00 | 0x47 | 0x18 | 24 bytes | XX | 0xE0 |

**TABLE 6-13: TOTAL HARMONIC DISTORTION DESCRIPTION**

| Data Field Byte | Description | Value |
|---|---|---|
| 1-4 | Total Harmonic Distortion of Phase A Voltage | Float, 4 Bytes Total |
| 5-8 | Total Harmonic Distortion of Phase B Voltage | Float, 4 Bytes Total |
| 9-12 | Total Harmonic Distortion of Phase C Voltage | Float, 4 Bytes Total |
| 13-16 | Total Harmonic Distortion of Phase A Current | Float, 4 Bytes Total |
| 17-20 | Total Harmonic Distortion of Phase B Current | Float, 4 Bytes Total |
| 21-24 | Total Harmonic Distortion of Phase C Current | Float, 4 Bytes Total |

## 6.7 START ENERGY MEASUREMENT COMMAND

**TABLE 6-14: PC TO METER (7 BYTES)**

| START | Command | Data Length | Data Field | Check Sum | STOP |
|---|---|---|---|---|---|
| 0xFF, 0x00 | 0x47 | 0x00 | 0x00 | XX | 0xE0 |

**TABLE 6-15: METER RESPONSE (42 BYTES)**

| START | Command | Data Length | Data Field | Check Sum | STOP |
|---|---|---|---|---|---|
| 0xFF, 0x00 | 0x48 | 0x24 | 36 bytes | XX | 0xE0 |

**TABLE 6-16: TOTAL HARMONIC DISTORTION DESCRIPTION**

| Data Field Byte | Description | Value |
|---|---|---|
| 1-4 | First quadrant reactive energy | Float, 4 Bytes Total |
| 5-8 | Second quadrant reactive energy | Float, 4 Bytes Total |
| 9-12 | Third quadrant reactive energy | Float, 4 Bytes Total |
| 13-16 | Fouth quadrant reactive energy | Float, 4 Bytes Total |
| 17-20 | Forward Reactive energy | Float, 4 Bytes Total |
| 21-24 | Reverse Reactive Energy | Float, 4 Bytes Total |
| 25-28 | Forward Active Energy | Float, 4 Bytes Total |
| 29-32 | Reverse Active Energy | Float, 4 Bytes Total |
| 33-36 | Reverse Active Energy | Float, 4 Bytes Total |

## 6.8 STOP ENERGY MEASUREMENT COMMAND

**TABLE 6-17: PC TO METER (7 BYTES)**

| START | Command | Data Length | Data Field | Check Sum | STOP |
|---|---|---|---|---|---|
| 0xFF, 0x00 | 0x48 | 0x00 | 0x00 | XX | 0xE0 |

**TABLE 6-18: METER RESPONSE (7 BYTES)**

| START | Command | Data Length | Data Field | Check Sum | STOP |
|---|---|---|---|---|---|
| 0xFF, 0x00 | 0x49 | 0x00 | 0 bytes | XX | 0xE0 |

## 6.9 HARMONIC POWER COMMAND

**TABLE 6-19: PC TO METER (7 BYTES)**

| START | Command | Data Length | Data Field | Check Sum | STOP |
|---|---|---|---|---|---|
| 0xFF, 0x00 | 0x49 | 0x00 | 0x00 | XX | 0xE0 |

**TABLE 6-20: METER RESPONSE (54 BYTES)**

| START | Command | Data Length | Data Field | Check Sum | STOP |
|---|---|---|---|---|---|
| 0xFF, 0x00 | 0x4A | 0x30 | 48 bytes | XX | 0xE0 |

**TABLE 6-21: HARMONIC POWER MEASUREMENTS**

| Data Field Byte | Description | Value |
|---|---|---|
| 1-4 | Fundamental Active Power Of Phase A | Float, 4 Bytes Total |
| 5-8 | Fundamental Reactive Power Of Phase A | Float, 4 Bytes Total |
| 9-12 | Fundamental Active Power Of Phase B | Float, 4 Bytes Total |
| 13-16 | Fundamental Reactive Power Of Phase B | Float, 4 Bytes Total |
| 17-20 | Fundamental Active Power Of Phase C | Float, 4 Bytes Total |
| 21-24 | Fundamental Reactive Power Of Phase C | Float, 4 Bytes Total |
| 25-28 | Harmonic Active Power Of Phase A | Float, 4 Bytes Total |
| 29-32 | Harmonic Reactive Power Of Phase A | Float, 4 Bytes Total |
| 33-36 | Harmonic Active Power Of Phase B | Float, 4 Bytes Total |
| 37-40 | Harmonic Reactive Power Of Phase B | Float, 4 Bytes Total |
| 41-44 | Harmonic Active Power Of Phase C | Float, 4 Bytes Total |
| 45-48 | Harmonic Reactive Power Of Phase C | Float, 4 Bytes Total |

## 6.10 CALIBRATE METER VOLTAGE/CURRENT COMMAND

**TABLE 6-22: PC TO METER (7 BYTES)**

| START | Command | Data Length | Data Field | Check Sum | STOP |
|---|---|---|---|---|---|
| 0xFF, 0x00 | 0x63 | 7 | 0x07 | XX | 0xE0 |

**TABLE 6-23: METER RESPONSE (7 BYTES)**

| START | Command | Data Length | Data Field | Check Sum | STOP |
|---|---|---|---|---|---|
| 0xFF, 0x00 | 0x64 | 0 | 0x00 | XX | 0xE0 |

**TABLE 6-24: CALIBRATION OF GAIN AND OFFSET VALUES**

| Data Field Byte | Description | Value |
|---|---|---|
| 1 | Phase Select | 0x01 = Phase A<br>0x02 = Phase B<br>0x03 = Phase C |
| 2 | Range Select | 0x01 = 10%<br>0x02 = 100% |
| 3 | Channel Select | 0x00 = Current<br>0x01 = Voltage |
| 4-7 | Correction Factor (Error Being Calibrated Out) | Float, 4 Bytes Total |

## 6.11 CALIBRATE PHASE LAG COMMAND

**TABLE 6-25: PC TO METER (12 BYTES)**

| START | Command | Data Length | Data Field | Check Sum | STOP |
|---|---|---|---|---|---|
| 0xFF, 0x00 | 0x63 | 6 | 0x06 | XX | 0xE0 |

**TABLE 6-26: METER RESPONSE (7 BYTES)**

| START | Command | Data Length | Data Field | Check Sum | STOP |
|---|---|---|---|---|---|
| 0xFF, 0x00 | 0x64 | 0 | 0x00 | XX | 0xE0 |

**TABLE 6-27: CALIBRATION OF PHASE LAG**

| Data Field Byte | Description | Value |
|---|---|---|
| 1 | Phase Select | 0x01 = Phase A<br>0x02 = Phase B<br>0x03 = Phase C |
| 2 | Range Select | 1-7 |
| 3-6 | Correction Factor (Error Being Calibrated Out) | Float, 4 Bytes Total |

## 6.12 CALIBRATE APPARENT POWER COMMAND

**TABLE 6-28: PC TO METER (12 BYTES)**

| START | Command | Data Length | Data Field | Check Sum | STOP |
|---|---|---|---|---|---|
| 0xFF, 0x00 | 0x64 | 6 | 0x06 | XX | 0xE0 |

**TABLE 6-29: METER RESPONSE (7 BYTES)**

| START | Command | Data Length | Data Field | Check Sum | STOP |
|---|---|---|---|---|---|
| 0xFF, 0x00 | 0x65 | 0 | 0x00 | XX | 0xE0 |

**TABLE 6-30: CALIBRATION OF POWER**

| Data Field Byte | Description | Value |
|---|---|---|
| 1 | Phase Select | 0x01 = Phase A<br>0x02 = Phase B<br>0x03 = Phase C |
| 2 | Current Range Select | 1-7 |
| 3-6 | Correction Factor (Error Being Calibrated Out) | Float, 4 Bytes Total |

## 6.13 CALIBRATE ENERGY PULSE COMMAND

**TABLE 6-31: PC TO METER (12 BYTES)**

| START | Command | Data Length | Data Field | Check Sum | STOP |
|---|---|---|---|---|---|
| 0xFF, 0x00 | 0x65 | 2 | 0x02 | XX | 0xE0 |

**TABLE 6-32: METER RESPONSE (7 BYTES)**

| START | Command | Data Length | Data Field | Check Sum | STOP |
|---|---|---|---|---|---|
| 0xFF, 0x00 | 0x66 | 0 | 0x00 | XX | 0xE0 |

**TABLE 6-33: CALIBRATION OF POWER**

| Data Field Byte | Description | Value |
|---|---|---|
| 1 | Phase Select | 0x01 = Phase A<br>0x02 = Phase B<br>0x03 = Phase C |
| 2 | Energy Output Mode | 0x00 = Active Power<br>0x01 = Apparent Power |

## 6.14 RESET ALL METER CALIBRATION VALUES COMMAND

**TABLE 6-34: PC TO METER (12 BYTES)**

| START | Command | Data Length | Data Field | Check Sum | STOP |
|---|---|---|---|---|---|
| 0x00, 0xFF | 0x66 | 4 | 0x04 | XX | 0xE0 |

**TABLE 6-35: METER RESPONSE (7 BYTES)**

| START | Command | Data Length | Data Field | Check Sum | STOP |
|---|---|---|---|---|---|
| 0xFF, 0x00 | 0x67 | 0 | 0x00 | XX | 0xE0 |

**TABLE 6-36: RESET METER OPTIONS**

| Data Field Byte | Description | Value |
|---|---|---|
| 1 | Command Type | 0x55 - Reset All<br>0xA1 = Reset<br>0xA2 - Reset Power Calibration Only<br>0xA3 - Reset Phase Calibration |
| 2 | Phase Select | 0x01 = Phase A<br>0x02 = Phase B<br>0x03 = Phase C |
| 3 | Current Range Select | |
| 4 | Reserved | |

## 6.15 CALIBRATE METER CONSTANT (ENERGY PULSE OUTPUT CONSTANT)

**TABLE 6-37: PC TO METER (9 BYTES)**

| START | Command | Data Length | Data Field | Check Sum | STOP |
|---|---|---|---|---|---|
| 0x00, 0xFF | 0x67 | 2 | 0x02 | XX | 0xE0 |

**TABLE 6-38: METER RESPONSE (7 BYTES)**

| START | Command | Data Length | Data Field | Check Sum | STOP |
|---|---|---|---|---|---|
| 0xFF, 0x00 | 0x68 | 0 | 0x00 | XX | 0xE0 |

**TABLE 6-39: ENERGY CONSTANT OPTIONS OPTIONS**

| Data Field Byte | Description | Value |
|---|---|---|
| 1-2 | Energy Constant | Range of 10064000 (Decimal) |

**NOTES:**

# Appendix A. Schematics and Layouts

## A.1 INTRODUCTION

This appendix contains the following schematics and layouts for the MCP3909 / dsPIC33F 3-Phase Energy Meter Reference Design.

- Power Supply Board Schematic
- Main Board Schematic - Page 1
- Main Board Schematic - Page 2
- Power Supply Board - Assembly Drawing
- Power Supply Board - Composite Drawing
- Main Board - Assembly Drawing
- Main Board - Composite Drawing

## A.2 SCHEMATICS AND PCB LAYOUT

**FIGURE A-1: LAYER ORDER**

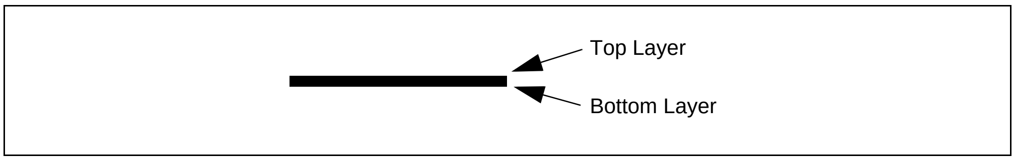


 

**FIGURE A-2: POWER SUPPLY BOARD SCHEMATIC**

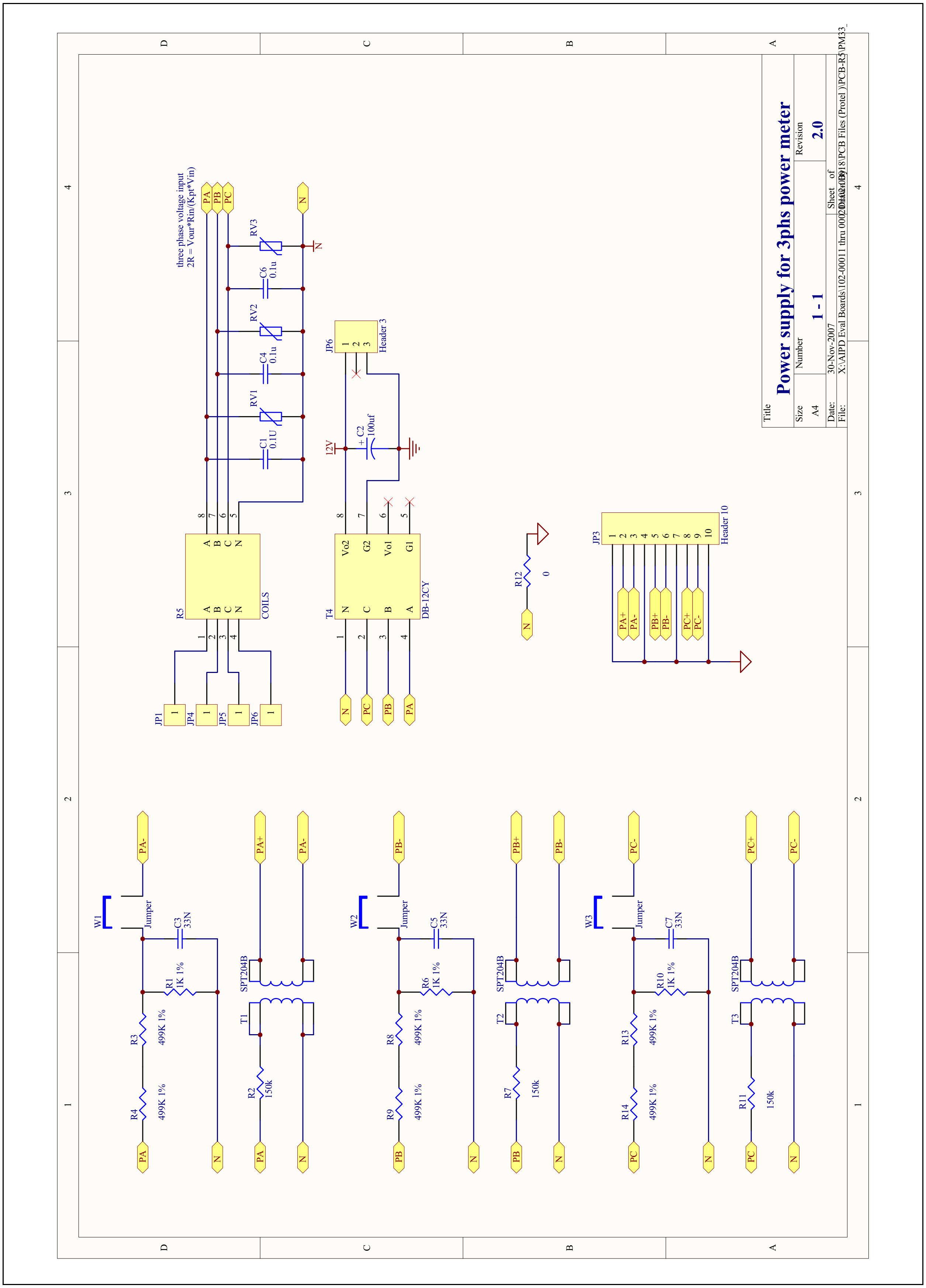

**FIGURE A-3: MAIN BOARD SCHEMATIC - PAGE 1**

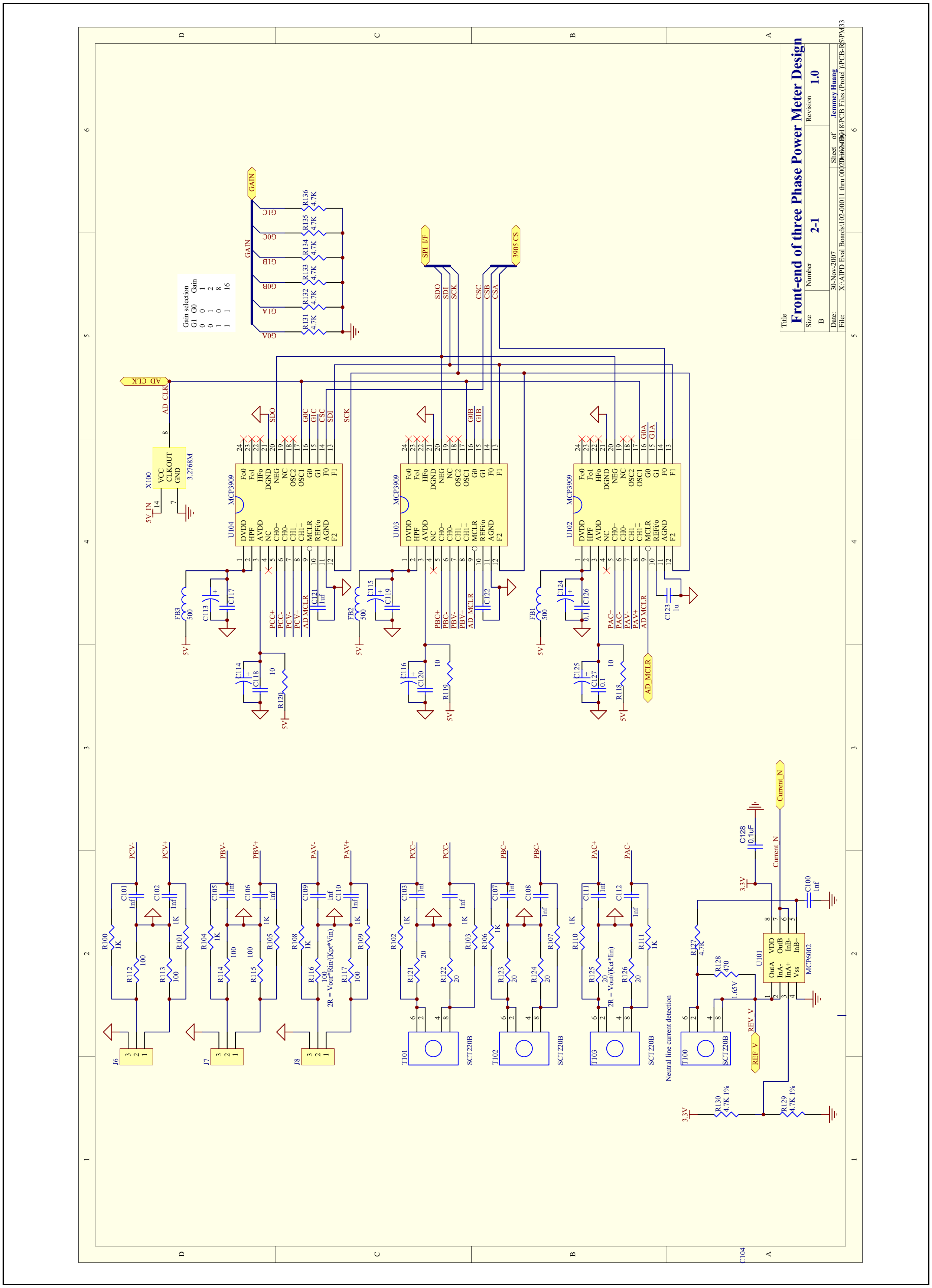

**FIGURE A-4: MAIN BOARD SCHEMATIC - PAGE 2**

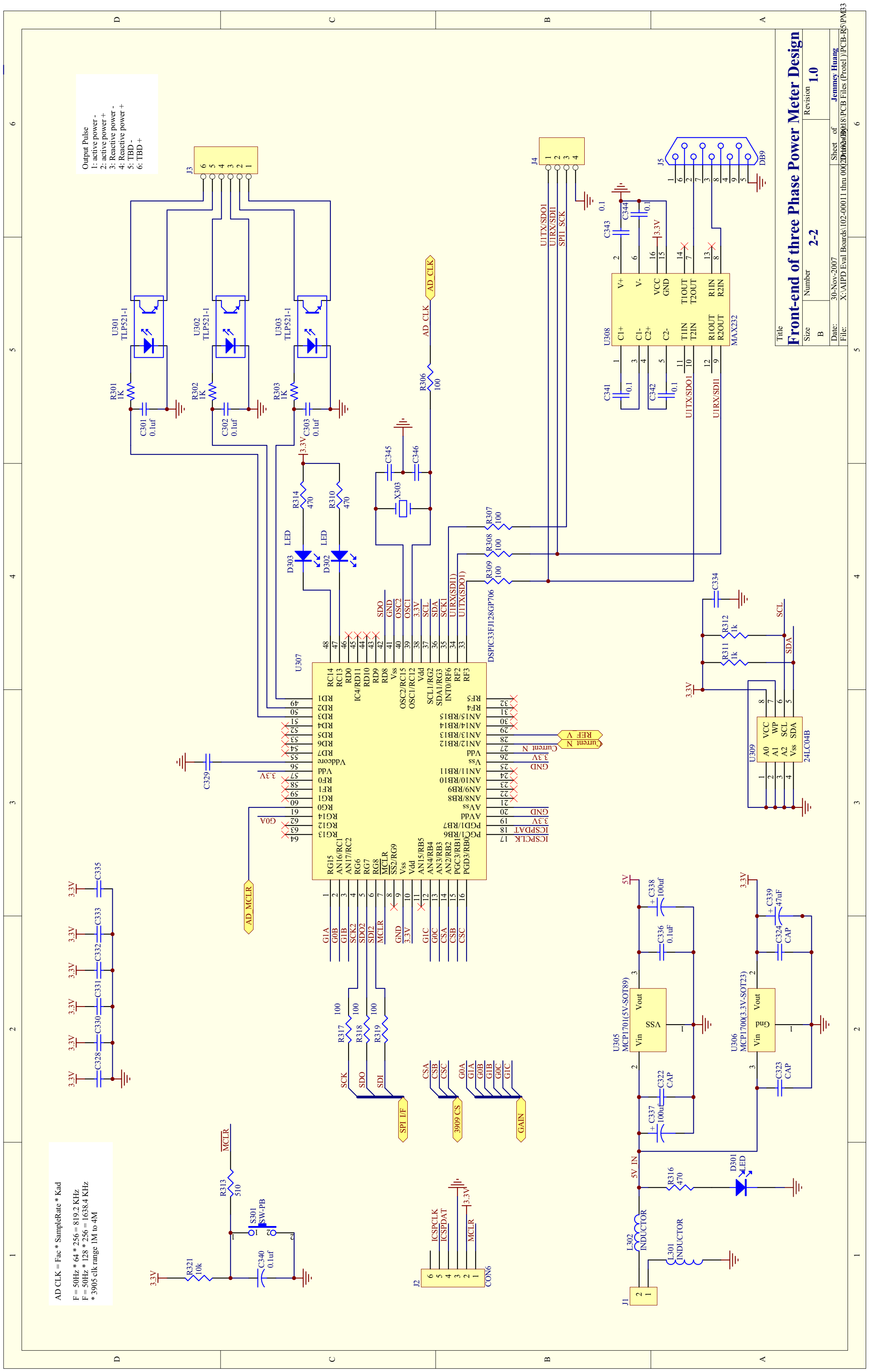

**FIGURE A-5: POWER SUPPLY BOARD LAYOUT - ASSEMBLY DRAWING**

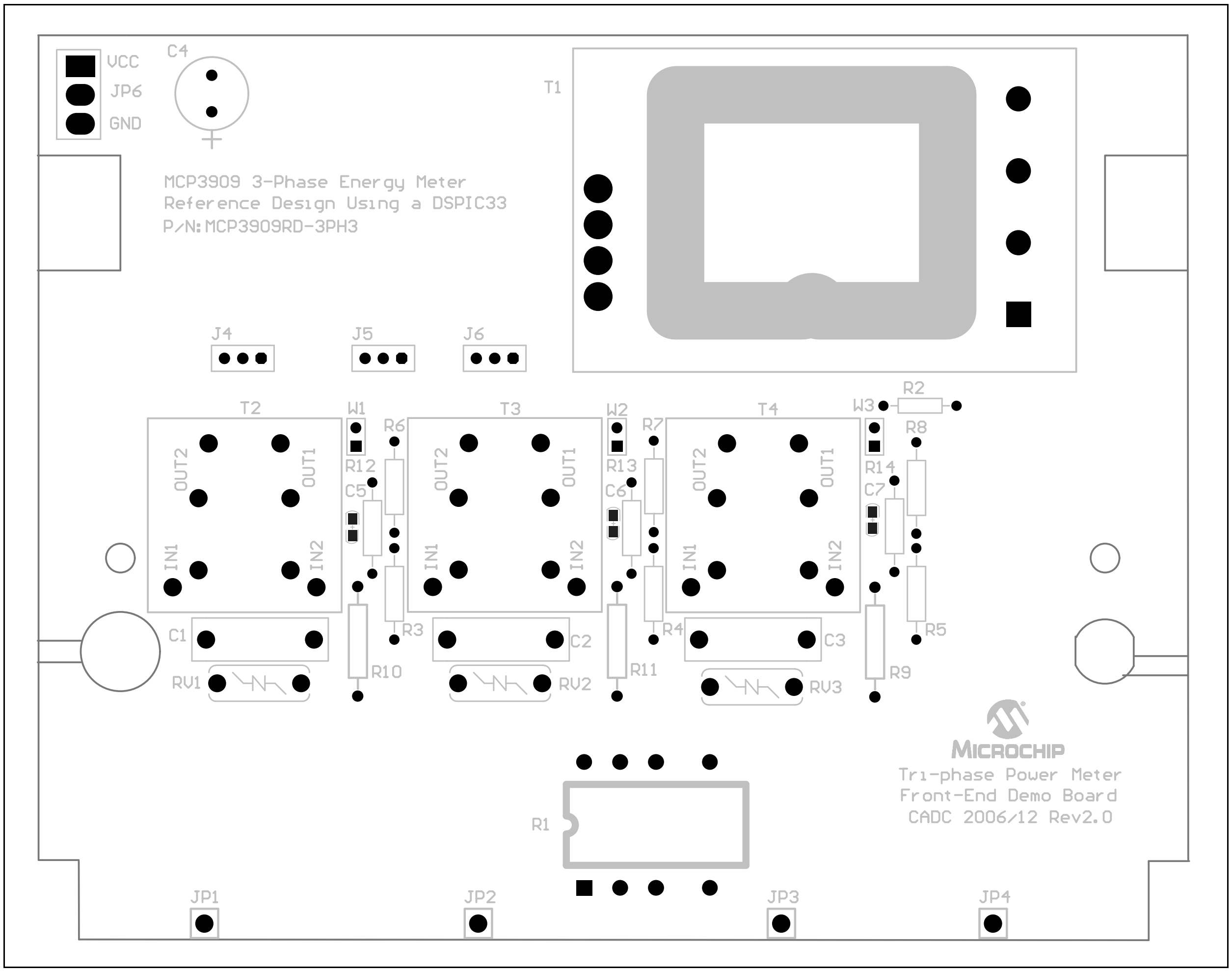

**FIGURE A-6: POWER SUPPLY BOARD LAYOUT - COMPOSITE DRAWING**

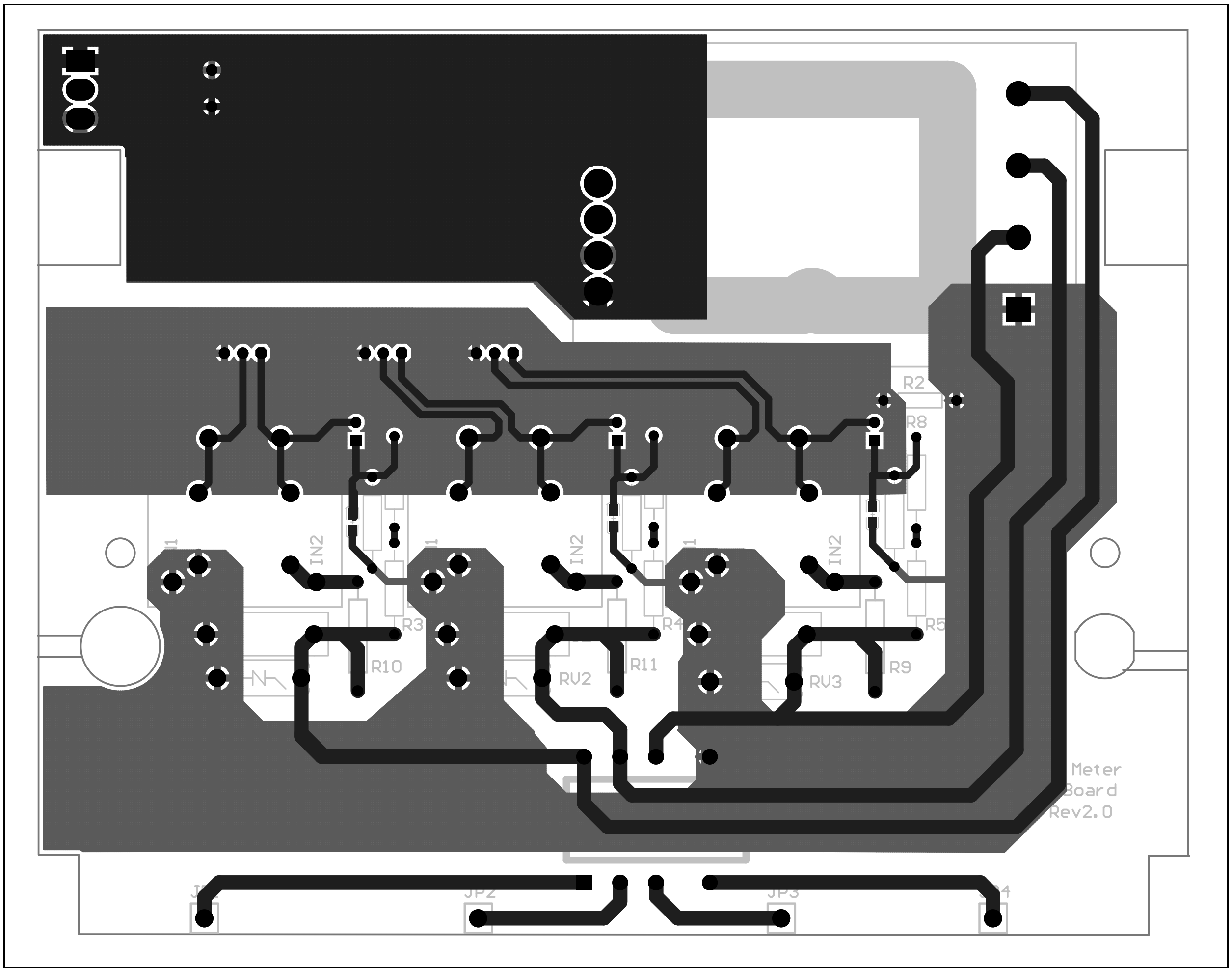


 

**FIGURE A-7: MAIN BOARD LAYOUT - ASSEMBLY DRAWING**

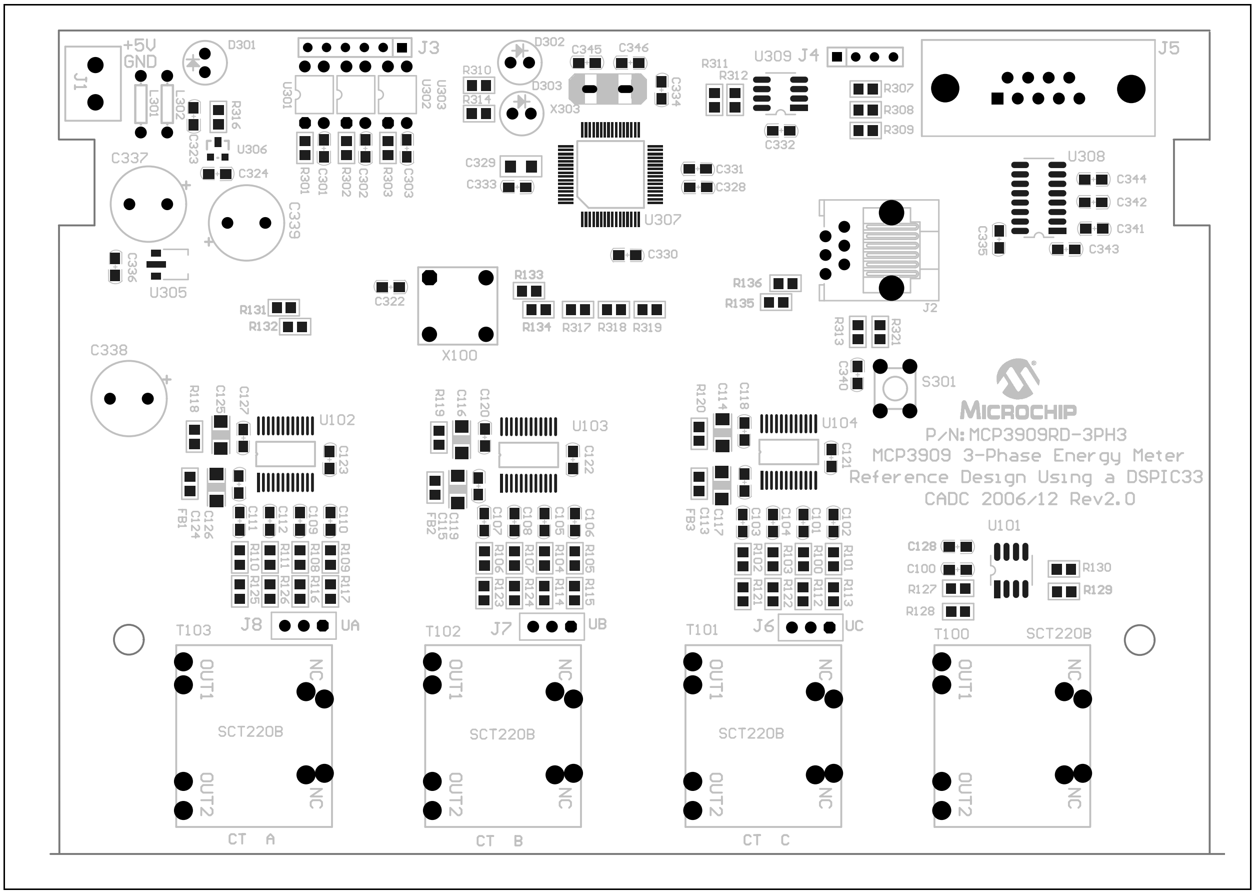

**FIGURE A-8: MAIN BOARD LAYOUT - COMPOSITE DRAWING**

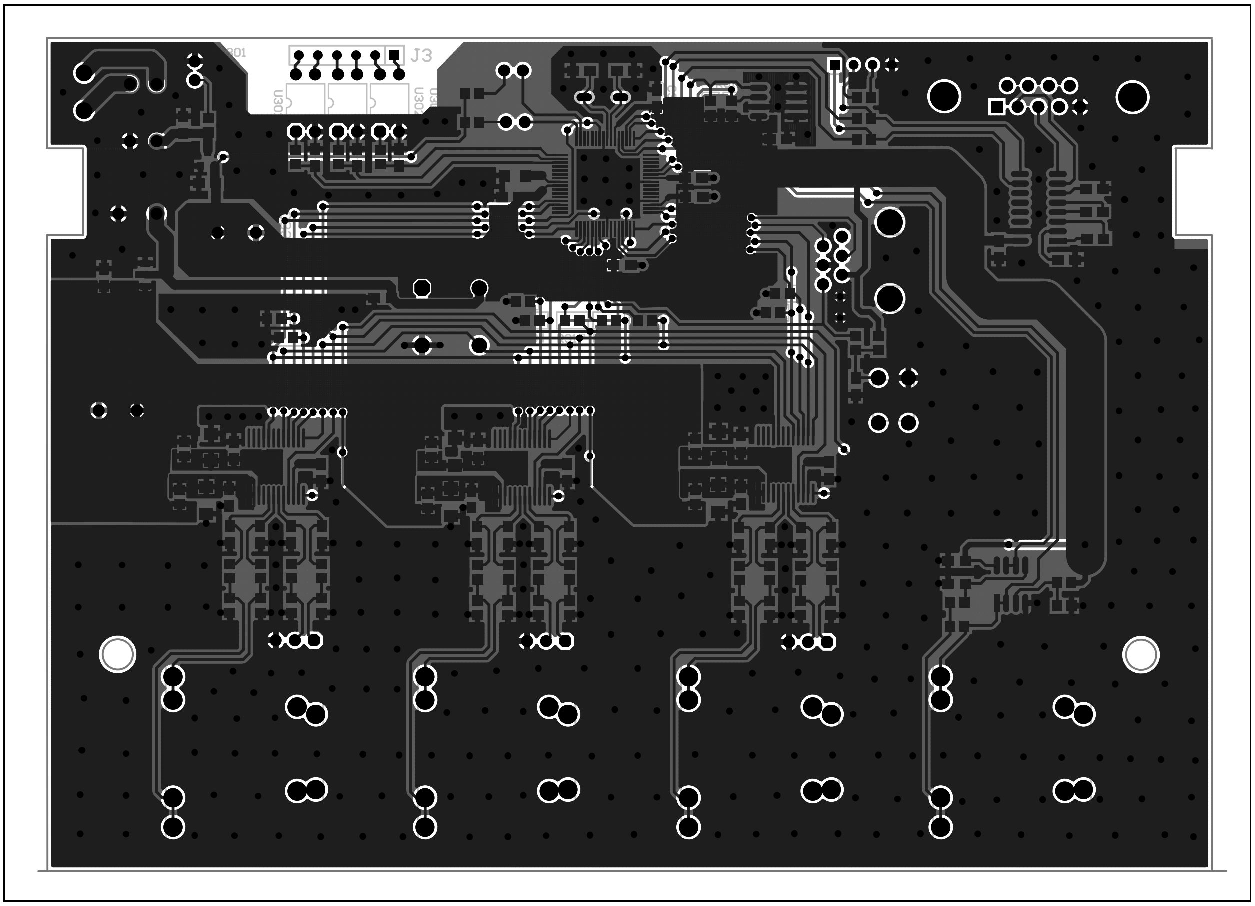


 

# Appendix B. Bill Of Materials (BOM)

**TABLE B-1: BILL OF MATERIALS - POWER SUPPLY (BOTTOM BOARD)**

| Qty | Reference | Description | Manufacturer | Part Number |
|---|---|---|---|---|
| 3 | C1, C2, C3 | CAP 0.1UF 305VAC EMI SUPPRESS | EPCOS Inc | B32922A2104M |
| 1 | C4 | CAP 470UF 25V ALUM LYTIC RADIAL | Panasonic® - ECG | ECA-1EM471 |
| 3 | C5, C6, C7 | DO NOT POPULATE | — | — |
| 3 | J4, J5, J6 | CONN HEADER 3POS .100 VERT TIN | Molex®/Waldom Electronics Corp | 22-23-2031 |
| 4 | JP1, JP2, JP3, JP4 | HOOK-UP WIRE 18AWG STRAND RED | Alpha Wire Company | 3055 RD005 |
| 4 | JP1, JP2, JP3, JP4 | CONN RING TERM #6 18-22AWG | Molex/Waldom Electronics Corp | 19070-0040 |
| 1 | JP6 | CONN HEADER 3POS .156 VERT TIN | Molex/Waldom Electronics Corp | 26-48-1035 |
| 1 | JP6 | CONN HOUSING 3POS .156 W/O RAMP | Molex/Waldom Electronics Corp | 09-50-7031 |
| 3 | JP6 | CONN TERM FEMALE 18-24AWG TIN | Molex/Waldom Electronics Corp | 08-50-0105 |
| 1 | PCB | RoHS Compliant Bare PCB, dsPIC33F and MCP3909 3-Phase Energy Meter (Power) Bottom Bd. | Microchip Technology Inc. | 104-00158 |
| 3 | P4, P5, P6 | CONN HOUS 3POS .100 W/RAMP/RIB (Connects to Above) | Molex/Waldom Electronics Corp | 22-01-3037 |
| 9 | P4, P5, P6 | CRIMP TERM FEMALE 22-30AWG TIN | Molex/Waldom Electronics Corp | 08-65-0805 |
| 1 | R1 | Part of T1 | Sanki | — |
| 1 | R2 | DO NOT POPULATE | — | — |
| 6 | R3, R4, R5, R6, R7, R8 | DO NOT POPULATE | — | — |
| 3 | R9, R10, R11 | RES 150K OHM METAL FILM .50W 1% | Vishay®/Phoenix Passive Components | 5033ED150K0F12AF5 |
| 3 | R12, R13, R14 | DO NOT POPULATE | — | — |
| 3 | RV1, RV2, RV3 | VARISTOR 300V RMS 14MM RADIAL | EPCOS Inc | S14K300E2 |
| 1 | T1 | 3P AC-DC converter, 220V - 12V/5V | Sanki | DB-12CY220 |
| 3 | T2, T3, T4 | 2mA/2mA Current transformer | Xinge | SPT204 |
| 3 | W1, W2, W3 | DO NOT POPULATE | — | — |

**Note 1:** The components listed in this Bill of Materials are representative of the PCB assembly. The released BOM used in manufacturing uses all RoHS-compliant components.

**TABLE B-2: BILL OF MATERIALS - TOP BOARD**

| Qty | Reference | Description | Manufacturer | Part Number |
|---|---|---|---|---|
| 13 | C100, C101, C102, C103, C104, C105, C106, C107, C108, C109, C110, C111, C112 | CAP 1000PF 50V CERAMIC X7R 0805 | Kemet® Electronics Corp | C0805C102K5RACTU |
| 6 | C113, C114, C115, C116, C124, C125 | CAP CER 10UF 16V X7R 1206 | Murata Electronics® North America | GRM31CR71C106KAC7L |
| 26 | C117, C118, C119, C120, C126, C127, C128, C301, C302, C303, C322, C323, C324, C328, C330, C331, C332, C333, C334, C335, C336, C340, C341, C342, C343, C344 | CAP .1UF 25V CERAMIC X7R 0805 | Panasonic® - ECG | ECJ-2VB1E104K |
| 4 | C121, C122, C123, C329 | CAP 1.0UF 10V CERAMIC X7R 0805 | Kemet Electronics Corp | C0805C105K8RACTU |
| 3 | C337, C338, C339 | CAP 470UF 25V ALUM LYTIC RADIAL | Panasonic - ECG | ECA-1EM471 |
| 2 | C345, C346 | CAP 22PF 50V CERM CHIP 0805 SMD | Panasonic - ECG | ECJ-2VC1H220J |
| 3 | 6" Wire Thru CT | HOOK-UP WIRE 16AWG STRAND RED | Alpha Wire Company | 3057 RD005 |
| 6 | CT Wire terminals | CONN RING TERM #6 18-22AWG | Molex/Waldom Electronics Corp | 19070-0040 |
| 1 | D301 | LED 3MM ALGAAS RED CLEAR | LITE-ON INC | LTL-4266N |
| 1 | D302 | LED 3MM GREEN CLEAR | LITE-ON INC | LTL-4236N |
| 1 | D303 | LED 3MM YELLOW CLEAR | LITE-ON INC | LTL-4256N |
| 3 | FB1, FB2, FB3 | FERRITE SMT | luying | STBL2012-121 |
| 1 | J1 | CONN HOUSING 3POS .156 W/O RAMP | Molex/Waldom Electronics Corp | 09-50-7031 |
| 1 | J1 | CONN TERM FEMALE 18-24AWG TIN | Molex/Waldom Electronics Corp | 08-50-0105 |
| 1 | J1 | HOOK-UP WIRE 22AWG STRAND RED | Alpha Wire Company | 3051 RD005 |
| 1 | J1 | HOOK-UP WIRE 22AWG STRAND BLACK | Alpha Wire Company | 3051 BK005 |
| 1 | J2 | CONN MOD JACK 6-6 VERT PCB 50AU | Tyco Electronics/Amp | 5520258-3 |
| 1 | J3 | CONN HEADER 6POS .100 VERT TIN | Molex/Waldom Electronics Corp | 22-27-2061 |
| 1 | J4 | CONN HEADER 4POS .100 VERT TIN | Molex/Waldom Electronics Corp | 22-27-2041 |
| 1 | J5 | DB9 Female vertical | Tyco Electronics/Amp | 747091-2 |
| 3 | J6,J7 & J8 | CONN HOUS 3POS .100 W/RAMP/RIB (Connects to J4,J5 & J6 of Lower Board) | — | — |
| 9 | J6,J7 & J8 | CRIMP TERM FEMALE 22-30AWG TIN | Molex/Waldom Electronics Corp | 08-65-0805 |

**Note 1:** The components listed in this Bill of Materials are representative of the PCB assembly. The released BOM used in manufacturing uses all RoHS-compliant components.

**TABLE B-2: BILL OF MATERIALS - TOP BOARD**

| Qty | Reference | Description | Manufacturer | Part Number |
|---|---|---|---|---|
| 3 | J6,J7 & J8 | HOOK-UP WIRE 22AWG STRAND GREEN | Alpha Wire Company | 3051 GR005 |
| 3 | J6,J7 & J8 | HOOK-UP WIRE 22AWG STRAND RED | Alpha Wire Company | 3051 RD005 |
| 3 | J6,J7 & J8 | HOOK-UP WIRE 22AWG STRAND BLACK | Alpha Wire Company | 3051 BK005 |
| 2 | L301, L302 | 60ohm bead | Jones | B60 |
| 1 | PCB | RoHS Compliant Bare PCB, dsPIC33F and MCP3909 3-Phase Energy Meter (Power) Bottom Bd. | — | 104-00159 |
| 17 | R100, R101, R102, R103, R104, R105, R106, R107, R108, R109, R110, R111, R301, R302, R303, R311, R312 | RES 1.00K OHM 1/8W 1% 0805 SMD | Panasonic - ECG | ERJ-6ENF1001V |
| 12 | R112, R113, R114, R115, R116, R117, R307, R308, R309, R317, R318, R319 | RES 100 OHM 1/8W 1% 0805 SMD | Panasonic - ECG | ERJ-6ENF1000V |
| 3 | R118, R119, R120 | RES 10.0 OHM 1/8W 1% 0805 SMD | Panasonic - ECG | ERJ-6ENF10R0V |
| 6 | R121, R122, R123, R124, R125, R126 | RES 20.0 OHM 1/8W 1% 0805 SMD | Panasonic - ECG | ERJ-6ENF20R0V |
| 7 | R127, R131, R132, R133, R134, R135, R136 | RES 4.7K OHM 1/8W 5% 0805 SMD | Panasonic - ECG | ERJ-6GEYJ472V |
| 4 | R128, R310, R314, R316 | RES 470 OHM 1/8W 5% 0805 SMD | Panasonic - ECG | ERJ-6GEYJ471V |
| 2 | R129, R130 | RES 4.70K OHM 1/8W 1% 0805 SMD | Yageo Corporation | 9C08052A4701FKHFT |
| 1 | R313 | RES 510 OHM 1/8W 5% 0805 SMD | Panasonic - ECG | ERJ-6GEYJ511V |
| 1 | R321 | RES 10.0K OHM 1/8W 1% 0805 SMD | Panasonic - ECG | ERJ-6ENF1002V |
| 1 | S301 | SWITCH TACT 6MM MOMENTARY 250GF | E-Switch | TL1105BF250Q |
| 1 | X100 | 3.2768Mhz Crystal | Koan | DIP-8-3.2768M |
| 1 | X303 | 7.3728Mhz Crystal | Koan | HC-49S-SMD-7.3728M |
| 1 | U305 | 2uA Low Dropout Positive Voltage Regulator | Microchip Technology Inc | MCP1701T-5002I/MB |
| 1 | U306 | Low Quiescent Current LDO | Microchip Technology Inc | MCP1700T-3302E/TT |
| 1 | U307 | High-Performance, 16-bit Digital Signal Controllers | Microchip Technology Inc | dsPIC33FJ128GP206 |
| 1 | U308 | IC DRVR/RCVR MULTCH RS232 16SOIC | Texas Instruments | MAX3232CDR |
| 1 | U309 | 4K I2C™ Serial EEPROM | Microchip Technology Inc | 24LC04B-E/SN |
| 3 | U102, U103 U104 | Energy Metering IC with SPI Interface and Active Power Pulse Output | Microchip Technology Inc | MCP3909-I/SS |
| 1 | U101 | 1MHz, Low Power Op-Amp | Microchip Technology Inc | MCP6002-I/SN |
| 3 | T101 T102, T103 | 5A/5mA Current transformer | Xinge | SCT954F |
| 1 | T100 | " DO NOT POPULATE | — | — |

**Note 1:** The components listed in this Bill of Materials are representative of the PCB assembly. The released BOM used in manufacturing uses all RoHS-compliant components.

**NOTES:**

# Appendix C. Power Calculation Theory

## C.1 OVERVIEW

This MCP3909 / dsPIC33F 3-Phase Energy Meter Reference Design is unique in that all calculations are done in the frequency domain. This is easily realized using the DSP engine core of the advanced 16-bit MCU, the dsPIC33F. In addition to performing direct fourier transforms (DFTs) on all the input channel measurements, an additional firmware function is included, quasi-synchronous sampling.

## C.2 SYNCHRONOUS SAMPLING AND QUASI-SYNCHRONOUS SAMPLING

The fundamentals of quasi-synchronous sampling and corresponding methods for measuring AC electrical parameters are discussed in this section. Typically, a synchronous sampling method is used for measuring electrical parameters. The method requires synchronization between sampling intervals and power grid frequency. For these types of meter designs, an external hardware PLL circuit is used to track power grid frequency, and the clock of the MCP3909 device is automatically updated to change the sampling frequency. Since the PLL output frequency drops behind the power grid frequency, a synchronous error exists in the system, and fully synchronous sampling is hard to achieve. In addition, as non-sine waves exist in the power grid, which may affect zero-crossing detection, when such conditions worsen, it may cause PLL failure, preventing the system from working normally.

For the MCP3909 / dsPIC33F 3-Phase Energy Meter Reference Design presented here, the dsPIC33F performs additionall calculations that eliminates the need for a costly external PLL circuit. This quasi-synchronous sampling method has an advantage in the engineering practice, which actually is periodic sampling, without synchronizing with the power grid frequency. Therefore, the zero-crossing detection and PLL circuit can be reduced to lower the hardware complexity. The tradeoff is the increased software requirements of the system, easily realized using the powerful dsPIC33F.

For DFT or FFT harmonic analysis of periodic signals, a Fourier transform may only bring accurate spectrum analysis when the sampling points satisfy $N > 2M$ for each line cycle and strict synchronous sampling is realized. (Where M is the maximal harmonic order of periodic signals, and N is the number of samples per line cycle).

Otherwise, if $N \leq 2M$, it will cause spectrum aliasing. In addition, if strict synchronous sampling cannot be realized, spectral-leakage will occur (the Hurdle Effect). However, in the quasi-synchronous sampling method emplyed here, strict synchronization between sampling intervals and the period of sampled signal is not guaranteed but is overcome through post-processing and iteration of the collected data. To reduce the error caused by this problem and to obtain better accuracy when measuring the fundamental and harmonics of higher orders, an increase in the number of iterations when processing data to improve accuracy is performed.

The iterations can effectively reduce the impact of synchronization error over the measurement accuracy, and is one of the methods to realize accurate measurement of the frequency and harmonics under steady-state conditions.

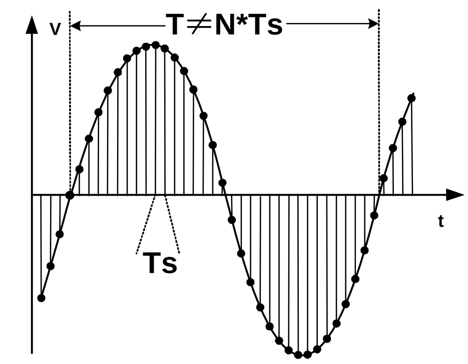


*FIGURE C-1: Quasi Synchronous Sampline.*

### C.2.1 Basic Idea of Quasi-Synchronous Sampling

Assuming that the average of a periodic signal in one cycle is $\overline{g(t)}$,

**EQUATION C-1:**

$$\overline{g(t)} = \frac{1}{T} \cdot \int_{0}^{T} g(t)dt = \frac{1}{T} \cdot \int_{TO}^{(TO+T)} g(t)dt$$

Make $t = x/\omega$, then,

**EQUATION C-2:**

$$\overline{g(t)} = \frac{1}{2\pi} \cdot \int_{0}^{2\pi} f(x)dx = \overline{f(x)}$$

where $f(x) = g(x/\omega)$, and the period is $2\pi$.

If the entire period sampling cannot be realized while a sampling frequency deviation $\Delta$ exists, then:

**EQUATION C-3:**

$$\overline{f(x)} \neq \frac{1}{2\pi+\Delta} \cdot \int_{0}^{(2\pi+\Delta)} f(x)dx \neq \frac{1}{2\pi+\Delta} \cdot \int_{\alpha}^{(\alpha+2\pi+\Delta)} f(x)dx$$

We have:

**EQUATION C-4:**

$$F^1(\alpha) = \frac{1}{2\pi+\Delta} \cdot \int_{\alpha}^{(\alpha+2\pi+\Delta)} f(x)dx$$

The value of $F^1(\alpha)$ is a function of $\alpha$ and also a function with $2\pi$ as its perod. The non--synchronous sampling error $E = \overline{f(x)} - F^1(\alpha)$.

As $F^1(\alpha)$ is function with $2\pi$ as its period, its value may be averaged through integration within the range of 0-$2\pi$, and it can be deduced that $\overline{f(x)} = \overline{F^1(\alpha)}$.

 

Assuming that the integral starts at β, then:

**EQUATION C-5:**

$$\overline{f(x)} = \overline{F^1(\alpha)} = \frac{1}{2\pi} \cdot \int_{\beta}^{(\beta + 2\pi)} F^1(\alpha) d\alpha$$

Likewise, as strict integration cannot be realized in the entire cycle, so:

**EQUATION C-6:**

$$\overline{f(x)} = \overline{F^1(\alpha)} \neq \frac{1}{2\pi + \Delta} \cdot \int_{\beta}^{(\beta + 2\pi + \Delta)} F^1(\alpha) d\alpha$$

Similarly, the integral value of above equation is related to β with 2π as its period, let's denote it as $F^2(\beta)$. If it won't confuse people, we'll write $F^1(\alpha)$ and $F^2(\beta)$ as $F^1(x)$ and $F^2(x)$, and a recurrence formula can be obtained as the following:

**EQUATION C-7:**

$$\overline{F^n(\alpha)} = \frac{1}{2\pi + \Delta} \cdot \int_{x}^{(x + 2\pi + \Delta)} F^{n-1}(x) dx$$

It can be proved that,

**EQUATION C-8:**

$$\lim_{n - \infty} F^n(\alpha) = \overline{f(x)}$$

In practical applications, it is necessary to sample the continuous analog signals and process the data obtained with discrete algorithms. The quasi-synchronous recursive process mentioned above can be expressed as follows:

For Equation C-4, the integral interval $[x_0, x_0 + n$ x $(2\pi + \Delta)]$ whose width is $n$ x $(2\pi + \Delta)$ can be divided equally into $n$ x $N$ sections, which results in $n$ x $N + 1$ sampled data, $f(x_i)$, (i=0,1,...,nxN), and we can iterate as follows:

First iteration:

$$F_0^{\,1} = \frac{1}{\sum_{i=0}^{N} \rho_i} \cdot \sum_{i=0}^{N} \rho_i \cdot f(x_i)$$

$$F_1^{\,1} = \frac{1}{\sum_{i=1}^{N+1} \rho_i} \cdot \sum_{i=1}^{N+1} \rho_i \cdot f(x_i)$$

…

$$F^{1}_{(n-1)\times N} = \frac{1}{\sum_{i=(n-1)\times N}^{N\times n} \rho_i} \cdot \sum_{i=(n-1)\times N}^{N\times n} \rho_i \cdot f(x_i)$$

Second iteration:

$$F_0^{\,2} = \frac{1}{\sum_{i=0}^{N} \rho_i} \cdot \sum_{i=0}^{N} \rho_i \cdot F_i^{\,1}$$

$$F_1^{\,2} = \frac{1}{\sum_{i=1}^{N+1} \rho_i} \cdot \sum_{i=1}^{N+1} \rho_i \cdot F_i^{\,1}$$

…

$$F^{2}_{(n-2)\times N} = \frac{1}{\sum_{i=(n-2)\times N}^{N\times(n-1)} \rho_i} \cdot \sum_{i=(n-2)\times N}^{N\times(n-1)} \rho_i \cdot F_i^{\,1}$$

Third iteration:

$$F_0^{\,3} = \frac{1}{\sum\limits_{i=0}^{N} \rho_i} \cdot \sum_{i=0}^{N} \rho_i \cdot F_i^{\,2}$$

$$F_1^{\,3} = \frac{1}{\sum\limits_{i=1}^{N+1} \rho_i} \cdot \sum_{i=1}^{N+1} \rho_i \cdot F_i^{\,2}$$

…

$$F^3_{(n-3)\times N} = \frac{1}{\sum\limits_{i=(n-3)\times N}^{N\times(n-2)} \rho_i} \cdot \sum_{i=(n-3)\times N}^{N\times(n-2)} \rho_i \cdot F_i^{\,2}$$

…

N-th iteration:

$$F_0^n = \frac{1}{\sum_{i=0}^{N} \rho_i} \cdot \sum_{i=0}^{N} \rho_i \cdot F_i^{n-1}$$

Where $\rho_i$ is the weight coefficient which is decided by the digital quadrature formula. Complex rectangular quadrature algorithm or complex trapezoidal quadrature algorithm is usually used in quasi-synchronous sampling.

Figure C-2 shows a 3-cycle interative process.

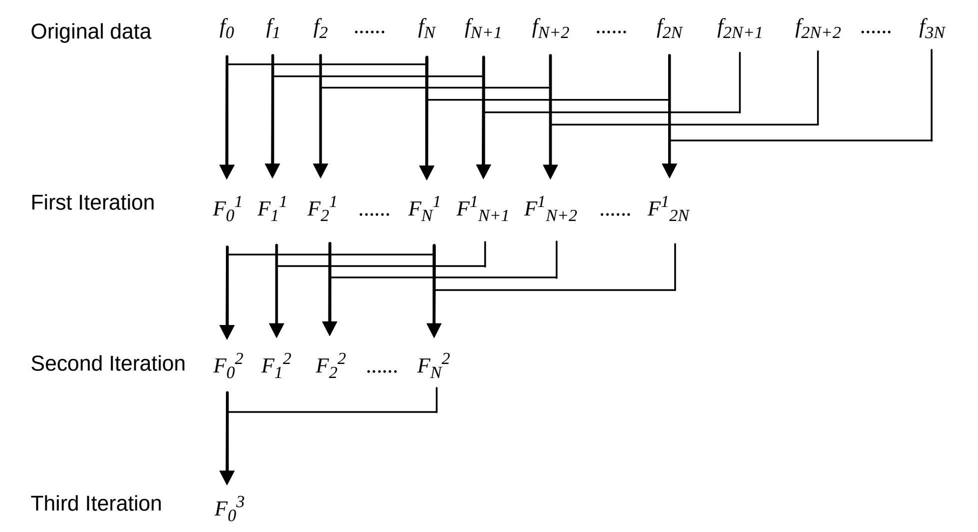


***FIGURE C-2:*** *3-Cycle Iterative Process.*

In practical applicatons, a frequency offset $\Delta$ is usually small, and good results may usually be obtained through 3-5 iterations.

As mentioned above, the iterative process will result in a group of weight coefficients $\eta_i$, called weight coefficients of quasi-synchronous algorithm, they may be deduced from the numeric quadrature formula. The relationship between the iterative result and original data is shown in Equation C-9.

**EQUATION C-9:**

$$F_0^n = \frac{1}{\sum_{i=0}^{n \times N} \eta_i} \cdot \sum_{i=0}^{n \times N} \eta_i \cdot f(x_i)$$

$$= \frac{1}{N^n} \cdot \sum_{i=0}^{n \times N} \eta_i \cdot f(x_i)$$

$$= \sum_{i=0}^{n \times N} R_i \cdot f(x_i)$$

Where:

**EQUATION C-10:**

$$R_i = \frac{1}{N^n} \cdot \eta_i \qquad (i = 0 \sim n \times N)$$

Equation C-10 is called the quasi-synchronous window function. After determining the sampling points, the number of iterations and numerical quadrature method, the coefficients of quasi-synchronous window function will become definite, and a quasi-synchronous window function arrays may be established in advance.

Using the quasi-synchronous window function to carry out the weighted process of the original data is equivalent to carrying out data synchronization one time, and the algorithm realization is also very simple that only a multiplication of the original data and quasi-synchronous window function arrays is required. After processing, the new periodic signal will have the same period and frequency components as the original signal, and the synchronization error of the new signal becomes smaller.

Figure C-3 is a schematic of the quasi-synchronous window function characteristics in the time domain and data processing. In Figure C-3, the red curve is the characteristic of the window function, and the blue curve is input signal, and the green curve is the output signal.

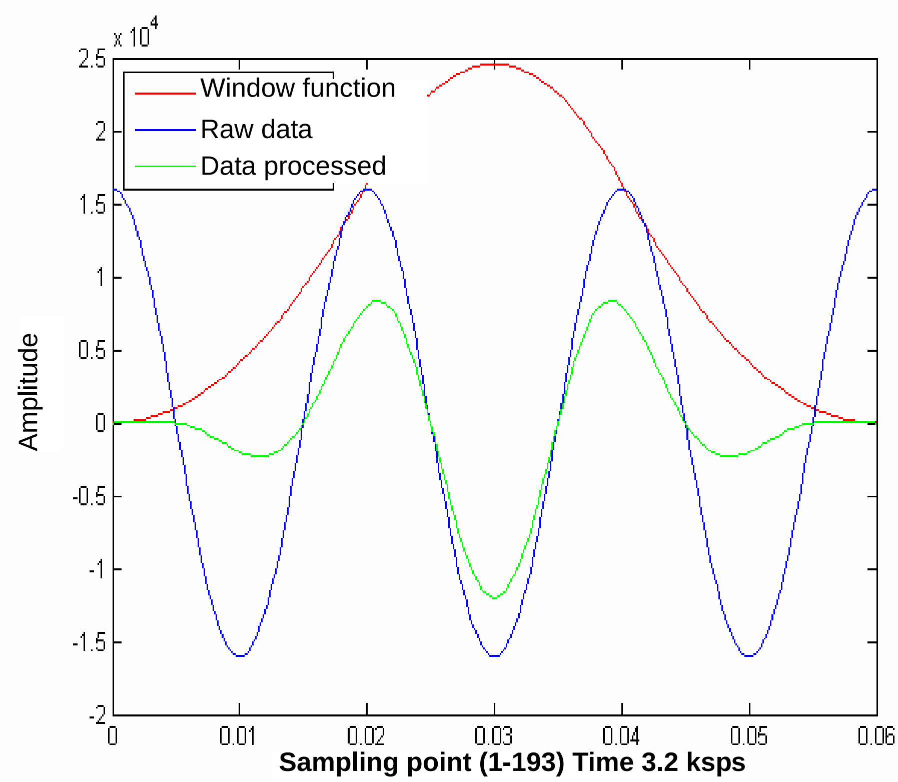


***FIGURE C-3:*** *Quasi-Synchronous Window Function Characteristics Curve and Data Processing.*

 

## C.3 THE HARMONIC ANALYSIS ALGORITHM OF QUASI-SYNCHRONOUS SAMPLING

Periodic signal can be expressed as trigonometric Fourier series or exponential Fourier series. A periodic signal with a period of T can be expressed as :

**EQUATION C-11:**

$$f(t) = \frac{\alpha_0}{2} + \sum_{k=1}^{\infty} (\alpha_k cos(k \cdot \omega \cdot t) + \beta cos(k \cdot \omega \cdot t))$$

where:

**EQUATION C-12:**

$$a_k = \frac{2}{T} \cdot \int_0^T f(t) \cdot cos(k \cdot \omega \cdot t) dt$$

**EQUATION C-13:**

$$b_k = \frac{2}{T} \cdot \int_0^T f(t) \cdot sin(k \cdot \omega \cdot t) dt$$

or as:

**EQUATION C-14:**

$$f(t) = a_0 + \sum_{k=1}^{\infty} c_k sin(k \cdot \omega \cdot t + \varphi_k)$$

where the relationship between $a_k$, $b_k$, $c_k$ and $\varphi_k$ is:

**EQUATION C-15:**

$$c_k = \sqrt{a_k^2 + b_k^2}$$

**EQUATION C-16:**

$$\varphi_k = atan\frac{a_k}{b_k}$$

**EQUATION C-17:**

$$a_k = c_k sin\,\varphi_k$$

**EQUATION C-18:**

$$b_k = c_k \cos\varphi_k$$

Make $g(t) = f(t) \bullet \cos(K \bullet \omega \bullet t)$, it can be proved that $g(t)$ is also a periondic function with $T$ as its period. Averaging $g(t)$ in the range of $[0 \sim T]$ results in:

**EQUATION C-19:**

$$\overline{g(t)} = \frac{1}{T} \cdot \int_0^T f(t) \cdot \cos(k \cdot \omega \cdot t)dt$$

So $a_k = 2 \times \overline{g(t)}$. Therefore, $a_k$ can be obtained if only $\overline{g(t)}$ can be calculated.

**EQUATION C-20:**

$$a_k = 2\overline{g(t)} = \frac{2}{N^n} \cdot \sum_{i=0}^{n \times N} \eta_i \cdot g_i$$

$$= \frac{2}{N^n} \cdot \sum_{i=0}^{n \times N} \eta_i \cdot f_i \cdot \cos\left(k \cdot \frac{2\pi}{N} \cdot i\right)$$

**EQUATION C-21:**

$$b_k = \frac{2}{N^n} \cdot \sum_{i=0}^{n \times N} \eta_i \cdot f_i \cdot \sin\left(k \cdot \frac{2\pi}{N} \cdot i\right)$$

Where $N$, $n$ and $\eta_i$ are constants. The equation may therefore be written as:

**EQUATION C-22:**

$$a_k = \sum_{i=0}^{n \times N} I_i \cdot f_i \cdot \cos\left(k \cdot \frac{2\pi}{N} \cdot i\right)$$

**EQUATION C-23:**

$$b_k = \sum_{i=0}^{n \times N} I_i \cdot f_i \cdot \sin\left(k \cdot \frac{2\pi}{N} \cdot i\right)$$

Where:

**EQUATION C-24:**

$$I_i = \frac{2}{N^n} \cdot \eta_1 = R_1 \times 2 \qquad (i = 0 \sim n \times N)$$

## C.4 MEASURING THE VOLTAGE/CURRENT RMS VALUE AND POWER USING QUASI-SYNCHRONOUS SAMPLING ALGORITHM

From Equation C-11, a periodic voltage can be expressed as:

**EQUATION C-25:**

$$U(t) = \frac{U_{a0}}{2} + \sum_{k=1}^{\infty} (u_{ak} cos(k \cdot \omega \cdot t) + u_{bk} sin(k \cdot \omega \cdot t))$$

So the voltage fundamental and the voltage of each harmonic can be expressed as:

**EQUATION C-26:**

$$U_k(t) = u_{ak} cos(k \cdot \omega \cdot t) + u_k sin(k \cdot \omega \cdot t)$$

From Equation C-25, the fundamental voltage and voltage of each harmonic can also be expressed as:

**EQUATION C-27:**

$$U_k(t) = u_{ck} sin(k \cdot \omega \cdot t + \varphi_{uk})$$

Where:

**EQUATION C-28:**

$$u_{ck} = \sqrt{u_{ak}^2 + u_{bk}^2}$$

**EQUATION C-29:**

$$\varphi_{uk} = atan\frac{u_{ak}}{u_{bk}}$$

The voltage RMS value of each harmonic, then can be expressed as shown in Equation C-31 with its initial phase angle shown in Equation C-29.

**EQUATION C-30:**

$$U_k = \frac{1}{\sqrt{2}} \cdot u_{ck} = \sqrt{\frac{u_{ak}^2 + u_{bk}^2}{2}}$$

The relationship between $u_{ak}$, $u_{bk}$ and $U_k$ can be expressed as:

**EQUATION C-31:**

$$u_{ak} = \sqrt{2} \cdot U_k \cdot \sin\varphi_{uk}$$

**EQUATION C-32:**

$$u_{bk} = \sqrt{2} \cdot U_k \cdot \cos\varphi_{uk}$$

Total effective voltage can be expressed as:

**EQUATION C-33:**

$$U_{total} = \sqrt{\sum_{k=0}^{\infty} U_k^2}$$

Similarly, the effective values and initial phase angles of fundamental current and current of each other harmonic can be expressed as:

**EQUATION C-34:**

$$I_k = \frac{1}{\sqrt{2}} \cdot i_{ck} = \sqrt{\frac{i_{ak}^2 + i_{bk}^2}{2}}$$

**EQUATION C-35:**

$$\varphi_{ik} = atan\frac{i_{ak}}{i_{bk}}$$

The relationship between $i_{ak}$, $i_{bk}$ and $I_k$ can be expressed as:

**EQUATION C-36:**

$$i_{ak} = \sqrt{2} \cdot I_k \cdot \sin\varphi_{ik}$$

**EQUATION C-37:**

$$i_{bk} = \sqrt{2} \cdot I_k \cdot \cos\varphi_{ik}$$

Total current RMS can be expressed as:

**EQUATION C-38:**

$$I_{total} = \sqrt{\sum_{k=0}^{\infty} I_k^2}$$

 

According to the definition of power measurement, the active power and reactive power of the fundamental and each other harmonic can be expressed as:

**EQUATION C-39:**

$$P_k = U_k I_k cos(\varphi_{uk} - \varphi_{ik})$$
$$= \frac{1}{2} \cdot U_k I_k (sin\,\varphi_{uk} sin\,\varphi_{ik} + cos\,\varphi_{uk} cos\,\varphi_{ik})$$

**EQUATION C-40:**

$$Q_k = U_k I_k \sin(\varphi_{uk} - \varphi_{ik})$$
$$= \frac{1}{2} \cdot U_k I_k (sin\,\varphi_{uk} cos\,\varphi_{ik} - cos\,\varphi_{uk} sin\,\varphi_{ik})$$

Substituting Equation C-31, C-32, C-33 and C-37 into Equation C-39 and C-40, the power of each harmonic component can be obtained with the following:

**EQUATION C-41:**

$$P_k = \frac{1}{2} \cdot (u_{ak} i_{ak} + u_{bk} i_{ik})$$

**EQUATION C-42:**

$$Q_k = \frac{1}{2} \cdot (u_{ak} i_{ak} - u_{bk} i_{ik})$$

Total active power and reactive power can be expressed as:

**EQUATION C-43:**

$$P_{total} = \sum_{k=0}^{\infty} P_k$$

**EQUATION C-44:**

$$Q_{total} = \sum_{k=0}^{\infty} Q_k$$

## C.5 MEASURING FREQUENCY

There are many ways to measure frequency, with the most common being counting the signal cycle. In this method, a counter increments each time a zero-crossing is detected. Based on the counts, the width of a cycle can be measured. If the zero-crossing is accurate and the counter precision is high enough, cycle counting can be a simple and practical method. But if the input signal has large harmonic components, causing distortion around zero-crossing, then this approach may produce large errors.

Another method is to analyze and process the sampled data and calculate the frequencies. Analysis may be carried out in time domain, such as digital differential ND and interpolation method; or may be carried out in frequency domain after DFT transformation, such as gravity center method, spectrum zoom method and phase difference method, among which the phase difference method is the most common one. It is not sensitive to signal distortion around zero-crossing points.

The basic idea of the phase difference method is: if the rough range of to-be-measured signal frequency is known, then we may assume a frequency that is close to the actual frequency and then acquire an array of samples based on the assumed frequency. In the sampled data, the phase of the 1st cycle and the subsequent N-th cycle are meaured and their difference may be calculated. Then the phase difference may be used to calculate the difference between the actual freqency and the assumed frequence, thus figuring out the actual frequency.

If the frequency $f_0$ to be measured is known to be a definite value f, i.e., $f_0 = f + \Delta f$, $\Delta f << f$, then from Equation C-27, the fundamental signal can be expressed as:

**EQUATION C-45:**

$$U_1(t) = u_{c1} sin(\omega \cdot t + \varphi_{u1}) = u_{c1} sin(2\pi f_0 t + \varphi_{u1})$$

If:

**EQUATION C-46:**

$$T = \frac{1}{f}$$

**EQUATION C-47:**

$$u_a = \frac{2}{T} \cdot \int_0^T U_1(t) cos(\omega t) dt$$

$$= \frac{2}{T} \cdot \int_0^T u_{c1} sin(2\pi f_0 t + \varphi_{u1}) cos(2\pi f t) dt$$

**EQUATION C-48:**

$$u_b = \frac{2}{T} \cdot \int_0^T U_1(t) sin(\omega t) dt$$

$$= \frac{2}{T} \cdot \int_0^T u_{c1} sin(2\pi f_0 t + \varphi_{u1}) sin(2\pi f t) dt$$

We get:

**EQUATION C-49:**

$$u_a = \frac{2u_{c1}}{T} \cdot \frac{(f + \Delta f) \cdot sin(\varphi_{u1}) \cdot sin\left(\frac{\pi \Delta f}{f}\right)}{\pi \cdot (2f + \Delta f) \cdot \Delta f}$$

**EQUATION C-50:**

$$u_b = \frac{2u_{c1}}{T} \cdot \frac{f \cdot cos(\varphi_{u1}) \cdot sin\left(\frac{\pi \Delta f}{f}\right)}{\pi \cdot (2f + \Delta f) \cdot \Delta f}$$

As $\Delta f << f$, from Equation C-49 and C-50, we have:

**EQUATION C-51:**

$$\frac{u_a}{u_b} \approx \frac{sin(\varphi_{u1})}{cos(\varphi_{u1})}$$

Therefore,

**EQUATION C-52:**

$$\varphi_{u1} \approx \begin{cases} \frac{\pi}{2}, (u_b = 0, u_a > 0) \\ \frac{3\pi}{2}, (u_b = 0, u_a < 0) \\ tg^{-1}(\frac{u_a}{u_b}), (u_b > 0, u_a > 0) \\ tg^{-1}(\frac{u_a}{u_b}) + \pi, (u_b > 0, u_a < 0) \\ tg^{-1}(\frac{u_a}{u_b}) + 2\pi, (u_b < 0, u_a > 0) \end{cases}$$

Assuming that the signal's initial phase angle measured in the 1st cycle is $\varphi_1$ and in the N-th is $\varphi_N$, then the difference between actual frequency and the assumed frequency is:

**EQUATION C-53:**

$$\Delta f \approx \begin{cases} \frac{(\varphi_N - \varphi_1) \cdot f}{2\pi \cdot N}, (|\varphi_N - \varphi_1| < \pi) \\ \frac{(\varphi_N - \varphi_1 + 2\pi) \cdot f}{2\pi \cdot N}, (\varphi_N - \varphi_1 < -\pi) \\ \frac{(\varphi_N - \varphi_1 - 2\pi) \cdot f}{2\pi \cdot N}, (\varphi_N - \varphi_1 > \pi) \end{cases}$$

## C.6 IMPROVING MEASUREMENT PRECISION OF QUASI-SYNCHRONOUS SAMPLING ALGORITHM

When using the quasi-synchronous sampling method for harmonic analysis and calculation of power as well as voltage and current, strict restrictions apply for the algorithm and compensation, (i.e., the frequency offset must not exceed 1% of the central frequency). Precision of the result increases as the frequency offset gets less. Measurement accuracy is not guaranteed, if this condition can not be met. Figure C-4 shows the quasi-synchronization algorithm using 3 iterations with input signal ranging from 47.5 Hz to 52.5 Hz. The algorithm is for calculating the active power, the reactive power and the relative error of current and voltage. Figure C-4 shows that the algorithm works well when the frequency falls in the range of 47.5 Hz to 52.5 Hz. As the frequency deviates from the range, the error increases significantly. Therefore, the algorithm needs to be improved to fit into more applications with a more relaxed restriction.

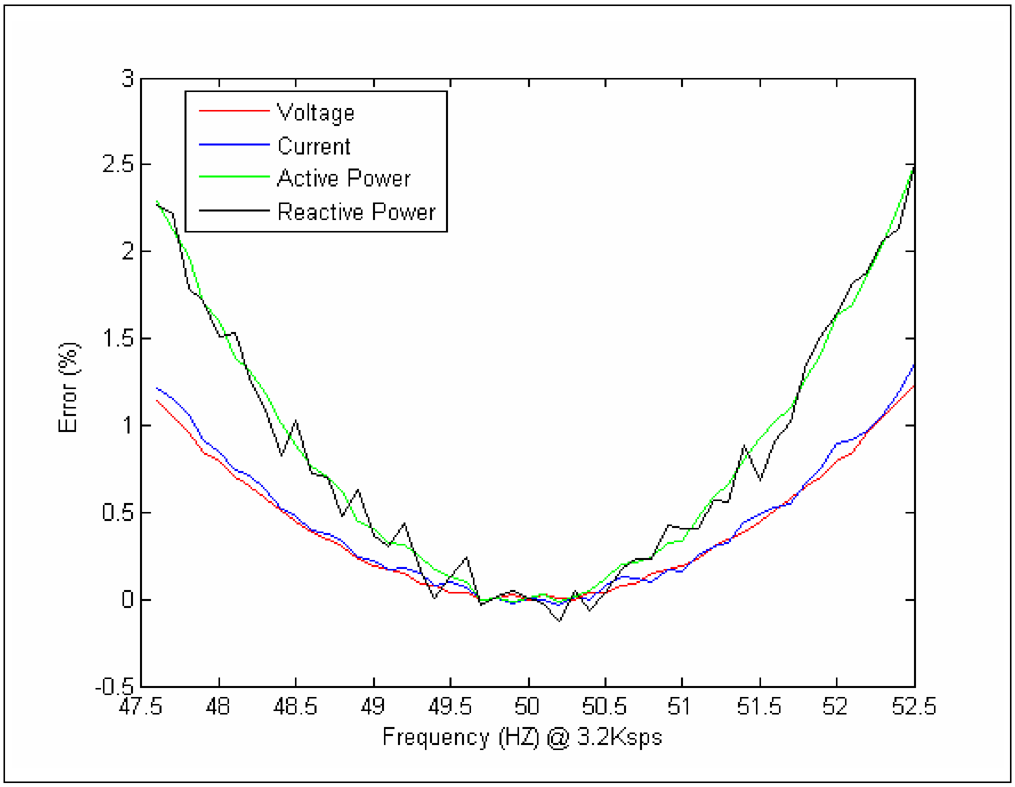


***FIGURE C-4:*** *Quasi-sync Algorithm Error Analysis of 3 Iterations.*

The quasi-sync sampling algorithm has relative high accuracy in frequency measurement and the error can be less than 0.005 Hz. If the frequency range to be measured can be segmented to make the frequency input closest to the multiple of cycle point, and processed using appropriate quasi-sync window function and sine/cosine tale, then the algorithm can be used for a much wider range of frequency .

Figure C-5 is the error analysis of the improved 3-iteration quasi-synchronous algorithm at 3.2 ksps. It shows that the relative error for each result can be well controlled when the frequency of the input signal falls in the range of 47.5 Hz to 52.5 Hz.

Figure C-5 clearly shows that the relative errors of the current, voltage, active power and reactive power in the entire frequency range are less than 0.08%. Also, when the input frequency is around the multiple of cycle frequencies (52.459 Hz, 51.613 Hz, 50.794 Hz, 50.0 Hz, 49.231 Hz, 48.485 Hz and 47.761 Hz), the calculateion error is minimal (<0.01%). When the input frequency deviates from the multiple of cycle frequencies, the calculation error increases rapidly. As the calculation error is related to the frequency offset to the multiple of freqency point, the calculation error caused by frequency offset can be corrected. Figure C-6 is the error analysis after frequency offset correction using simple parabolic interpolation. Calcultion errors for all parameters are shown to be less than 0.015% after the correction.

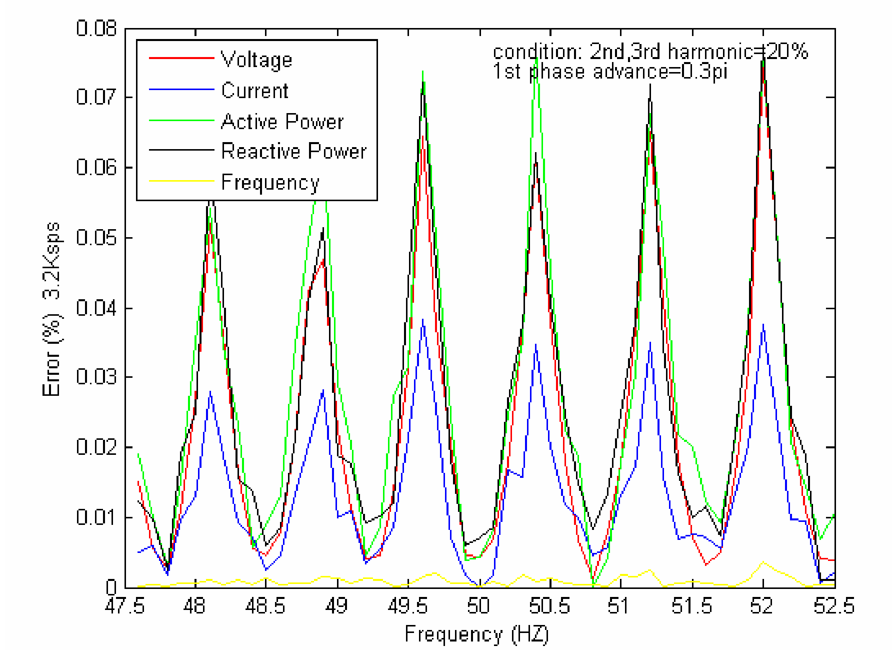


***FIGURE C-5:*** *Error Analysis Of Improved Quasi-sync Calculation Using 3 Iterations.*

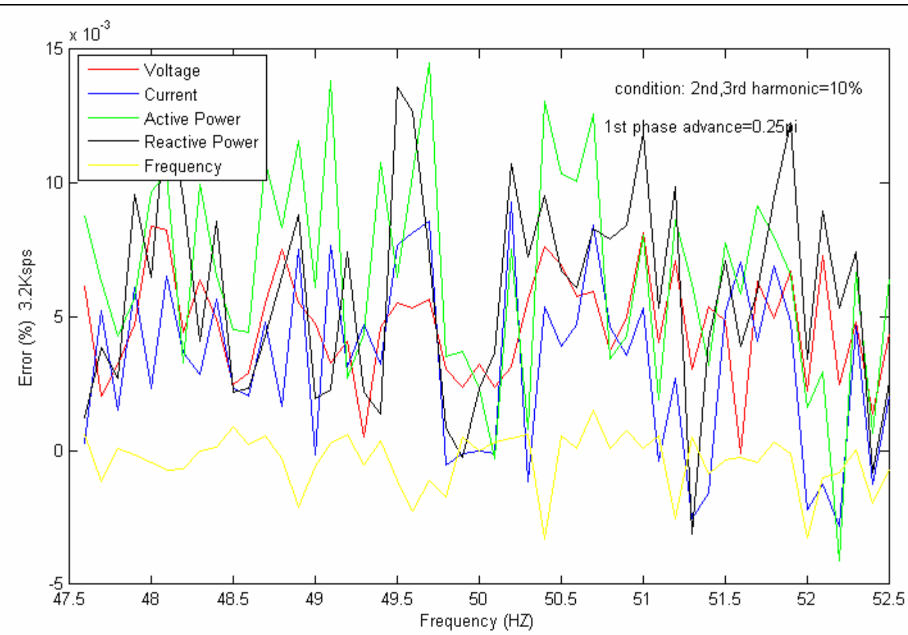


***FIGURE C-6:*** *Calculation Error Analysis After The Frequency Offset Compensation.*

## C.7 MEASURING SECONDARY PARAMETERS

The methods of measuring parameters such as RMS values of voltage and current, active power, reactive power and frequency have been discussed in previous sections. These are primary parameters that need to be calculated from the original data. There are some other parameters called secondary parameter, such as power factor of each phase, total reactive power, total active power, total power factor, harmonic components and cumulative energy. They are obtained indirectly from primary parameters.

The measurement of secondary parameters is discussed in this section.

### C.7.0.1 TOTAL ACTIVE POWER AND TOTAL REACTIVE POWER

For 3-phase 4-wire systems, 3-phase total active power and recative power are the sum of power of each phase, respectively, which can be expressed as:

**EQUATION C-54:**

$$P = P_A + P_B + P_C$$

**EQUATION C-55:**

$$Q = Q_A + Q_B + Q_C$$

## C.8 APPARENT POWER OF EACH PHASE AND TOTAL APPARENT POWER

Apparent power is defined as:

**EQUATION C-56:**

$$S = \sqrt{Q^2 + p^2}$$

## C.9 POWER FACTOR OF EACH PHASE AND TOTAL POWER FACTOR

Power factor is defined as the ratio of active power to apparent power. The definition can be represented as shown in Equation C-57:

**EQUATION C-57:**

$$PF = \frac{|P|}{\sqrt{P^2 + Q^2}}$$

## C.10 Active Energy AND REACTIVE ENERGY

Active energy is defined as the integral of active power over time, which is:

**EQUATION C-58:**

$$W = \int_0^T P(t)dt = \sum_{k=0}^{N} u(k) \cdot i(k) \cdot \Delta t$$

In this design, active energy is obtained from multiplying the voltage by the current sampled each time. The phase angle difference is compensated after each power measurement is completed.

For reactive power, the cumulative reactive energy over a time period can be calculated by measuring the average power and calculating the time interval between 2 measurements.

**EQUATION C-59:**

$$V_r = \int_0^T Q(t)dt$$

## C.11 POSITIVE/NEGATIVE ACTIVE ENERGY, POSITIVE/NEGATIVE REACTIVE ENERGY AND FOUR-QUADRANT REACTIVE ENERGY

In the measurement plane, the horizontal axis denotes voltage vector U (fixed on the horizontal axis). The instantaneous current vector is used to represent the power transfer, and has a phase angle $\phi$ against vector U. $\phi$ is positive in counter-clockwise direction. Power exchange can be defined in 4 scenarios:

- Quadrant I (P>0, Q>0): active energy and reactive energy are sent out at the same time;
- Quadrant II (P<0, Q>0): active energy is sent in while reactive energy is sent out;
- Quadrant III (P<0, Q<0): active energy is sent in while reactive energy is absorbed;
- Quadrant IV (P>0, Q<0): active energy is sent out while the reactive energy is absorbed.

1. **Positive active energy and negative active energy:** accumulated active energy can be defined as positive and negative depending on the direction of active current. When the direction of active current is positive (from power grid to loads), active energy is positive (where active power P>0, corresponding to quadrants I and IV, which means that loads are drawing energy from grid). When current moves from loads to power grid, it is defined as negative active energy (where active power P < 0, corresponding to quadrants II and III, which means energy is provided to grid). Usually only positive active energy is taken into account in active energy, but in practice negative active energy may be taken into account as well, if necessary.
2. **Positive reactive energy and negative reactive energy:** If reactive power Q > 0 (corresponding to quadrants I and II), it means power grid is providing reactive energy to loads, so the energy is defined as positive reactive energy. When reactive power Q < 0 (corresponding to quadrants III and IV), it means that loads are providing reactive energy to power grid, so the energy is defined as negative reactive energy.

3. **Four-quadrant reactive energy:** metering reactive energy in positive/negative reactive energy cannot truly reflect the status of reactive energy, whereas 4-quandrant reactive energy measuring gives a true picture of energy exchange. Reactive energy in four quadrants represents four different reactive energy (see Figure C-7). And the reactive energy  is accumulated depending on which quadrant it is located.

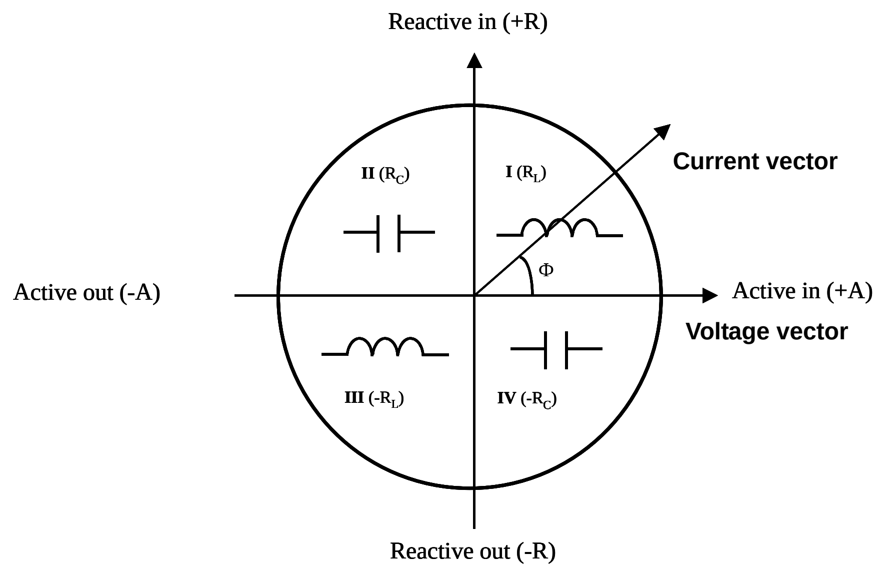


Where:

| | | |
|---|---|---|
| A | = | is active energy, |
| R | = | is reactive energy |
| $R_L$ | = | is inductive reactive energy |
| $R_C$ | = | s capacitive reactive energy |

***FIGURE C-7:*** *Definition Of 4 Quadrants To Measure Electrical Energy.*

 

## C.12 HARMONIC COMPONENTS OF CURRENT, VOLTAGE AND TOTAL HARMONIC DISTORTION

In **Section C.3 "The Harmonic Analysis Algorithm Of Quasi-synchronous Sampling"**, we discussed the measuring of current and voltage signals for each order of harmonics. 3 parameters are used to show to what extent a distorted wave deviates from a sine wave. They are: harmonic content, total distortion and harmonic ratio of the k-th harmonic. The term harmonic content means the root of square of effective values for all harmonics, which is defined as:

**EQUATION C-60:**

$$U_H = \sqrt{\sum_{k=2}^{N} U_k 2}$$

The total voltage distortion ratio of harmonics is the ratio of harmonic content to the fundamental in percentage, which is defined as:

**EQUATION C-61:**

$$THD_U = \frac{U_H}{U_I} \times 100\% \sqrt{\sum_{k=2}^{N} (THD_{Uk})^2}$$

The k-th harmonic ratio for voltage is the ratio of the k-th harmonic to the fundamental in percentage, defined as:

**EQUATION C-62:**

$$THD_{Uk} = \frac{U_k}{U_1} \times 100\%$$

Similarly, harmonics of each order for the current and total distortion ratio can be sorted out.

 

## C.13 COMPENSATION FOR RATIO ERROR AND PHASE LAG

The error of the current transformer (CT) is a complex, which can usually be expressed by two orthogonal parts, current error (f) and phase lag (δ).

**EQUATION C-63:**

$$\varepsilon = f + j \cdot \delta$$

The current error, also known as ratio error, can be written in percentage as:

**EQUATION C-64:**

$$f = 100\frac{(k_n I_2 - I_1)}{I_1}$$

Where:

$K_n$ = the rated current ratio

$I_1$ = the primary current

$I_2$ = the secondary current that passes $I_1$ under the test condition

Phase lag, also known as angle error, is the phase difference between primary and secondary current vector, in 'minute'.

Different current transformers have different errors. Current transformers are classified into different accuracy classes depending on their error magnitudes. The accuracy class of a transformer is nominated by the percentage of the maximal ratio error allowed for a given rated current.

Accuracy classes and corresponding error limits for a current transformer are listed in Table C-1.

**TABLE C-1: ACCURACY CLASS AND ERROR LIMIT FOR THE CURRENT TRANSFORMER**

| Accurate Class | Ratio Error± (%) | | | | | Phase lag | | | | | | | | | |
|---|---|---|---|---|---|---|---|---|---|---|---|---|---|---|---|
| | Rated Current (%) | | | | | ± (%) | | | | | ± (Grad) | | | | |
| | | | | | | Rated Current (%) | | | | | Rated Current (%) | | | | |
| | 1 | 5 | 20 | 100 | 120 | 1 | 5 | 20 | 100 | 120 | 1 | 5 | 20 | 100 | 120 |
| **0.1** | | 0.4 | 0.2 | 0.1 | 0.1 | | 15 | 8 | 5 | 5 | | 0.45 | 0.24 | 0.15 | 0.15 |
| **0.2** | | 0.75 | 0.35 | 0.2 | 0.2 | | 30 | 15 | 10 | 10 | | 0.9 | 0.45 | 0.3 | 0.3 |
| **0.5** | | 1.5 | 0.75 | 0.5 | 0.5 | | 90 | 45 | 30 | 30 | | 2.7 | 1.35 | 0.9 | 0.9 |
| **1** | | 3 | 1.5 | 1.0 | 1.0 | | 180 | 90 | 60 | 60 | | 5.4 | 2.7 | 1.8 | 1.8 |
| | **Rated Current (%)** | | | | | **Phase difference** | | | | | | | | | |
| | 50 | | 120 | | | | | | | | | | | | |
| **3** | 3 | | 3 | | | Phase difference of class 3 and class 5 are not specified. | | | | | | | | | |
| **5** | 5 | | 5 | | | | | | | | | | | | |

## C.14 RELATIONSHIP BETWEEN ERROR AND CURRENT

For a given load and frequency, the absolute ratio error and angle error increase when the primary current decreases from the rated value for un-compensated current transformer. The reason is that with the decrease of the secondary current, the magnetic permeability µ of the iron core varies non-linearly, resulting in less reduction in the field ampere turns.

Figure C-8 is a typical curve for load current and the phase lag of a CT. Generally, phase lag of the output signal is great when the load current is small, and also increases at a fast rate.

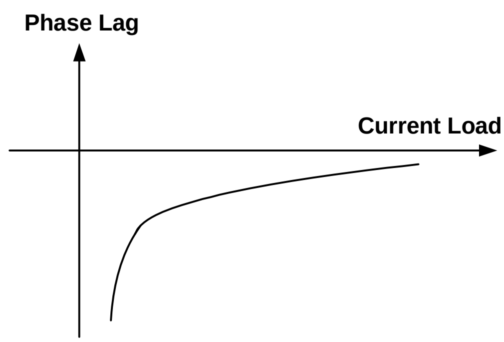


***FIGURE C-8:*** *Current Load Versus CT Phase Lag.*

 

## C.15 RATIO ERROR COMPENSATION

As non-linearity and inconsistency exist in the sampling circuit (including CT and back-end shunt resistors) and the ADC circuit, it is necessary to compensate for ratio error to the system. Figure C-9 is the transfer link of the voltage and current channels.

The compensation for ratio error is quite simple. It compares the measured value against the actual input value under certain input conditions and obtains a correction coefficient.

**EQUATION C-65:**

$$\text{Correction coefficient} = \text{Coefficient before correction} \times \frac{\text{Calibration Value}}{\text{Measured Value}}$$

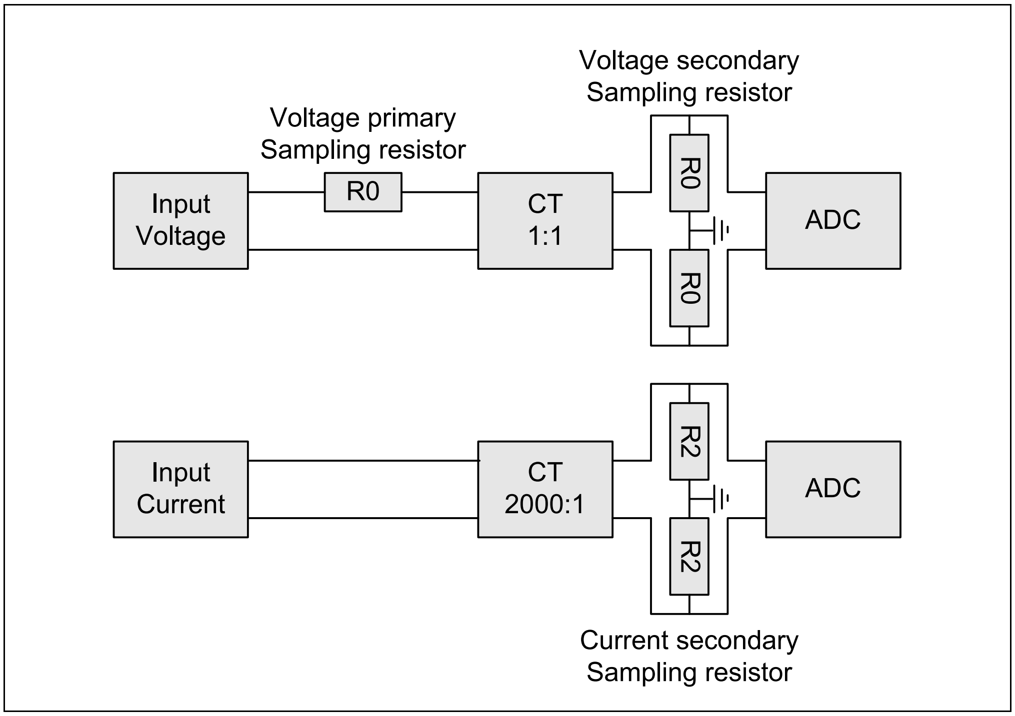


***FIGURE C-9:*** *Error Caused By Sampling Circuit And ADC.*

Since current has a large dynamic range, for a meter which requires high accuracy (0.2s and 0.5s), the multi-point calibration method is needed to meet input requirement for full range. The MCP3909 device's current channel includes an adjustable gain amplifier. The ratio error must be recalibrated for different amplification, but only needs to be calibrated once under the same amplification conditions.

## C.16 PHASE LAG COMPENSATION

Phase lag of a CT has no effect on the metering of RMS current/voltage and apparent power, but will affect the metering of power, since the phase lag will change the phase relationship between the input current and the voltage. This will result in a deviation of the calculated active power from the calculated reactive power.

Figure C-10 shows how a transformer's phase lag affects the measured results under both inductive and capacitive loads. Let's assume that the output of CT has no phase lag from the input voltage, while the CT has a  phase lag from the input signal. With inductive loads, the phase angle increases between the volatge and the current because of the phase lag induced by the CT, resulting in a decrease of the measured active power and an increase of the reactive power. While with capacitive loads, the phase angle between the voltage and the current decreases because of the phase lag induced by the CT, resulting in a decrease of the measured reactive power and an increase of active power.

There are many methods for phase lag compensation. In this design the result correction method is used. It compensates with a coefficient after the active power and reactive power are figured out, which has a small amount of calculation.

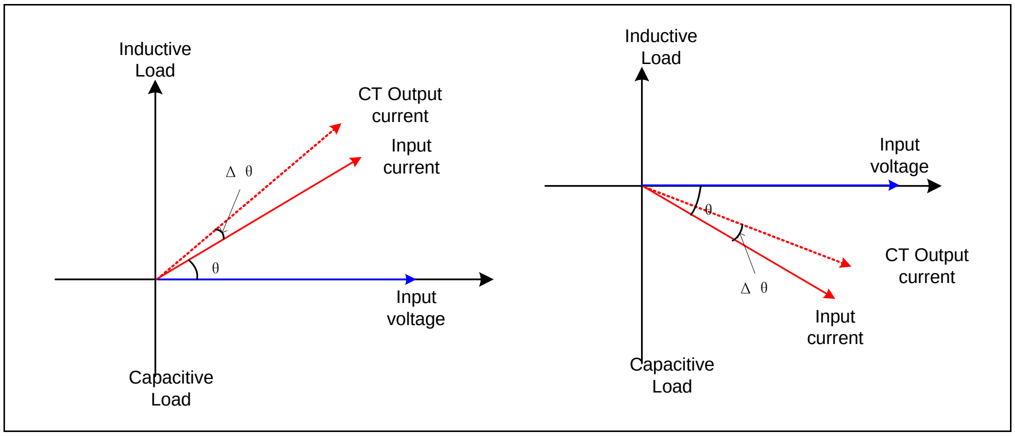


***FIGURE C-10:*** *Measurement Change Caused By Transformer Phase Lag.*

Assuming that the phase lag of CT is $\varphi_i$, of PT is $\varphi_u$, after PT and CT, the variation of phase lag between current and voltage is: $\Delta\varphi = \varphi_u - \varphi_i$.

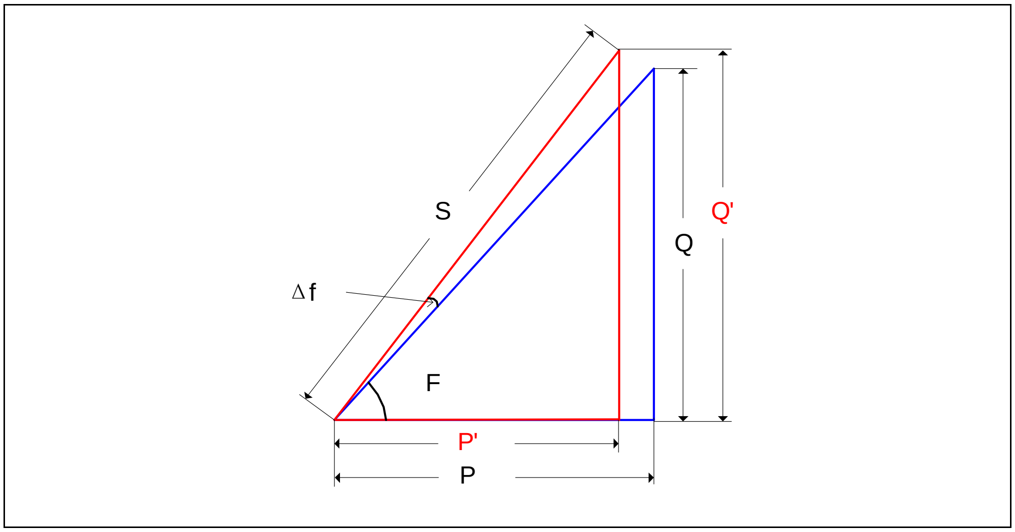


***FIGURE C-11:*** *Principle Of Phase Lag Correction.*

 

Given that the phase lag between the input voltage and current is $\phi$, after PT and CT, the actual measured active power is P', reactive power is Q'. RMS current is I, RMS voltage is V, input apparent power is S, actual input active power is P and reactive power is Q, then Figure C-11 can be drawn based on the principles of power triangle.

**EQUATION C-66:**

$$P' = V \cdot I \cdot cos(\phi + \Delta\varphi) = P cos\Delta\varphi - Q sin\Delta\varphi$$

**EQUATION C-67:**

$$Q' = V \cdot I \cdot sin(\phi + \Delta\varphi) = Q cos\Delta\varphi - P sin\Delta\varphi$$

From the above 2 equations, we have:

**EQUATION C-68:**

$$P = k_1 P' + k_2 Q'$$

**EQUATION C-69:**

$$Q = k_1 Q' - k_2 P'$$

Where:

**EQUATION C-70:**

$$k_1 = cos\Delta\varphi$$

**EQUATION C-71:**

$$k_1 = sin\Delta\varphi$$

By setting up certain input conditions, $\Delta\varphi$ can be measured, and then $k_1$ and $k_2$ can be calculated.

In this design, we use an input of 0.5L for calibration. With this condition, $\Delta\varphi$ can be calculated using the difference between the meaured and the actual input value of active power. For accurate calculations, the user may also use the difference between the measured cumulative energy and the actual cumulative energy to calculate the difference.

**EQUATION C-72:**

$$\Delta\varphi = a cos\left(\frac{P'}{2 \cdot P}\right) - \frac{\pi}{3} = a cos\left((0.5 \cdot (1 + err)) - \frac{\pi}{3}\right)$$

Where $err$ is the error rate of the energy measurement, which results from calculating the error between the actual energy measured by a standard meter and the energy measured by the dsPIC devices. The error can be obtained from the output of the meter calibration workbench.

**EQUATION C-73:**

$$err = \frac{P' - P}{P} = \frac{\Delta P}{P} \times 100$$

 

Since the phase lag of a CT's output signal is related to the magnitude of current, different correction coefficients, K, can be set according to different RMS current values. In this design, 5 calibration points can be set. If it does not require high-precision, fewer points can be set to simplify calibration.

If one-time calibration cannot meet the precision requirement, more calibrations can be done. The new angle error may still be calculated using Equation C-72. The new correction coefficient is:

**EQUATION C-74:**

$$k'_1 = cos(\Delta\varphi_1 + \Delta\varphi_2) = k_1 \cdot cos\Delta\varphi_2 - k_2 \cdot sin\Delta\varphi_2$$

**EQUATION C-75:**

$$k'_2 = sin(\Delta\varphi_1 + \Delta\varphi_2) = k_2 \cdot cos\Delta\varphi_2 - k_1 \cdot sin\Delta\varphi_2$$

#### C.16.0.1 PHASE LAG COMPENSATION WHEN FREQUENCY VARIES

For the same current intensity, the signal delay caused by the CT is the same. When the frequency of the input signal varies, the phase lag will be different. Normally, calibration is done at 50 Hz. When the frequency varies, if the same phase lag compensation coefficient for 50 Hz is still used, it will cause an error in the power measurement. In most cases, the frequency varies in a small range (test specification requires ±2.5%), so it has little effect on the measurement accuracy. For meters with an accuracy of 0.5s or above, this measurement error can be ignored. But for 0.2s meters, the error cannot be ignored and the frequency variation needs to be corrected during calculation.

The phase lag compensation coefficient $k_1$ and $k_2$ are corrected during calculation. Assuming that the freqnency is 50 Hz, the signal delay caused by CT is t, then after correction, the compensation coefficient $k_1$ and $k_2$ will be:

**EQUATION C-76:**

$$k_1 = cos\Delta\varphi = cos(t \cdot 50 \cdot 2\pi)$$

**EQUATION C-77:**

$$k_2 = sin\Delta\varphi = sin(t \cdot 50 \cdot 2\pi)$$

When frequency varies, assuming that the frequency offset is $\Delta f$, i.e. the input signal frequency is $50 + \Delta f$, then the compensation coefficient will be:

**EQUATION C-78:**

$$k'_1 = cos\Delta\varphi = cos(t \cdot (50 + \Delta f) \cdot 2\pi)$$

**EQUATION C-79:**

$$k'_2 = sin\Delta\varphi = sin(t \cdot (50 + \Delta f) \cdot 2\pi)$$

To avoid complexity in calculation and to maximize the correction precision, the following equations may be used to approximate $K_1$ and $K_2$ when the phase angle is small.

**EQUATION C-80:**

$$\begin{aligned} k'_1 &= \cos\Delta\varphi \approx \cos\Delta\varphi - \frac{\Delta f}{50} \cdot \sin^2\Delta\varphi \\ &= k_1 - \frac{\Delta f}{50} \cdot k_2 \cdot k_2 \end{aligned}$$

**EQUATION C-81:**

$$\begin{aligned} k'_2 &= \sin\Delta\varphi \approx \sin\Delta\varphi - \frac{\Delta f}{50} \cdot \sin\Delta\varphi \cdot \cos\Delta\varphi \\ &= k_2 - \frac{\Delta f}{50} \cdot k_1 \cdot k_2 \end{aligned}$$

**NOTES:**

# Appendix D. 50/60 Hz Meter Operation

## D.1 FIRMWARE VERSIONS

There are two versions of firmware for the meter due to the quasi-synchronous sampling scheme employed by the dsPIC33F firmware. The design covers the frequency of rated frequency ±2.5 Hz.

To change the rated frequency, just change the definition in the beginning of cacul.h - #define STD_FREQ  50.0.

This is provided for download from Microchip's website, file names and checksums below.

At the same time you need to change the crystal to provide clock for metering IC.

**TABLE D-1: FIRMWARE FILES**

| Line Frequency | Firmware Name | Hex File Checksum | YXX VALUE |
|---|---|---|---|
| 50 Hz | PM_1_50.ZIP | TBD | 3.857 MHz |
| 60 Hz | PM_1_60.ZIP | TBD | TBD |

# WORLDWIDE SALES AND SERVICE

## AMERICAS

**Corporate Office**
2355 West Chandler Blvd.
Chandler, AZ 85224-6199
Tel: 480-792-7200
Fax: 480-792-7277
Technical Support:
http://support.microchip.com
Web Address:
www.microchip.com

**Atlanta**
Duluth, GA
Tel: 678-957-9614
Fax: 678-957-1455

**Boston**
Westborough, MA
Tel: 774-760-0087
Fax: 774-760-0088

**Chicago**
Itasca, IL
Tel: 630-285-0071
Fax: 630-285-0075

**Cleveland**
Independence, OH
Tel: 216-447-0464
Fax: 216-447-0643

**Dallas**
Addison, TX
Tel: 972-818-7423
Fax: 972-818-2924

**Detroit**
Farmington Hills, MI
Tel: 248-538-2250
Fax: 248-538-2260

**Kokomo**
Kokomo, IN
Tel: 765-864-8360
Fax: 765-864-8387

**Los Angeles**
Mission Viejo, CA
Tel: 949-462-9523
Fax: 949-462-9608

**Santa Clara**
Santa Clara, CA
Tel: 408-961-6444
Fax: 408-961-6445

**Toronto**
Mississauga, Ontario,
Canada
Tel: 905-673-0699
Fax: 905-673-6509

## ASIA/PACIFIC

**Asia Pacific Office**
Suites 3707-14, 37th Floor
Tower 6, The Gateway
Harbour City, Kowloon
Hong Kong
Tel: 852-2401-1200
Fax: 852-2401-3431

**Australia - Sydney**
Tel: 61-2-9868-6733
Fax: 61-2-9868-6755

**China - Beijing**
Tel: 86-10-8528-2100
Fax: 86-10-8528-2104

**China - Chengdu**
Tel: 86-28-8665-5511
Fax: 86-28-8665-7889

**China - Hong Kong SAR**
Tel: 852-2401-1200
Fax: 852-2401-3431

**China - Nanjing**
Tel: 86-25-8473-2460
Fax: 86-25-8473-2470

**China - Qingdao**
Tel: 86-532-8502-7355
Fax: 86-532-8502-7205

**China - Shanghai**
Tel: 86-21-5407-5533
Fax: 86-21-5407-5066

**China - Shenyang**
Tel: 86-24-2334-2829
Fax: 86-24-2334-2393

**China - Shenzhen**
Tel: 86-755-8203-2660
Fax: 86-755-8203-1760

**China - Wuhan**
Tel: 86-27-5980-5300
Fax: 86-27-5980-5118

**China - Xiamen**
Tel: 86-592-2388138
Fax: 86-592-2388130

**China - Xian**
Tel: 86-29-8833-7252
Fax: 86-29-8833-7256

**China - Zhuhai**
Tel: 86-756-3210040
Fax: 86-756-3210049

## ASIA/PACIFIC

**India - Bangalore**
Tel: 91-80-3090-4444
Fax: 91-80-3090-4080

**India - New Delhi**
Tel: 91-11-4160-8631
Fax: 91-11-4160-8632

**India - Pune**
Tel: 91-20-2566-1512
Fax: 91-20-2566-1513

**Japan - Yokohama**
Tel: 81-45-471- 6166
Fax: 81-45-471-6122

**Korea - Daegu**
Tel: 82-53-744-4301
Fax: 82-53-744-4302

**Korea - Seoul**
Tel: 82-2-554-7200
Fax: 82-2-558-5932 or
82-2-558-5934

**Malaysia - Kuala Lumpur**
Tel: 60-3-6201-9857
Fax: 60-3-6201-9859

**Malaysia - Penang**
Tel: 60-4-227-8870
Fax: 60-4-227-4068

**Philippines - Manila**
Tel: 63-2-634-9065
Fax: 63-2-634-9069

**Singapore**
Tel: 65-6334-8870
Fax: 65-6334-8850

**Taiwan - Hsin Chu**
Tel: 886-3-6578-300
Fax: 886-3-6578-370

**Taiwan - Kaohsiung**
Tel: 886-7-536-4818
Fax: 886-7-536-4803

**Taiwan - Taipei**
Tel: 886-2-2500-6610
Fax: 886-2-2508-0102

**Thailand - Bangkok**
Tel: 66-2-694-1351
Fax: 66-2-694-1350

## EUROPE

**Austria - Wels**
Tel: 43-7242-2244-39
Fax: 43-7242-2244-393

**Denmark - Copenhagen**
Tel: 45-4450-2828
Fax: 45-4485-2829

**France - Paris**
Tel: 33-1-69-53-63-20
Fax: 33-1-69-30-90-79

**Germany - Munich**
Tel: 49-89-627-144-0
Fax: 49-89-627-144-44

**Italy - Milan**
Tel: 39-0331-742611
Fax: 39-0331-466781

**Netherlands - Drunen**
Tel: 31-416-690399
Fax: 31-416-690340

**Spain - Madrid**
Tel: 34-91-708-08-90
Fax: 34-91-708-08-91

**UK - Wokingham**
Tel: 44-118-921-5869
Fax: 44-118-921-5820

03/26/09